Growth of a Tectonic Ridge

by

Robert W. Fleming

Arvid M. Johnson

and

James A. Messerich

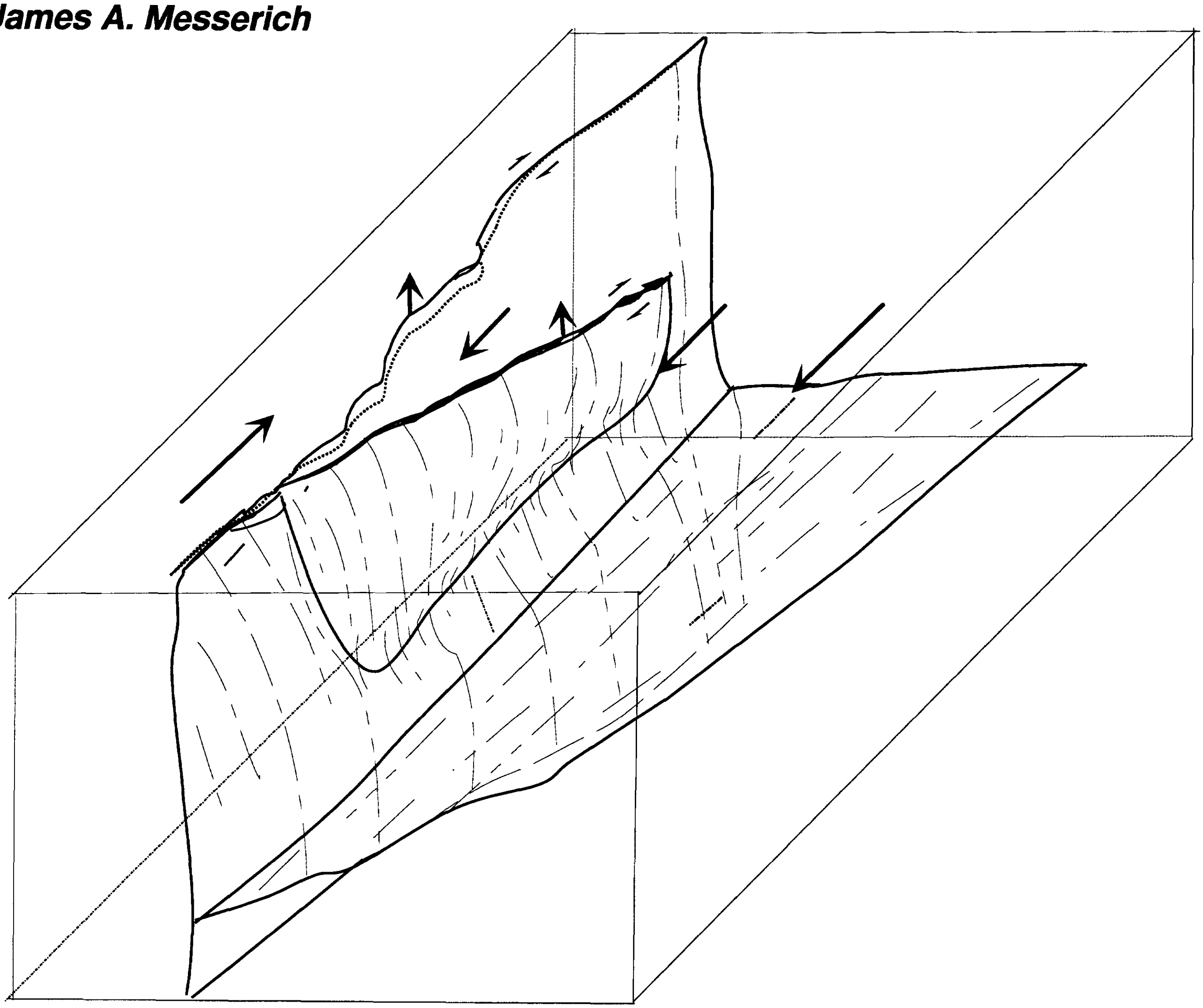

U.S. Geological Survey
Open File Report 97-153
Denver, Colorado 80225
1997

Growth of a Tectonic Ridge

Robert W. Fleming
Geologic Hazards Team
U.S. Geological Survey, Mail Stop 966
Denver, Colorado 80225
Tel.: (303) 273–8603 • FAX: (303) 273–8600

Arvid M. Johnson
Department of Earth and Atmospheric Sciences
Purdue University
West Lafayette, Indiana 47907–1397
Tel.: (317) 494–0250 • FAX: (317) 496–1210)

James A. Messerich
Geologic Photogrammetry Laboratory
U.S. Geological Survey, MS 913
Denver, CO 80225
Tel.: (303) 236-0914 • FAX: (303) 236-5690

Table of Contents

List of Figures

List of Tables

List of Plates (in pocket)

Abstract

Tortoise Hill ridge incrementally grew in height during the 1992-Landers, California, earthquake. The ridge is in strike-slip terrain, within the right-lateral, Emerson fault zone. Tortoise Hill was elevated along bounding shear zones on the northeast and southwest up to 1 m as about 3 m of right-lateral shift was accommodated across the fault zone. Fortuitously, we located a group of survey points in the Tortoise Hill area that had been placed by a public utility company. Data for the measured deformation comes from a resurvey of those points and from analytical photogrammetric measurements on pre- and post-earthquake aerial photography.

Global Position System (GPS) and triangulation studies for length of base-line changes on the scale of kilometers by others indicate that the regional deformation east and west of the Landers rupture is *left-lateral* shearing on the order of 10^{-5}. This deformation reflects the elastic rebound. Our studies of a small area within the region indicate that deformations in the form of normalized length changes are smaller than our limit of accuracy (about 3×10^{-4}) to within about 100 m of the belt of shear zones. Within the shear zones and ridge, we measure right-lateral deformations up to 10^{-2}. At the center of the ridge, the deformation is smaller than 3×10^{-4}. There is also dilation normal to the long axis of the ridge suggesting that the rock within the ridge may have increased in volume. A displacement vector for a point in the center of the ridge indicates that ground in the ridge was thrusted toward the southwest as well as displaced laterally, parallel to the Emerson fault zone. The displacement vector is about 0.8 m oriented at about 45° to the bounding belts of shear zones relative to a point several kilometers to the south of the ridge.

Leveling measurements of differential vertical displacement indicate that ground more than 3 to 4 km southwest away from the ridge was not uplifted. Where uplift began, it gradually increased from about 5 cm/km to perhaps 10 cm/km at the southwest side of the ridge. Total uplift to the southwest side of the ridge was about 0.2 m. From there, the uplift became localized and quickly reached a peak value of about 1 m within the ridge. The pattern is gentle tilting of a broad area to the southwest and an abrupt uplift of the ridge within the bounds of the surrounding belts of shear zones. The greatest growth of the ridge is at the crest of an elliptically-shaped area centered on the high ground of the ridge. Toward the northwest from the ridge, uplift ended within about 1 km of the ridge; the area on the northeast side of the Emerson fault zone in this area was down-dropped at least 0.3 m as part of the releasing stepover to the Camp Rock fault zone. Measurements of horizontal strain and displacement within and outside the ridge combined with elevation changes and detailed maps of surface rupture constrain potential models of the deformation.

The northeast side of Emerson fault zone is a fault that accommodated most of the 3.1 m of right-lateral shift across the fault zone. On part of the southwest side of the fault zone there is also a bounding fault, but in most places the fault zone consists of fractures distributed across a zone that is tens of meters wide. The fault on the northeast side is broken into four elements separated by shorter stepovers. The two northern elements are each 400 m long and trend N55°W. Stepovers are duplex structures; the trend of the stepovers is N35°W. Adjacent to Tortoise Hill, the traces of elements trend about N65°W; whereas traces of fractures with stepovers trend about N45°W. The areas in the stepovers of both fault elements adjacent to Tortoise Hill contain complicated patterns of surface rupture. In particular, the zone between the element that trends N55°W and N65°W has a structure indicating compressive deformation on both sides of the rupture zone. One is a blister-like structure composed of a swarm of tension cracks on the southwest side. The orientation of the tension cracks is consistent with maximum compression directed about normal to the stepover. On the northeast side of the rupture zone, several thrust faults and buckle folds also signal compression at the same place.

In the same area, left-lateral faults directed about normal to the main rupture zone trend northeast across the valley of Galway Lake. These fractures appear to be the local response to misalignment of the fault elements bounding the Emerson fault zone. This structural response to misalignment is small compared to the scale of deformation in the ridge.

The deformation in the belt of shear zones on the northeast side of the ridge indicates that the ridge grew relative to materials outside the zone along a near-vertical rupture. On the southwest side of the ridge, the rupture zone was mixed mode—right lateral and thrusting—on a fault dipping to the northeast. The models that seem to apply to these geometric constraints include wedging or localized dilation of material within the fault zone.

Introduction

The 28 June 1992 Landers, California, earthquake of M 7.6 created an impressive record of surface rupture and ground deformation. Fractures extend over a length of more than 80 km including zones of right-lateral shift, steps in the fault zones, fault intersections and vertical changes. Among the vertical changes was the growth of a tectonic ridge described here.

The ground rupture and vertical deformation occurred in the desert, extending 80 to 90 km along an arc, north-south at the south end of the rupture and northwest-southeast at the north end of the rupture, from about 10 km north of Yucca Valley, California. Fracture details were preserved and patterns were largely unaffected by houses and roads. Deformation was dominated by right-lateral shearing that extended over elements of no fewer than four distinct faults arranged broadly *en echelon* (fig. 1).

In the process of documenting the surface rupture in different tectonic settings, we began to suspect that, in places, deformation was complimentary to existing topography. Areas of positive relief in the rupture zones appeared to have been uplifted during this earthquake. And, areas that might be tectonically positioned to be down-dropped were covered with very young alluvium. In our minds, the landscape began to take on the form of the tectonic deformation that seemed to have occurred during the earthquake. One of these areas, Tortoise Hill, appeared to have been uplifted significantly during the earthquake. We mapped a part of the area and decided that the amount of vertical growth was in the range of 0.5 to 2 m. But through mapping alone we could get only hints of how much growth had actually occurred.

During the same period, a concerted effort was being made to locate low-altitude, pre-earthquake aerial photographs of the rupture zone. We had previously used pre- and post-event aerial photographs to document deformation on landslide surfaces (Fleming and others, 1991), and wanted to test whether deformation caused by an earthquake could be measured photogrammetrically. We were largely unsuccessful in finding large-scale photos from the usual governmental sources (USGS, BLM, USDA, city, county, etc.) that covered any part of the rupture trace. The two groups of high-voltage transmission lines that crossed the rupture zone beginning about 1.3 km north of Tortoise Hill led us to the principal public utility of the greater Los Angeles area, the Southern California Edison Company (SoCalEd). While the pre-earthquake aerial photographs of the power-transmission lines were not well-enough controlled for analytical measurements, we did learn that Tortoise Hill had been part of a site that had been photographed and surveyed for a potential generating station. A relatively dense array of bench marks extends over about 10 land sections, from one side of the Emerson fault zone to the other,

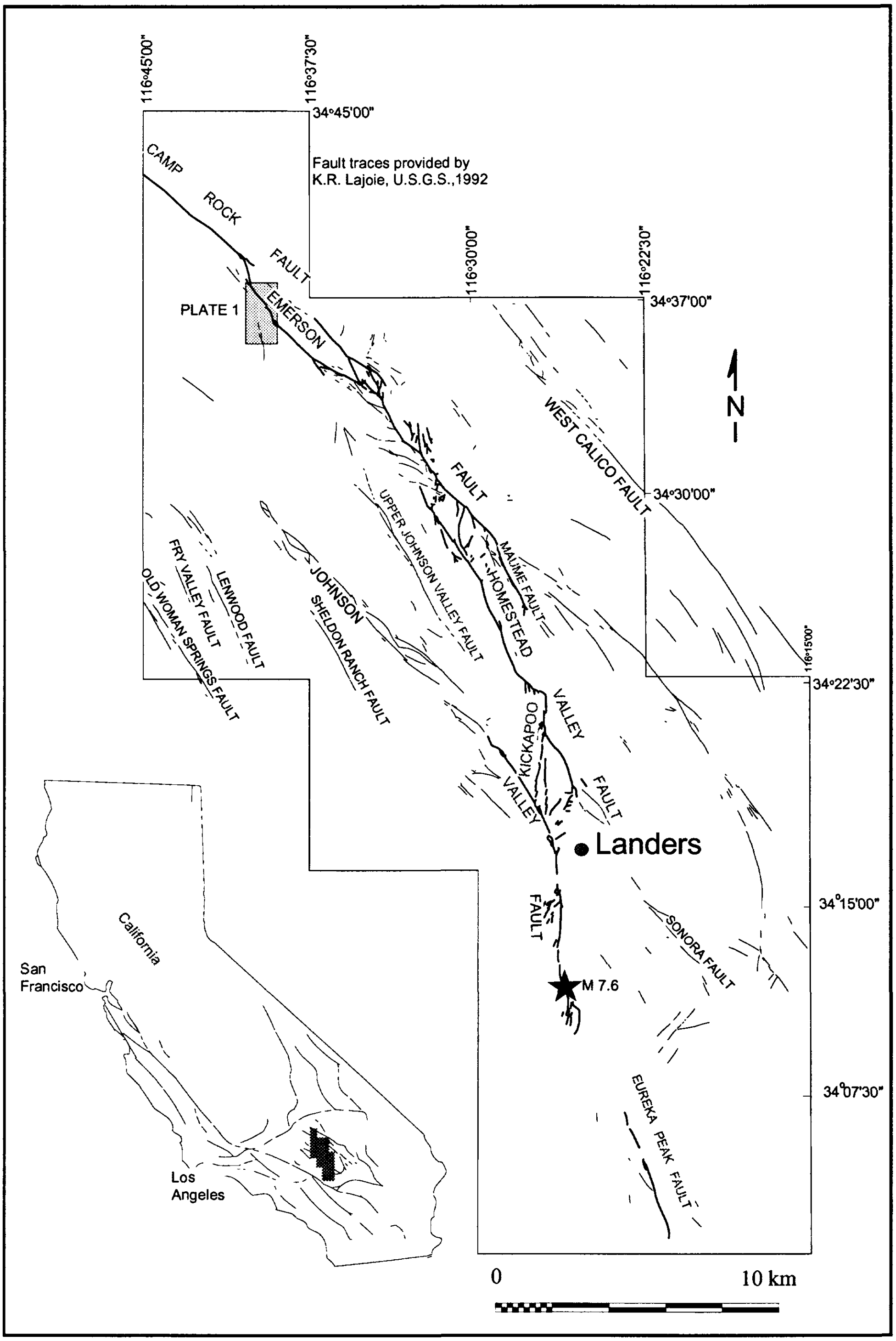

Figure 1. Location map, showing en echelon fault zones that activated during the 1992 Landers, California, earthquake. Epicenter of main shock (M 7.6) was near Landers at the south end of the ruptures. Inset figure shows some of the major faults in southern California. Parts of the Camp Rock, Emerson, Homestead Valley and Johnson Valley fault zones shown as (heavier lines) ruptured in a right-lateral sense, generally with up to 4 meters of shift.

that had been surveyed by the utility company in the 1970's. The network of survey monuments crosses Tortoise Hill near the northwest end of the Emerson fault zone, where faulting steps across the valley of Galway Lake to the Camp Rock fault zone (Plate 1)[1]. The area is between Bessemer Mine Road in the south and the Rodman Mountains in the north. The Single-Tower Transmission Line is in the northwest and the Emerson fault zone cuts obliquely from northwest to southeast in the northern part of the area (Plate 1 and Plate 2).

As part of the surveying project, SoCalEd had flown sets of aerial photographs of the site at 1:6000 and 1:12000 in the 1970's that could be compared to aerial photographs flown by I.K. Curtis Aerial Services, Inc. at 1:6000 along the traces of the ground ruptures immediately after the earthquake. Thus we were provided with an opportunity to use a new method of determining details of displacements and strains in the vicinity of earthquake ruptures. The detailed survey information on the benchmarks from the 1970's provided an additional data set that could be evaluated with a resurvey of the same benchmarks, thereby providing access to two somewhat different methods of obtaining near-field deformational data. A level line that had been established for all the control and wing points provided the basis for learning elevation changes in the area of the ridge and extending for about 5 km south. The SoCalEd gave access to the pre-earthquake data and the aerial photographs, and we contracted with them for a resurvey of the bench marks. The basic survey information from both surveys are in the appendices to this report. We did not contract for bringing control to the site from a distant bench mark, so we cannot determine rotations of the entire surveyed field.

In this paper we describe the Emerson fault zone and the Tortoise Hill ridge including the relations between the fault zone and the ridge. We present data on the horizontal deformation at several scales associated with activity within the ridge and belt of shear zones and show the differential vertical uplifts. And, we conclude with a discussion of potential models for the observed deformation.

Acknowledgments

This research has been supported through grants from the Nuclear Regulatory Commission (Fleming), Department of Energy DE FG02 93ER14365 (Johnson), the Southern California Earthquake Center NTP2898 (Johnson), and the National Science Foundation Grant EAR 9416760 (Johnson and Cruikshank) for research and Grant EAR-9304047 (Johnson) for equipment. Nils Johnson drafted the maps and Jim Gardner edited the manuscript. The Southern California Edison Company made all their pre-earthquake survey data available and conducted the resurvey of the site. Kenneth Cruikshank (Portland State University) and William Smith (USGS) surveyed control points for analysis of the post-earthquake aerial photographs. Kenneth Cruikshank helped with the fracture mapping in Tortoise Hill. We are grateful to all these individuals and organizations for the support. We, of course, are responsible for remaining errors.

[1]The plates are large folded sheets in the envelope at the end of this report.

Emerson Fault Zone

The Emerson fault zone was mapped by Dibblee (1964) and Jennings (1973, 1994) as extending some 55 km in the southeasterly direction from the vicinity of the Single-Tower Transmission Line (Section 15, T6N, R3E), along the west side of Emerson Lake, to at least as far south as the latitude of Landers (to Section 18, T2N, R7E). About half of the known extent of the fault zone activated in 1992; it extended about 25 km from its northwest end to the vicinity of Galway Lake. Near its northwest end it stepped through a series of tension cracks northeastward to the Camp Rock fault zone; and, at its southeast end, it stepped southward across a mountain to the Homestead Valley fault zone (Zachariasen and Sieh, 1995). According to the California fault map by Jennings (1973, 1994), the Emerson fault zone was recognized to be a right-lateral, strike-slip fault; it was known as a Quaternary fault without historic activity implying active slip between the past 200 and the past 2 million years.

Traces of fractures were mapped within part of the Emerson fault zone between Tortoise Hill in the southeast and the Single-Tower Transmission Line in the northwest (Plates 1 and 2). Where the fractures are shown in detail, along with measurements of differential displacements, they were mapped using plane-table methods at scales of 1:200 to 1:500. Where the fractures are shown only as traces, they were mapped from aerial photographs at a scale of 1:6000. Comparison of fracture traces mapped by the two different methods indicates that the traces mapped photogrammetrically are generally incomplete and a subset of those mapped with plane-table methods.

The Emerson fault zone accommodated about 2.9 m of right-lateral shift at the Single-Tower Transmission Line and 3.1 m at Tortoise Hill ridge. Shift on the Emerson fault zone caused near collapse of a high–voltage transmission tower because its legs straddled the largest break (fig. 2) in the belt of shear zones. Using the distances between the legs of the deformed tower, and the corresponding distances between the legs of neighboring undeformed towers, we calculated that the part of the rupture zone that passed through the legs of the tower accommodated 2.7 m of right–lateral differential displacement (Appendix I). By sighting along the other towers of the powerline we determined that an additional 21 cm of right–lateral relative displacement occurred within the fault zone to the southwest of the deformed tower. An additional 69 cm of relative displacement outside the shear zone to the northeast of the deformed tower accounts for the entire right–lateral component of differential displacement, 3.6 m, accommodated over a length of several transmission towers in the direction of the power line.

The additional 69 cm appears to be a result of tension cracking, not fault slip. To the northeast of the belt of shear zones at the damaged transmission tower, there are numerous open tension cracks trending about N10-15°E across the valley of Galway Lake toward the Camp Rock fault zone (Plates 2 and 3). The tension cracks outside the belt are correctly oriented to transfer right-lateral displacement across the valley of Galway Lake between the Emerson and Camp Rock fault zones. The 69 cm of displacement seen in the offset between transmission towers to the northeast is the displacement in the direction of the power line produced by opening of the tension cracks. Correcting for the orientation of the measurement with respect to the opening direction of the tension cracks, perhaps about 1 m of right-lateral shift was transferred across the valley to the Camp Rock fault zone in the form of open fractures. We expect that the displacement on the Emerson fault zone continuing to the northwest diminishes by that amount, but we have no measurements of displacement in that area. (The method of displacement measurement on the transmission towers and results are in Appendix 1.)

In general, the trace of the rupture zone of the Emerson fault is simple and relatively straight

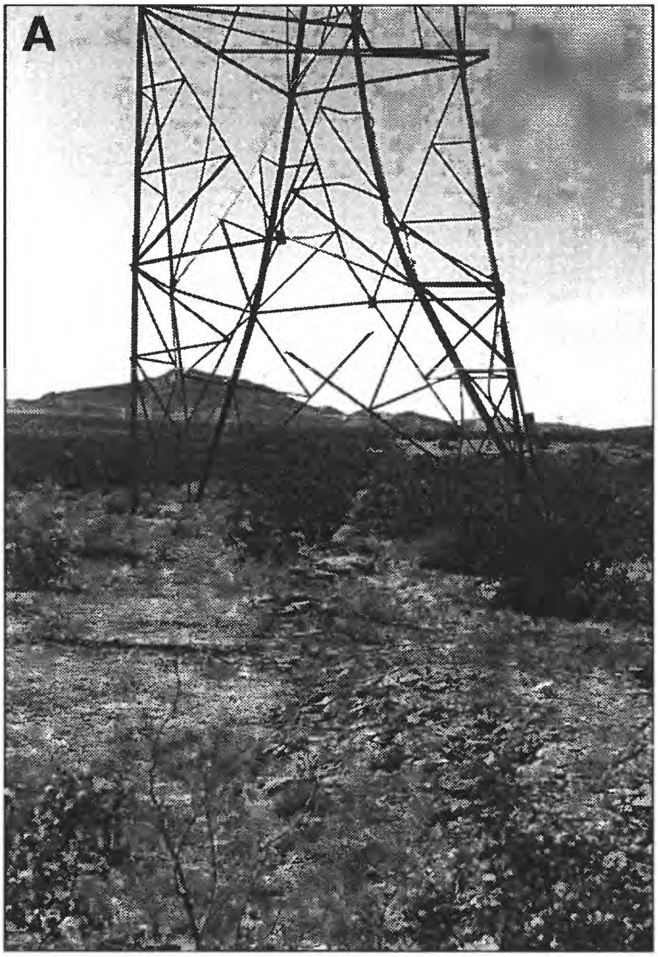

Figure 2. Rupture that passed between legs of tower. Views looking northwest along northeast edge of belt of shear zones at single-tower powerline.

A. Damaged transmission tower (Photo by A.G. Barrows).

B. Same view direction with parts of dismantled tower visible in middle of view to left. In foreground is trough about 2 m wide in sandy soil that represents the main break. Two fault elements, represented by narrow troughs and oriented about 15° clockwise from main rupture are also visible in foreground. The main rupture, visible in this view, offset the legs of the tower about 2.7 m in a right-lateral sense.

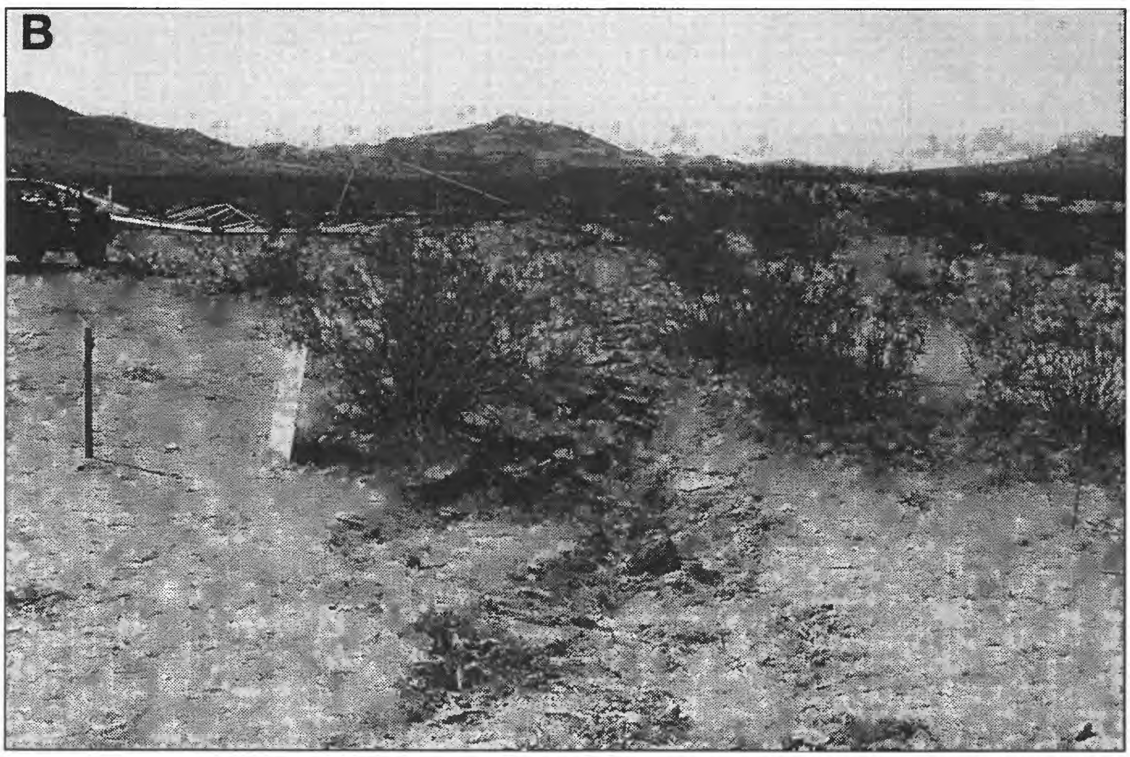

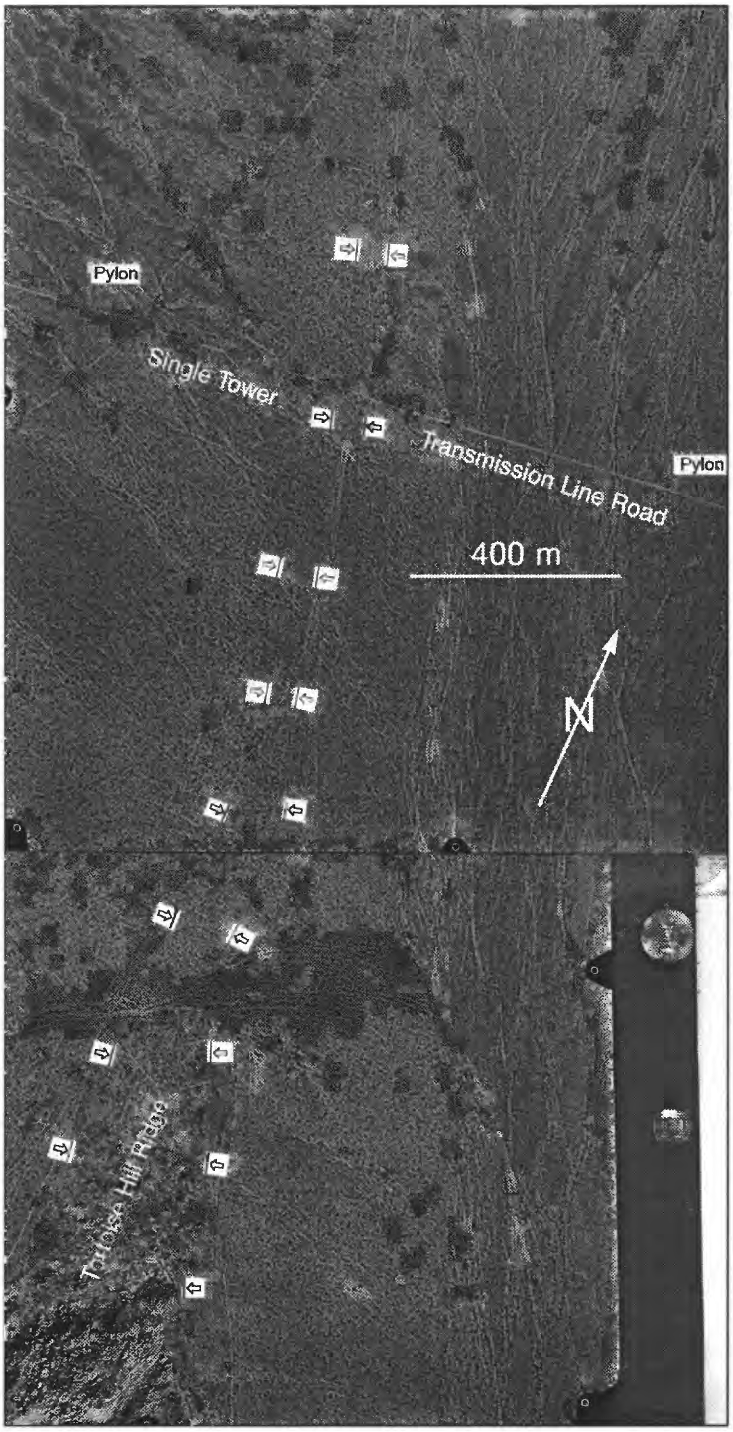

Figure 3. Vertical aerial photograph (about 1:12000 scale) showing belt of shear zones along Emerson fault zone about 6 km northwest of Bessemer Mine Road. Road in upper part of area is along Single-Tower Transmission Line. At south end of photo is north end of Tortoise Hill ridge. Edges of belt shown with arrows. East (right) side of belt is defined by the main fault in this area. The belt is about 70 m wide at transmission line road and 400 m wide in part of ridge shown.

for about 2 km to the northwest and 1 km to the southeast of the Single-Tower Transmission Line. The fault zone is characterized by a belt of shear zones 60-70 m wide (fig. 3 and Plate 3). The overall trend of the belt is N45° to 50° W. As is typical of belts of shear zones (Johnson and others, 1993, 1994), the belts contain fractures such as individual tension cracks, *en-echelon* tension cracks, and right-lateral fault elements.

Tension cracks, oriented about 30° to 45° (N15°W to north-south) at clockwise angles from the strike of the fault zone are clearly different in terms of both pattern and orientation from those outside the belt. The cracks occur sparsely throughout the width of the broad belt on either side of the collapsed tower (Plate 3). The tension cracks are open fractures with highly irregular, interlocking traces that have accommodated only opening (mode I), but no shear. The high irregularity is characteristic of tension cracks that form where the normal compression parallel to the fracture is relatively low (e.g., Cruikshank and others, 1991a). The tension cracks that formed at about 45° to the walls of the broad belt of the Emerson fault zone (Plate 3) seem to reflect only simple shear, without dilation, across a shear zone at depth. Those oriented at 30° seem to reflect a combination of shear and dilation (Fleming and Johnson, 1989; Johnson and others, 1997).

The tension cracks are simple fractures because they were subjected to a single mode of deformation (Johnson and Fleming, 1993, Johnson and others, 1993). Some of the fractures, though, are complex because they first opened and then sheared (and perhaps opened further); these are typical of brittle fractures in shear zones (e.g., Johnson and Fleming, 1993; Johnson and others, 1993).

Several narrow shear zones accommodated a few centimeters to a few tens of centimeters of right-lateral shift within the Emerson fault zone northwest of the Single-Tower

Transmission Line (Plate 3). A narrow shear zone along the southwest wall accommodated 21 cm of right–lateral and 0 to 10 cm of vertical (downthrown on northeast side) relative displacement. For much of its length it consists of N–S oriented tension fractures, several meters long. The blocks of ground between the fractures typically end in low thrusts, directed toward the center of the broad shear zone (Plate 3).

The shear zone (or "mole track") along the northeast wall (fig. 2B and Plate 3) accommodated much more shift and is broader. It dominates the belt of shear zones. This shear zone or complex of shear zones ranges from perhaps 0.5 m wide at places in the northwest section of its trace to 10 m wide in the southeast section, and it has a beaded, or pinch–and–swell structure, which is particularly noticeable in the northwest section. The very narrow elements—the pinches—are a few tens of centimeters wide; they contain a narrow trough in the ground surface, about 10 cm deep and wide (fig. 2B) along parts of their spans. The broader elements—the swells—are several meters wide. Both the swells and the troughs contain long fractures, oriented at a clockwise angle of about 30° to the trend of the shear zone (fig. 2B).

These fractures in the belt of shear zones in the vicinity of the power-line crossing are representative of those seen in the fault zones throughout the Landers earthquake area (Johnson and others, 1993). They represent in a general way the expected style and array of fracturing in a simple shear zone in the absence of a complicating structure. The tension fractures that step to the Camp Rock fault zone to the northeast of the deformed transmission tower are a simple additional element that adds a minor, but interesting complexity to the fracturing in the shear zone. Departures in fracture kinematics from this nearly "normal" pattern are used to interpret the mechanics of a more complex structure. We describe the more complex fractures associated with Tortoise Hill as part of the description of the ridge.

Tortoise Hill Ridge and the Emerson Fault Zone

Tortoise Hill ridge is about 1 km southeast of the power-line crossing (Plate 1). Fractures surround the northwest end of the ridge, apparently as a result of splitting of the belt of shear zones into two, separate shear zones. The pattern of the split belt is like the prow of a Tortoise-Hill-ridge boat, or perhaps a canoe, steaming northwesterly. The bounding zone on the northeast side of the ridge continues to the southeast beyond the map area. The fault zone on the southwest side of the ridge extends only to the southeast end of the ridge and stops. Maximum uplift of the ridge is at about the point where the southwest-bounding fractures end (Plate 1).

The ridge protrudes above the general land surface in an upside-down, keel-shaped outcrop about 400 m wide and 1200 m long. It is about 40 m higher than the valley of Galway Lake on the northeast side and about 20 m higher than the projection of the tilted surface (fig. 4) on the southwest side. This southwest side of the ridge is a long, gently sloping surface much like a pediment except that evidence for beveling by erosion is absent. A distinct change in slope is visible about 1 km southwest of the ridge, but the topographic base map on the geologic map of Dibblee (1964) and on Plate 1 indicates that the change of slope is more one of direction than magnitude of slope.

The northeast side of the ridge is very steep and apparently a fault scarp (fig. 5). In the narrow shear zone along part of this scarp, 1 to 1.5 m of differential vertical uplift was evident with the ridge side upthrown. Measurements of offset features indicate that right-lateral shifts of up to 2.65 m were accommodated across the narrow belt of ruptures. Figure 6 shows a fault surface with striations plunging from right to left within the main rupture zone along the northeast side of Tortoise Hill. The fault surface here strikes N65°W and dips 86° south. The slickensides have a rake of 12°, and plunge S64°E. The adjacent

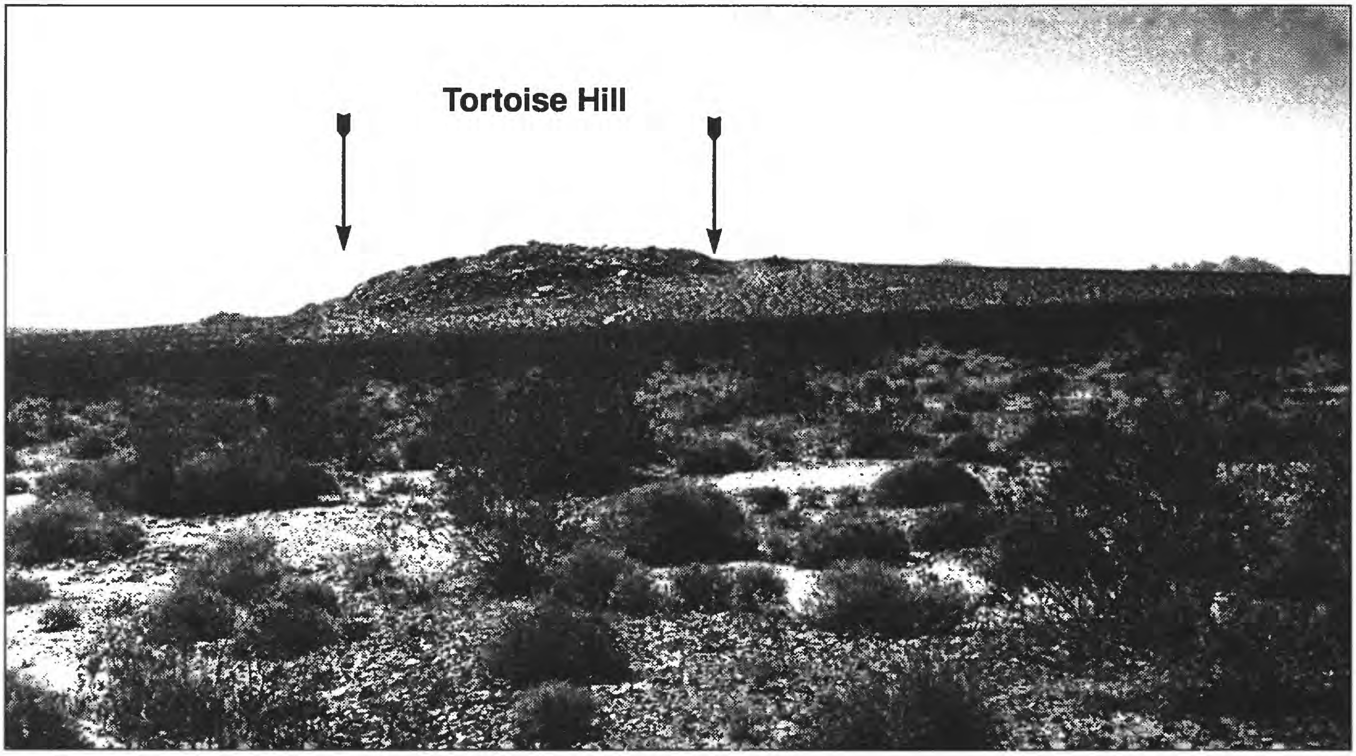

Figure 4. View southeast showing a profile of Tortoise Hill ridge. Valley of Galway Lake is on left and in foreground, and the pediment-like surface underlain by monzogranite on the right. Northeast face of ridge is a fault scarp. Southwest flank is gentle and projects slightly above the slope of pediment-like surface.

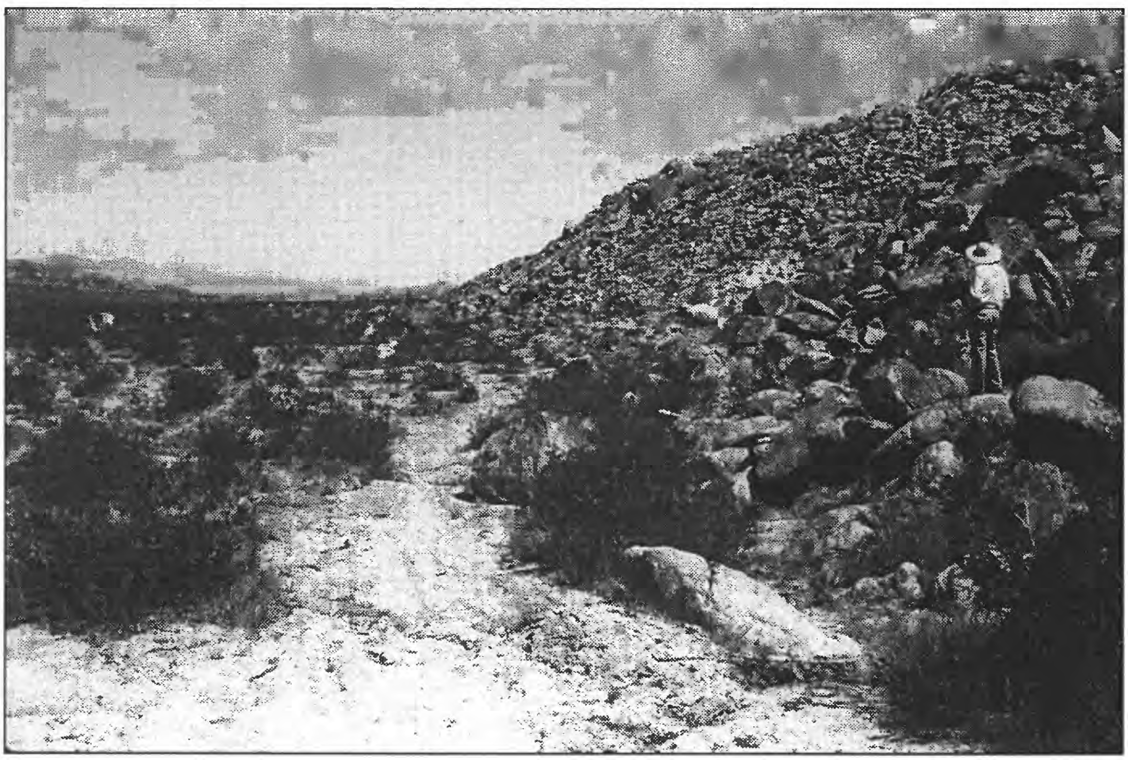

Figure 5. View southeast along Emerson fault zone. The steep, northeast face of Tortoise Hill has a compound slope; lower part is a fault scarp. Spheroidal weathering gives hill the appearance of a rock pile.

Figure 6. View southwest on northeast side of Tortoise Hill ridge of nearly vertical fault surface of main rupture about 1 m high. About 200 m south of Quad 3 (Plate 4) along northeast side of ridge. Light gray material in face beneath dark top soil is monzogranite. Striations plunge 17° to the left (SE).

materials are alluvial fill in the valley of Galway Lake. As we shall see from the survey data reported in subsequent sections, the valley of Galway Lake was downdropped by more than 0.3 m during the earthquake. In addition to the ridge being uplifted relative to the valley, the valley apparently has served repeatedly as a releasing stepover between the Emerson and Camp Rock fault zones.

The exposed rock at Tortoise Hill and over several square kilometers of ground to the southwest is Mesozoic monzogranite (D.M. Morton, written communication, 1996) containing local aplite dikes. Some of the aplite dikes were visible on the aerial photographs and were added to the information on Plates 2 and 4. We were interested in the extent of shearing in the ridge because one of the mechanisms of ridge growth might be dilatancy. The map of dikes is incomplete, but it does show that there are large blocks of intact rock throughout most of the ridge. We simply note here that the long intact dikes in the ridge therefore argue against large amounts of shearing of rock within the ridge, so the suggestion of ridge growth through dilatancy is weak.

In Tortoise Hill, the monzogranite has weathered into spheroidal boulders, and the ridge has the overall appearance of a large rock pile (fig. 5). Outcrops of the monzogranite also occur here and there over the pediment-like slope to the southwest (pediment-like surface is on right of ridge in fig. 4). The fault-parallel Galway Lake valley immediately northeast of Tortoise Hill is underlain by young alluvium, but small knobs and hills of older igneous and metamorphic rocks project through the alluvium on the northeast side of the valley (Dibblee, 1964).

Rather than Tortoise Hill ridge being one large, homogeneous structure bounded by shear zones, the ridge appears to consist of several pieces of ground that have moved differentially vertically with respect to one another. The pieces of ground are spine-shaped bodies that are not highly fractured internally but may be bounded by fractures. For example, one spine, about 120 m long, 50 m wide and 10 to 12 m high, occurs along the main rupture zone as shown at the northeast edge of Plate 4 and as the rocky mass on the left in figure 7. A smaller spine, about 40 m long, 20 m wide and 6 m high, occurs at a place corre-

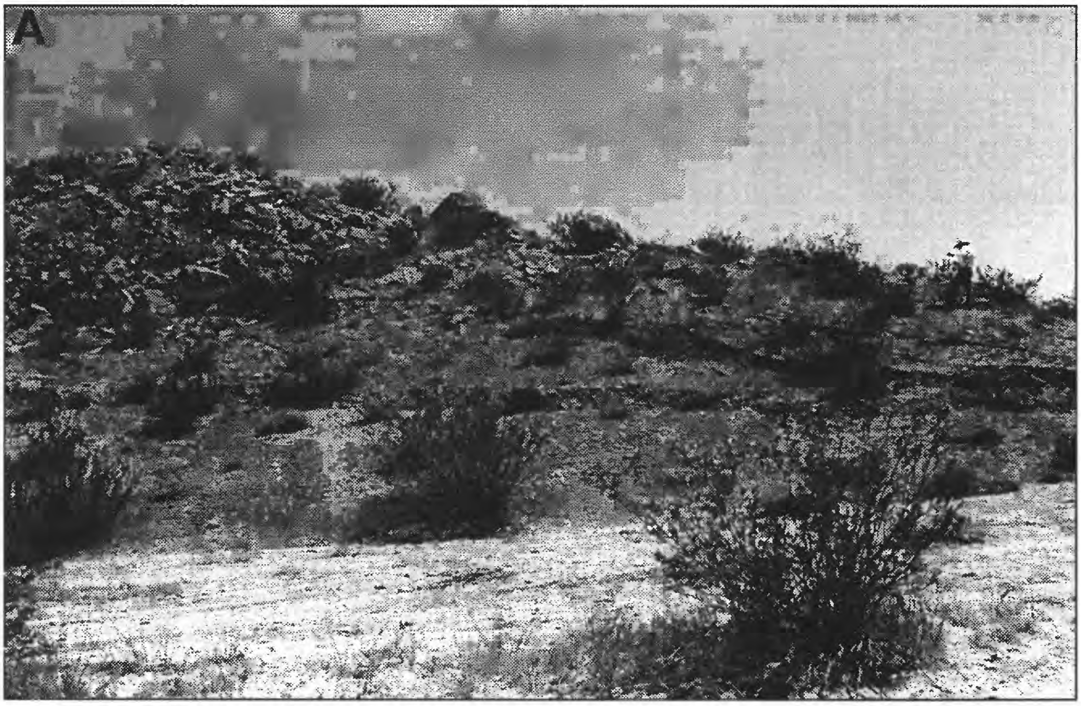

Figure 7. View toward southwest of northwest end of Tortoise Hill ridge.

A. More distant view of ridge. On the left is bouldery nose of hill 1080 (Plate 2). In middle distance on right is ragged fracture of the main rupture, which climbs up the bouldery nose, about 3 m on near side of two larger blocks on skyline. In middle distance in center and left is a low thrust fault, with a scarp 20 to 30 cm high, with downthrown side near observer.

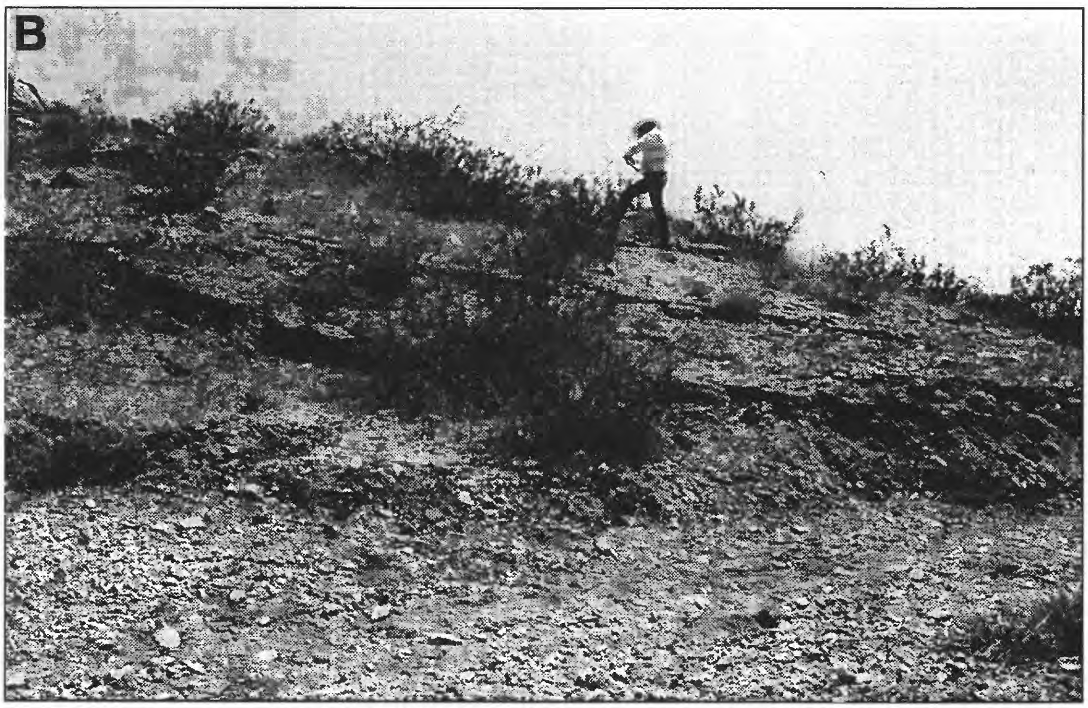

B. Closer view of ruptures. On left are two en-echelon thrusts about 30 cm high. They merge to right with main right-lateral rupture which, here, accommodated about 2.3 m of right-lateral and 0.5 m of vertical differential shift. Center of view shows the small pop-up structure shown in Plate 2, where the misalignment between fault elements produce a restraining structure in the stepover.

sponding to the quadrangle corner that moved upwards 0.4 m as indicated in Plate 4. There may be several other spines with similar ranges of scales visible in the contour map of Plate 4, but all are near the shear zone on the northeast side of the ridge. Our deformation measurements were too widely spaced to resolve any differential displacement of the spines.

There is a broad band of hummocky ground parallel to the unsheared monzogranite near midlength on the southwest side of the ridge (fig. 8). The ground surface is a group of low, rounded bumps that are perhaps 10 m across and 2 to 5 m high. Material in the small bumps is highly sheared monzogranite. In some places the monzogranite is recognizable, but in others the rock is completely pulverized. Mafic minerals, biotite and amphibole, are drawn out in streaks or altered. Bands containing altered mafic minerals about 1 cm thick alternate with pink or gray bands of clay-size material. Shearing is evident on most surfaces and directions of striae are different on different surfaces. We found places where the ground was split locally in this zone and small amounts of the white to pink material were extruded onto the ground surface. The surface rupture on the southwest side is mixed mode right-lateral and thrust faulting (Plate 2 and Plate 4). At the northeast end of the rupture, right-lateral shift predominates; at the southwest end, thrusting predominates (fig. 9).

The fault on the northeast side of the belt of shear zones in the Emerson fault zone throughout the mapped area carries most of the differen-

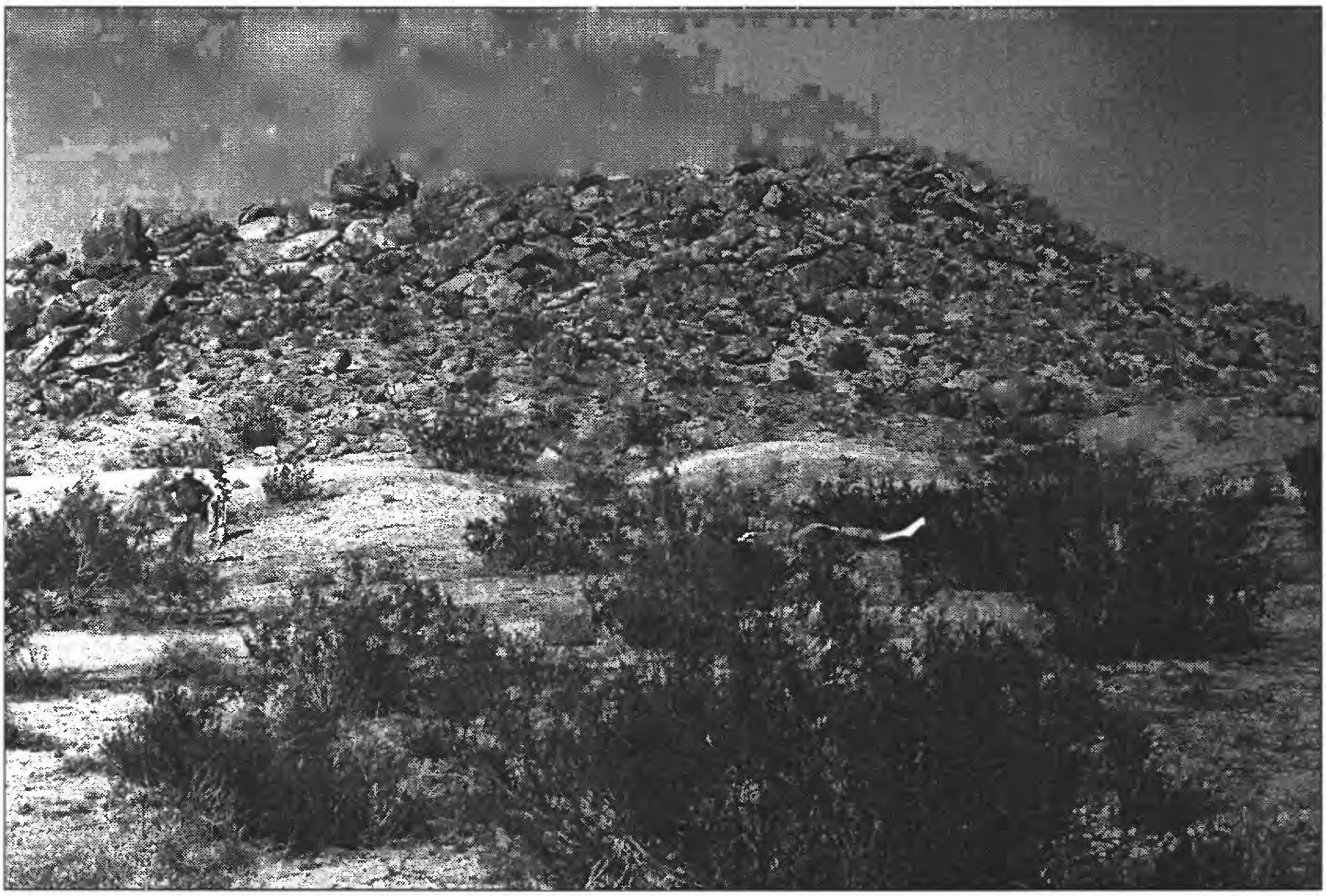

Figure 8. View toward northeast of southwest side of ridge. Light-colored low hummocks at base of Tortoise Hill are composed of highly sheared monzogranite.

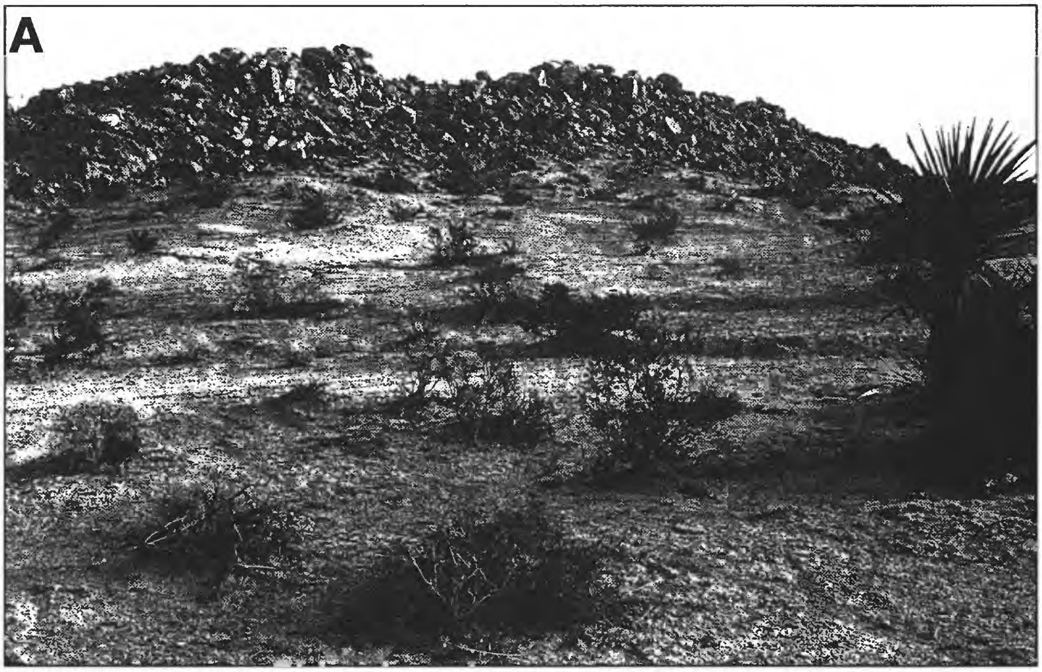

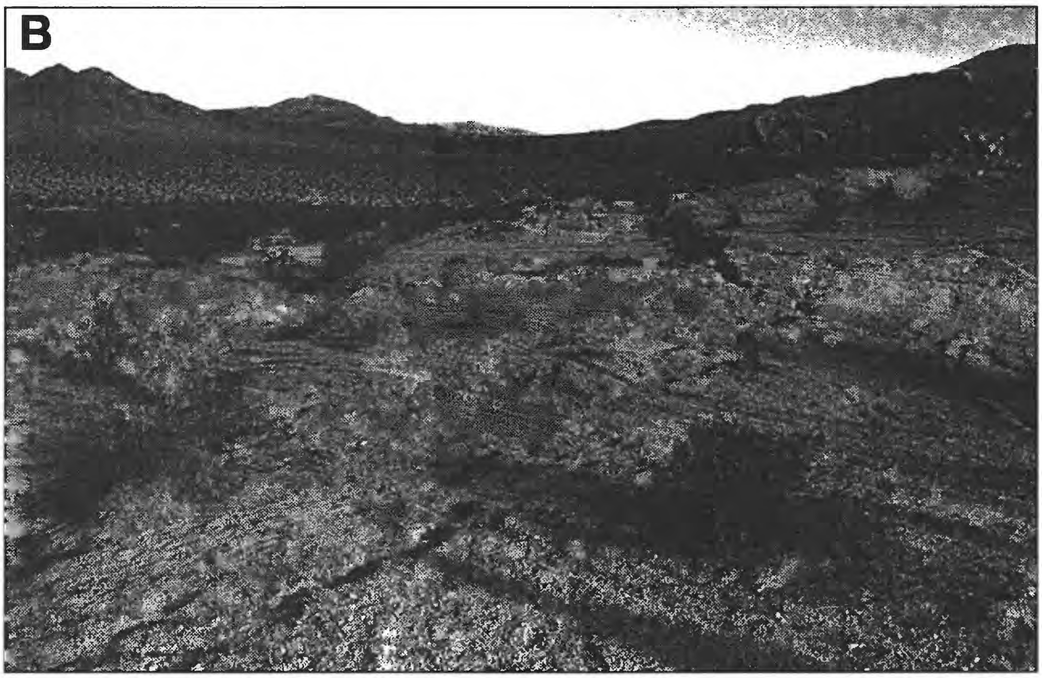

Figure 9. Thrust faults on southwest side of Tortoise Hill about 1 year after the earthquake.

A. View toward northeast at Tortoise Hill showing brows representing two thrust faults along southwest side of the ridge about 200 m southeast of side of Quad 2. Each brow is about 20 cm high, with ground in background thrown upward relative to ground in foreground. Some of tension cracks visible beyond brows on left side of view. Hummocky ground between brows and monzogranite is underlain by highly sheared material.

B. View northwest along southwest side of Tortoise Hill, which is on right. In left side is a step, which marks one of the blind thrust faults on the southwest side of the ridge. Ground on right uplifted one to two decimeters relative to ground on left. A tension crack, marked by series of depressions, extends from near lower left corner toward upper right corner. Orientation reflects right-lateral shearing.

tial displacement across the belt. At the power line, 2.7 of 2.9 m of displacement is on the northeast side. At Tortoise Hill, about 2.65 of 3.1 m is concentrated in a narrow belt on the northeast side. Eight kilometers to the southeast, the concentrated displacement shifts to the southwest side of the shear zone.

There is structure contained in the shear zone but it is difficult to recognize on the plates. In general, however, the rupture belt contains one sharp boundary to the fracturing and the other side is diffuse. The trend and steps in the sharp boundary of the rupture belt is useful to recognize structures.

There are virtually no fractures related to right-lateral strike-slip faulting farther to the northeast so we can use this sharp boundary as a reference line to describe the fracturing along the trend of the surface rupture. Beginning on the northwest end of Plate 2, the general trend of the rupture zone is N48°W. The ruptures on the boundary on the northeast side of the zone, however, are not in a straight line but rather form a consistent stepping pattern of four connected elements. The northwesternmost element is at least 400 m long and oriented about N55°W. Then, in a 100 m stretch that is oriented about N35°W, the sharp edge of the rupture belt is offset in a right step of about 40 m. There, another 400-m element begins that is oriented N55°W. This element is offset in a right-step by another shorter, 80-m element, also oriented N35°W. Within both steps are groups of fractures in the shear zone that diverge from the sharp boundary along the element and curve back toward it at the southeast end of each step. In other locations of surface rupture produced by the Landers earthquake, we have seen these same structures better developed. They are strike-slip duplex structures (Cruikshank and others, 1991a; Johnson and others, 1997). All the fracturing is right lateral in the duplex structure. The bounding shear zone contains right-lateral fault elements that are subparallel to the boundary. The curving fractures are also right-lateral fault elements. The net kinematic result of the duplex structure is a right offset of the bounding right-lateral fault zone.

The third, 350-m element, is oriented about 10° more westerly (N65°W) than the two elements farther north. Several narrow zones of fault elements diverge from the bounding rupture zone of the preceding element and curve back toward it at the end of the stepover and indicate that a duplex structure is in the stepover.

The fractures in this stepover zone, however, are more complicated than in the more northerly duplex. There is a difference in orientation between the two elements that produces a restraining bend of about 10°, and there are additional types and orientations of fractures in the area of the bend that were not evident farther northwest. The structures in the bend can be better understood by mentally eliminating the fractures that appear to be part of a duplex structure in the stepover zone.

Abundant fractures occur on both sides of the northeast-bounding fault (Plate 4). On the northeast side are several long tension cracks oriented about north-south and a group of thrust-fault-like fractures oriented about east-west (fig. 10). The thrust-like fractures have mixed north to south and south to north transport directions and therefore accomplish only shortening (e.g., Fleming and Johnson, 1989) in a north-south direction across the zone. Farther along on the northeast side of the principal rupture zone are about five narrow zones of left-lateral shearing that trend about normal to the direction of the overall shear zone. The left-lateral sense of shear is indicated by the orientations of the *en echelon* fractures. Offset of up to 10 cm was measured at one of these narrow zones.

A zone of tension cracks is shown on the southwest side of the bounding rupture zone in area "A" of figure 10 and on the left edge of Plate 4. This zone had the appearance in the field of a blister-like structure that had been uplifted and fractured in this small area of perhaps 20 by 30 m. Tension fractures of this orientation were confined to the southwest side of the rupture zone, but arching of a contour line on the northeast side of the rupture zone is perhaps indicative of uplift extending across the bounding shear zone

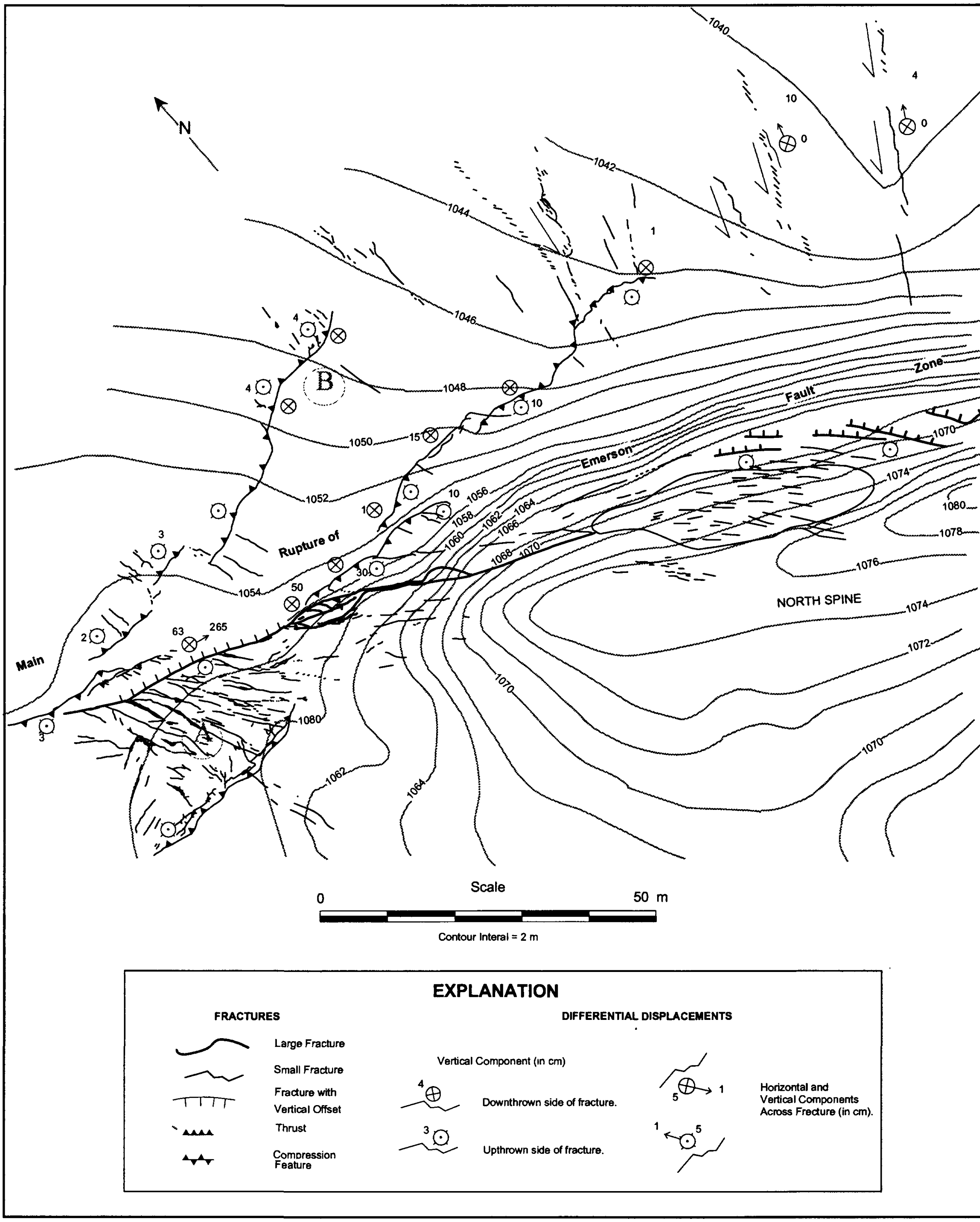

Figure 10. Fractures at left jog in Emerson fault zone at brow of Tortoise Hill, showing compression features on both sides of the jog. The main rupture of the Emerson fault had a scarp about 65 cm high near center of area shown and right-lateral slip was about 265 cm here. The main rupture trends southeast over the east edge of the elongated dome of North Spine. To the north of the rupture are opposite-facing thrusts, dipping north or south, indicating north-south compression. The brows are up to 10 or 15 cm high. To the south there is a welt marked by numerous tension cracks oriented north-south and bounded on the south by a thrust dipping northward.

to the other side as well. The zone of tension cracks was bounded on its southern end by a thrust fault. The thrusting is produced when the prisms of rock broken by tension cracks are rotated in right-lateral shear (fig. 10). The blocks are free to rotate on their sides but constrained on their ends; rotation thus produces the thrusting along the boundary of the blister-like structure. The arching of the contour line across the structure indicates that the total local uplift at the blister-like structure is between 1 and 5 m (Plate 4).

To the northwest of the blister-like structure are at least four narrow belts of left-lateral fractures that are subparallel to the right-lateral fractures in the duplex zone (Plate 2). The left-lateral fractures curve toward the small, blister-like structure composed mostly of tension cracks that is adjacent to the bounding rupture zone. This complicated structure is shown in more detail on the northwest (left) end of Plate 4. These fractures and bulging that are indicative of compression on both sides of the rupture zone are apparently the response to the misalignment of the fault elements. The weak duplex structure accounts for the stepover between the elements; but the misalignment produces compression that is manifest differently on the two sides of the bounding rupture belt.

The stepover at the southeast end of the complex rupture element trends N45°W and produces 30-40 m of right step. The next element, the southeasternmost element shown on Plate 2, is at least 500 m long and oriented parallel to the more complex element just northwest of it (N65°W). There is one left-lateral fault zone at the northwest end of the element that trends northeast across the valley of Galway Lake. There are also a few small fractures on the southwest side of the principal rupture belt at the stepover and a few apparently unorganized fractures in the block across from the left-lateral fault. This area was mapped photogrammetrically, and there is not enough fracture information to determine whether a duplex structure formed between the elements. Clearly, there was not a complex compressive structure like the one immediately to the northeast of this area that resulted from a misalignment of the elements.

In summary, the fault bounding the northeast side of the Emerson fault zone is composed of four right-stepping fault elements. The two elements that are farthest to the northwest are parallel and oriented N55°W. The stepover between the elements is oriented N35-40°W. This stepover contains connective fractures of a duplex structure. The two elements bounding the northeast side of Tortoise Hill are also about parallel to each other and oriented N65°W. The stepover between these southeastern most elements is oriented about N45°W. The area between these two elements lacks the fractures indicative of duplex structures seen farther northwest, but instead contains a left-lateral shear zone normal to the bounding shear zone and a few other fractures of uncertain origin. The middle stepover, between the second and third elements described above, contains both a duplex structure and complicated compressive structures. The compressive structures occur in the zone between the elements and apparently are a result of a 10° misalignment of the two fault elements. It is important to reiterate that the compressive structures occur on both sides of the bounding rupture belt and that the dimensions of the structures are about the same as the length of the stepover. The reasons for the differences in rupture style for what appears to be similar structural settings of stepping fault elements are unknown. It does appear that the complex fracturing and blister-like structure on the principal fault of the Emerson fault zone at Tortoise Hill is a localized response to the short, misoriented fault element. The change in orientaiton and the stepping of fault elements are not likely to have produced the uplift of Tortoise Hill ridge. The change in orientation is highly localized, so it could produce only a small structure; the size of the blister-like structure and the short thrusts are appropriate to the scale of the misoriented element. The steps should be releasing rather than compressing structures, so the ridge would therefore not be related to the stepping of fault elements.

The shear zone on the southwest side of Tortoise Hill ridge is south and directly across the ridge from the blister-like structure described above. This zone is also broken, and three crude but distinct elements can be identified. Elements are oriented about N45°W, 250-300 m long, and right stepping with 20-40 m of offset on each step. The fractures at the northwest end of the zone are predominantly right lateral with a small component of reverse movement on a surface dipping northeast. Farther southeast, the zone accommodates increasing reverse shift with the ridge side upthrown from a few centimeters to a few tens of centimeters (fig. 9).

This shear zone on the southwest side of the ridge has lifted the monzogranite in Tortoise Hill above the sloping, pediment-like surface farther to the southwest. Along this side of the ridge, the outcrops of white pulverized rock in zones essentially parallel to the surface-rupture fractures indicate that this side of the ridge has also been the site of repeated faulting.

Horizontal Deformations

Magnitudes of horizontal deformation are partly a function of where the measurement is taken and partly a function of length of measurement baseline. We have measurements of length- and angle-changes at length scales ranging over three orders of magnitude, from 10 km to 0.1 km. Close in to the rupture belt, we expect larger strains than several kilometers away. We have examined deformation at three levels of observation: Changes in length of long base lines (about 6 km or longer) using triangulation and Global Position System (GPS) surveys provide data for far-field strain analysis. Resurvey of a group of pre-earthquake bench marks ranging from about 7 km from the rupture zone to within the rupture zone and across it provides data for close-in deformation determination. Measurement lengths are typically in the range of 500 m to 1000 m. And, analytical aerial photogrammetry provides data on change in lengths of braced quadrilaterals where initial line lengths are in the range of 100 m and where measurement points are within and across the shear zones. These three levels of information show deformation as a function of position with respect to the surface rupture.

GPS Measurements

Calculations of changes of line lengths and angles using very long baseline trilateration networks across faults that have moved during earthquakes date back to the 1906 San Francisco earthquake (King and Savage, 1983; Prescott and Lisowski, 1983; Stein and Thatcher, 1981; Thatcher, 1975, 1979; and Thatcher and Fujita, 1984; Savage and Gu, 1985), and continue today with broad-scale Global Position System (GPS) surveys. Trilateration and GPS surveys at Landers (Hudnut and others, 1994; and Freymueller and others, 1994) provide considerable regional information about displacement fields on both sides of the rupture zone. Results of these surveys can be used to compute strains a few kilometers from the belts of surface rupture.

Trilateration data of Hudnut and others (1994) for monuments surveyed before and after the earthquake provide normalized length changes for triangles spanning relatively large areas on either side of the northern part of the Homestead Valley fault zone and the southern part of the Emerson fault zone. One triangle consists of stations CREO[2], MAUM, and LEDG, east of the fault zones (fig. 11). The other consists of stations BOUL, MEANS and ROCK, west of the fault zones.

The triangles have legs ranging from about 6 to 20 km long, and at that scale the *normalized length changes*[3] are:

E_n = (final length – initial length)/initial length.(1)

[2]Names defined by Hudnut and others (1994).

[3]We use the term normalized length changes because there may well be fracture discontinuities disrupting the line between the two measurement points. We avoid the closely related term, strain, which is defined only for a continuous body.

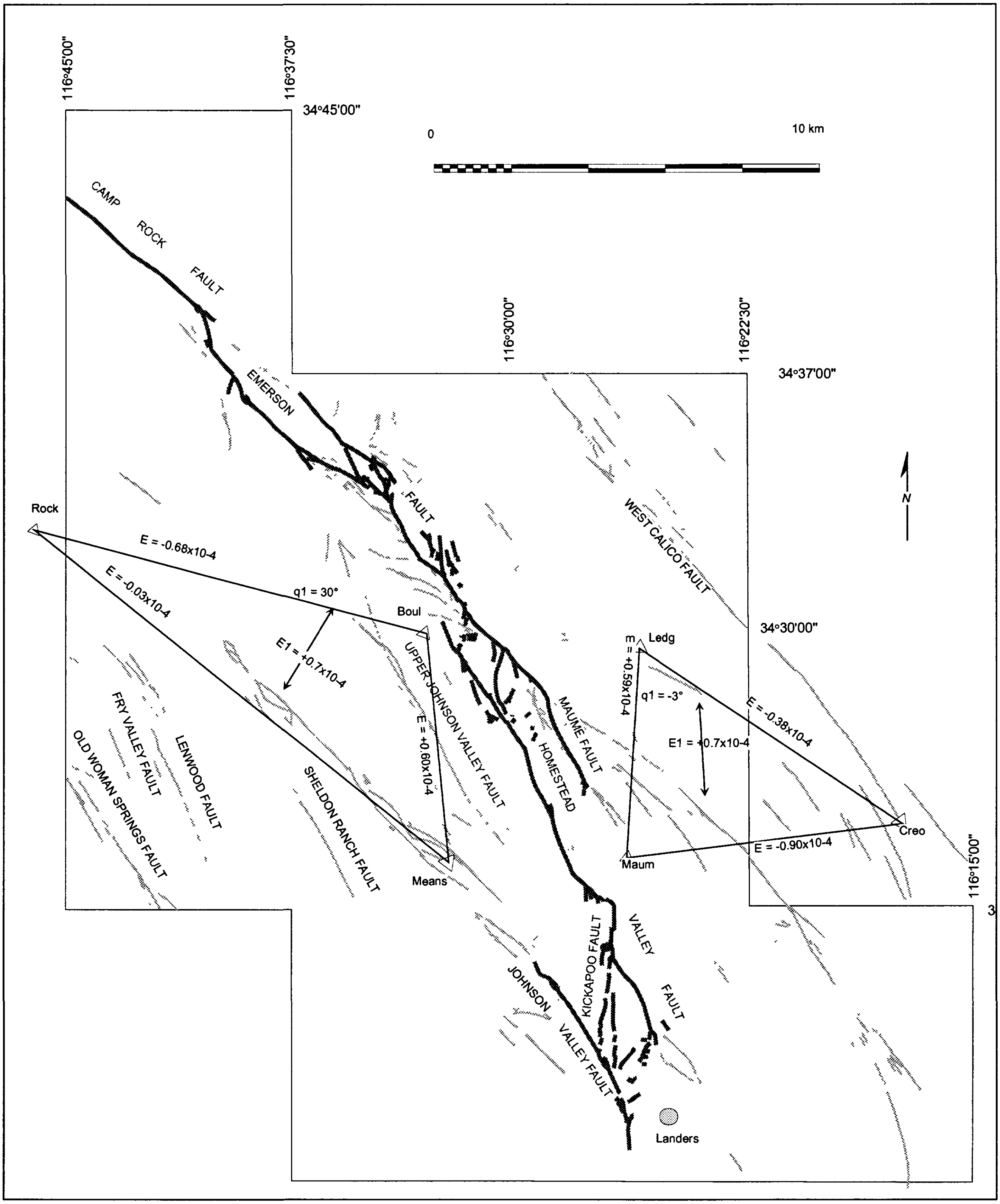

Figure 11. Triangles east and west of the ruptured faults were surveyed by trilateration and show normalized length changes. The direction and magnitude of maximum extension is indicated with double-headed arrows. The measurements reflect left-lateral shearing on the order of $7x10^{-5}$ that accompanied elastic, right-lateral unloading of the faults. Right-lateral deformations are concentrated in the vicinity of belts of shear zones along the faults.

The deformations for a triangle west of the Landers rupture are consistent with unloading during the earthquake sequence. For the triangle east of the surface rupture, changes are $-0.009\text{x}10^{-2}$ (compression) for MAUM/CREO, $-0.004\text{x}10^{-4}$ (compression) for LEDG/CREO, and $+0.006\text{x}10^{-2}$ (extension) for MAUM/LEDG. We note that the MAUM/LEDG leg trends roughly north-south, so the deformations are consistent with left-lateral shearing in the general direction N45°W, reflecting unloading of the right-lateral fault zones during the earthquake.

If we assume that the deformations are continuous, the direction of maximum extension would be N3°W and the principal extensions would be $E_1=+0.007\ \text{x}10^{-2}$ and $E_2=-0.007\text{x}10^{-2}$, that is, the deformation is pure shear (or simple shear).

For the triangle west of the fault zones, normalized length changes are $-0.7\ \text{x}10^{-4}$ (compression) for ROCK/BOUL, $-0.003\ \text{x}10^{-2}$ (compression) for ROCK/MEANS, and $+0.006\text{x}10^{-2}$ (extension) for BOUL/MEANS. The BOUL/MEANS leg is roughly north–south, again consistent with left-lateral shearing in the general direction N45°W. If the deformations are continuous, the direction of maximum extension would be N30°E and the principal extensions are $E_1=+0.007\ \text{x}10^{-2}$ and $E_2= -0.009\ \text{x}10^{-2}$, so there is both left-lateral shearing and slight area decrease.

Qualitatively, the long base-line changes support the suggestion of left-lateral shearing that is generally parallel to the direction of the rupture belt. Both sides of the rupture belt deformed in a manner consistent with unloading of the right-lateral fault zones.

Repeated Land Surveys

SoCalEd established bench marks, surveyed, and mapped an area of about 10 land sections during the mid-1970's as part of the control for photogrammetric surveying of a potential site for a power plant. The plant has not been built, but the survey benchmarks remain. The area included a set of section lines from Bessemer Mine Road in the southwest, across Tortoise Hill ridge and the surface rupture of the Emerson fault zone, and into the alluvial valley of Galway Lake to the northeast. Forty-six bench marks were set as primary *x-y-z* control and an additional 30 wing points were set for elevation control of aerial photography. Using a total station in 1995, SoCalEd repeated angle and length measurements that were made in 1973 and 1976 as part of our investigation of faulting and deformation in the area of the Landers rupture. Descriptions of the surveys are in Appendix II. The record of the earlier survey is on file in Book 31, page 90, of San Bernardino County. Plate 1 shows computed displacements, normalized length changes, and vertical changes.

Mr. Richard Moses, supervising surveyor for both the 1973/76 survey and the 1995 survey reported that the angles should be accurate to 5 seconds and the lengths should be accurate to within 10^{-5}. Thus, for a 1 km line, the length should be accurate to 1 cm. Through examination of normalized length changes, however, we infer that the actual errors are larger. The larger errors probably were introduced with the older surveying methods in 1973/76. We conclude that length changes of about $3\text{x}10^{-4}$ and larger should be significant but that inferred length changes of smaller magnitude are masked by error.

Some of the results of the repeated land surveys are in Plate 1. We have assumed that the bench mark near the corner of Sections 1 and 12 of R3E and Sections 6 and 7 of R4E did not move between the times of the two surveys. As with the GPS and trilateration measurements of length changes regionally (fig. 11), we do not report strain invariants or principal strains; rather we report normalized length changes. The reason we do not convert the length measurements into strain is that the deformation is almost certainly localized. The notion of strain is based on the assumption that, at the level of observation, the displacement distribution is homogeneous; strain is defined as a point quantity. Thus the strain tensor and strain invariants, including the principal strains, have no meaning where lines measured cross discontinuities. Also, we calculate the angular deformation, $\tan(\psi)$, from the relation,

$$\cot(\theta) = \tan(\psi) + \cot(\Theta) \quad (2)$$

in which Θ is the initial and θ is the final angle between two line elements and ψ is the angle of shearing (e.g., Johnson and others, 1996). If the deformations were strains, $\tan(\psi)$ would be the shear strain.

Measurements south of Section 25, T6N R3E, (Plate 1) which includes part of Tortoise Hill ridge, reflect such small length changes (or errors) that we are unable to obtain meaningful estimates of deformations. For example, the measurements between benchmarks in the vicinity of Bessemer Mine Road indicate normalized length changes and shearing on the order of 10^{-5}, which we judge to be insignificant. Nearby, at the common corner of Sections 1, 2, 11 and 12, T5N R3E, the normalized changes are on the order of 10^{-5}, but the magnitudes of an angular deformation and a normalized length change are about 2×10^{-4}. These must be negligible. Note that, even at the southern corners of Section 25, T6N R3E, about 1 mi south of Tortoise Hill, the normalized length changes and angular deformations are smaller than can be measured accurately with the repeated surveys. Even at the southwest corner of Section 24, T6N R3E, about 500 m southwest the edge of Tortoise Hill, the normalized length changes are negligible. The normalized length changes between the control points to the north and south are both below the level of significance, even though the control point to the north is within 200 m of the known rupture zones. The control point to the east is on the eastern side of a known fault, so the normalized length change of -0.03×10^{-2}, which is at the margin of significance, probably is a result of faulting.

According to these results, the normalized length changes are smaller than 2×10^{-4} in an area extending 6.5 km south of Tortoise Hill and about 4.5 km southwest the Emerson fault zone (Plate 1). The results suggest that normalized length changes and angle changes are below that level everywhere except where there are control points that span ruptured ground. The small normalized length changes are consistent with the regional GPS and trilateration measurements reported in figure 11, that the normalized length changes are on the order of 5×10^{-5}.

Photogrammetric Measurements

In order to determine supplementary length changes in relatively small areas near the rupture zone at Tortoise Hill, we have used a photogrammetric method and sequential aerial photography. The method was first used to make displacement measurements in specially designed landslide projects by Fraser and Gruendig (1985), who report sub-centimeter accuracy. We have since used sequential aerial photography to measure displacements in landslides (Baum and others, 1989; Fleming and others, 1991; Baum and Fleming, 1991), For landslides in Utah and Hawaii, the style of structural deformation to houses is confirmed with one-dimensional strain computed from closely-spaced measurements of displacement on photos (Baum and Fleming, 1991). At the active Slumgullion landslide in southern Colorado, photos taken in 1985 and 1990 are used to measure deformational changes by tracking the movement of photo-identifiable points as they are translated with the landslide (Smith and Savage, 1995). The *x-y-z* positions of photo-identifiable points on the moving ground are measured with an analytical stereoplotter, and measurements of the same moving point at two different times are converted into a displacement vector. The control points required to scale the photography and establish a reference coordinate system for the measurements is off the moving ground of the landslide.

The technique has not previously been used to determine displacements along active faults or strains in their vicinity, but we have been able to use the method for parts of the Landers earthquake rupture. We have pre-earthquake aerial photographs, taken in 1976, at a scale of 1:6000, of part of the area that later was in the belt of fault rupture. The photographs were flown by SoCalEd and are controlled with the array of points surveyed at that time. The second set of photographs was taken within hours of the Landers earthquake by I.K. Curtis Aerial Services, Inc. On 28 June 1992, aerial photographs at a scale of 1:6000 were taken of almost all the areas of ground rupture at Landers, including the northern part of the area covered by the 1976 photographs. We surveyed eight control points that could be identified precisely on the 1992 photography in 1994, using a total station for both horizontal and vertical control. Thus, each set of photographs had its own set of control points that was established at about the time of the photography.

Further details of the method, including replication and sorting of data used in calculations, and all our data are presented in Appendix III.

We used the photogrammetric method to measure lengths of legs and braces of a ladder of four quadrilaterals extending across Tortoise Hill ridge from the southwest to the northeast sides. The quadrilaterals, in relation to the fractures that we mapped and the topography of the hill are shown in figure 12 and Plate 4. The position of the control point in Tortoise Hill that moved horizontally southward is shown near the right-hand end of Plate 4 and with a displacement vector on Plate 1.

For each quadrilateral and each date of photography we determined a least-squares best fit plane and determined lengths within that plane. Then we determined normalized length changes by comparing lengths of legs and braces in 1973 and 1992. Our measurements discussed in Appendix III indicate that normalized length changes smaller in magnitude than about $3x10^{-4}$ are negligible.

Starting with the southwest edge of the quadrilateral (Quadrilateral Q2) in the southwest, the normalized length change is marginally significant, but shows a small extension in the northwest direction. The northeast-trending legs cross a rupture zone and both show compression about ten times larger, -1.4 to $-2x10^{-3}$. The compression certainly reflects the thrusting of Tortoise Hill relatively toward the southwest across the southwest rupture belt. The north-south diagonal brace was shortened and the east-west diagonal brace was lengthened, reflecting the right-lateral shear across the southwest rupture belt. Thus the measurements reflect small to negligible extension parallel to the southwest belt, but significant right-lateral shearing parallel and shortening normal to the southwest belt that bounds Tortoise Hill ridge.

The next quadrilateral to the northeast (Quad Q0) near the center of Tortoise Hill (Plate 4) indicates very small to negligible deformation (that is, normalized length changes smaller in magnitude than $3x10^{-4}$).

The northeast end of the next quadrilateral (Quadrilateral Q1) to the northeast is within the belt of shear zones on the northeast side of Tortoise Hill ridge. Normalized length changes are generally large, on the order of 10^{-3} and the deformation is clearly inhomogeneous within the quadrilateral. Thus the leg at the southwest edge of the quadrilateral shortened barely significantly, whereas the leg at the northeast edge shortened by $-1.5x10^{-3}$, apparently reflecting the fact that it traverses the right side of the belt of shear zones obliquely. Because the northwest end of the leg is deeper within the belt than the southwest end, the leg is shortened significantly. The shortening of the north-south brace and the lengthening of the east-west brace again reflect the right-lateral shearing in the belt of shear zones.

Another interesting result is that the southwest and northeast sides of the quadrilateral are both extended significantly. Because of the orientations of these sides relative to the orientation of the belt of shear zones, we would expect minor extension in the southwest side and minor compression in the southeast side if there were only simple shearing. We suggest that the significant extension in both sides reflects movement of the center of Tortoise Hill southward relative to the belt of shear zones on the northeast side of Tortoise Hill. We observed this sense of differential displacement for a control point, shown at the left-hand side of Plate 1, that moved 0.8 m toward the south.

The last quadrilateral (Quad Q3) extends from northeast of the belt of shear zones into the belt of shear zones. The northeast side of the quadrilateral stretched significantly, $1x10^{-3}$; the reason is unclear. The northwest and southeast sides also stretched large amounts, 1 to $2x10^{-2}$, apparently reflecting large right-lateral shearing. The minor northeastward thrusting visible in the belt of shear zones apparently was overwhelmed by the right-lateral shearing. The right-lateral shearing is also reflected in the shortening of the north-south brace and the lengthening in the east-west brace.

In summary, at the three levels of observation, (~10 km, 1 km, 0.1 km lengths), normalized length changes provide insight into the intensity and style of deformation. In the far-field, as measured by trilateration and GPS, principal extensions are in the range of 7 to $9x10^{-5}$. On both sides of the rupture belt in the far field, the deformation is left-lateral shear that is generally parallel to the belt of surface rupture. Re-survey of pre-earthquake bench marks near Tortoise Hill indicates that the deformation is generally below the limit of survey accuracy ($\sim 3x10^{-4}$) everywhere except where points cross a belt of surface rupture. The braced quadrilaterals spanning Tortoise Hill gave essentially the same result; normalized length changes were smaller than $3x10^{-4}$ except where quadralaterals cross faults. Normalized length changes were in agreement with the kinematic expression of fractures in the bounding shear zones.

Differential Displacements

Horizontal Displacements

The results of the land surveys also determine relative horizontal displacements assuming that one of the control points and the direction of a line element remained fixed. Because of probable errors in the survey farther south, we selected the southeast corner of Section 36, T7N R3E to be fixed and the orientation of the line between that corner and the control point immediately to the west (NE corner, Section 1) to be fixed. Then we followed the survey northward to determine displacements relative to these references. The horizontal displacements appear to be smaller than the error level south of Section 25 (T7N R3E).

The horizontal displacements are known primarily along the eastern and western section lines. Starting with the eastern section line, and the point farthest north (midheight of Section 24, T7N R3E), as well as its two neighbors to the south, the displacement is 3 to 3.1 m, right-lateral, roughly parallel to the northeast edge of the Emerson fault zone (Plate 1). This value is slightly larger than the value of differential displacement of 2.9 m we determined by sighting along legs of towers of the Single-Tower Transmission Line in Section 23, to the northwest (Appendix I). The next control point along the eastern side is immediately south of the main rupture zone along the northeast side of Tortoise Hill. That point and control points farther south have been displaced horizontally by negligible amounts, less than about 20 cm. Both the amounts and the directions for those points appear to be random (Appendix II).

The northernmost control point along the western section line is within the belt of shear zones, which, here, is about 50 m wide (Plate 2). The relative horizontal displacement is 0.6 m, directed about 30° east of south. Thus the horizontal displacement is oblique to the northeast wall of the rupture zone but roughly parallel to the southwest wall, which passes around the southwest side of Tortoise Hill ridge. The horizontal displacement of the control point immediately to the south is at the margin of error, about 0.2 m, and is toward the east. The horizontal displacements of control points farther south along the western section line apparently are negligible.

One of the control points is in the center of Tortoise Hill, at mid-length along the southern border of Section 24. The horizontal displacement here, relative to the assumed fixed point is 0.8 m south. This displacement is quite interesting because it reflects the combination of right-lateral differential displacement and southwest thrusting of the block of Tortoise Hill, presumably accommodated mainly by the belt of shear zones that passes around the southwest side of Tortoise Hill.

Differential horizontal displacements were determined relative to quadrilateral points assumed to be fixed immediately southwest Tortoise Hill (fig. 12 and Table 1). The two corners on the southwest end of the ladder of quadrilaterals (Q2-C & D), one of which moved upwards 0.21 m and the other 0.26 m (Plate 4), are points C on the right and D on the left in Table 1. Point A is in the upper left and point B is the upper right of quad Q2. Movement relative to points Q2-C & D is partitioned into components parallel and normal to the fault zone.

According to the bottom part of Table 1, the movement of point A of Quadrangle Q2 was δv=–0.18 m and δu=0.13 m. In combination with the data shown in Plate 4, point A thus moved vertically upward (δz) about 0.72 m, moved to the southeast about 0.13 m (δu), right-lateral, and southwest 0.16 m (δv), thrusting. Point B moved

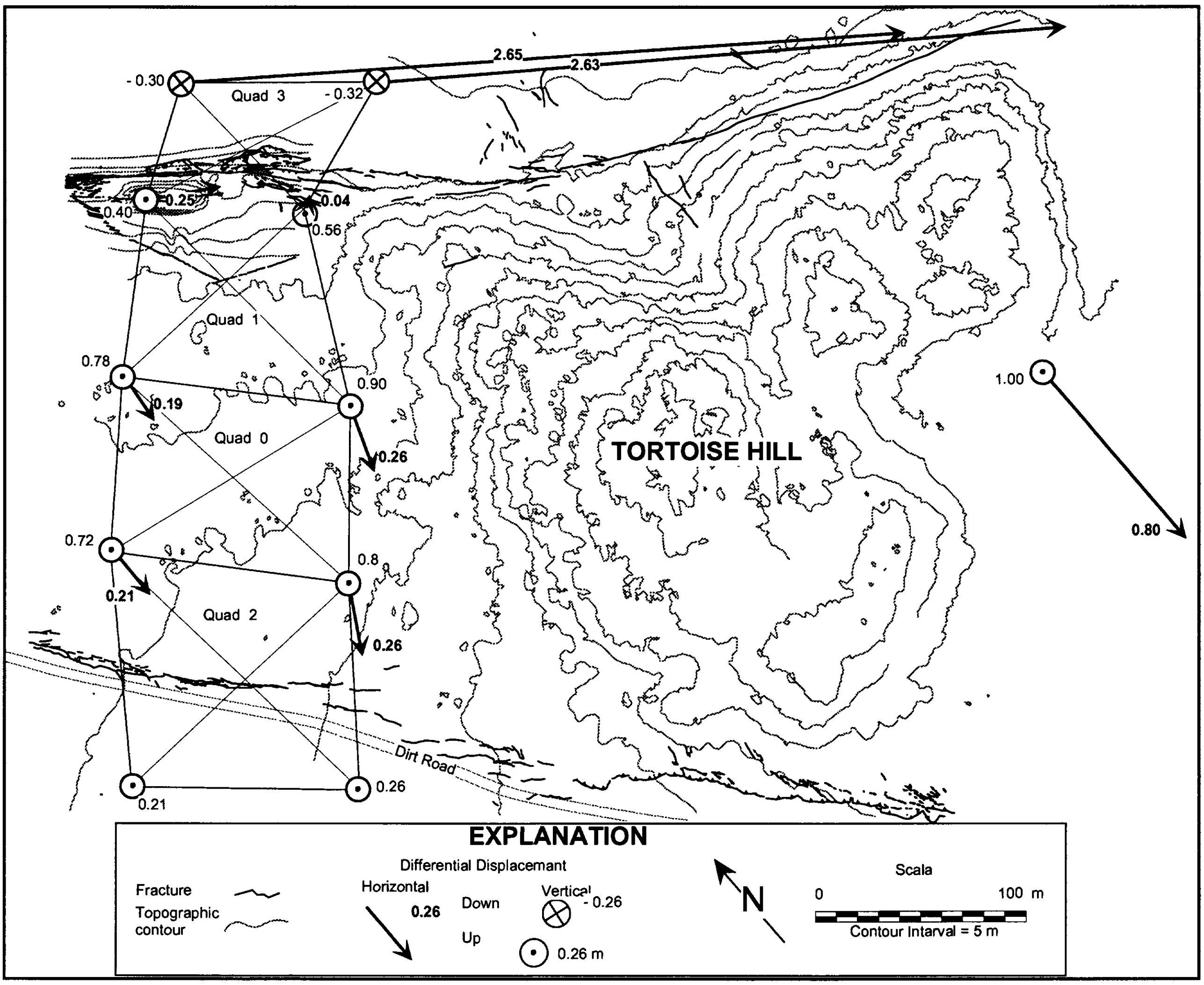

Figure 12. Map showing fractures bounding margins of Tortoise Hill ridge and differential displacements measured photogrammetically. A ladder of quadrilaterals extends across the ridge. At southeast edge, displacements were measured by land survey of regional grid. Maximum horizontal shift across ridge about 2.65 m. Maximum vertical displacement, relative to an assumed fixed point about 6 km south of ridge, is 1.0 m at center of ridge.

Table 1. Horizontal Displacements of Corners of Quadrilaterals

(Measurements in meters, relative to corners C and D on southwest side of Tortoise Hill ridge).

Quad.	Corner	δu (+SE -northwest) (Parallel to fault)	δv (+NE -SW) (Normal to fault)	Corner	δu	δv
	A	2.64	0.18	B	2.62	0.21
3						
	D	0.24	0.05	C	0.01	0.04
	A	0.24	0.05	B	0.01	0.04
1						
	D	0.11	–0.16	C	0.09	–0.24
	A	0.11	–0.16	B	0.09	–0.24
0						
	D	0.13	–0.16	C	0.05	–0.26
	A	0.13	–0.16	B	0.05	–0.26
2						
	D	0	0	C	0	0

similarly, 0.81 m vertically, 0.05 m right-lateral and 0.26 m of thrusting (δv=–0.26 m and δu=0.05 m). As indicated in Table 1, point C and D of quad 0 are the same as points A and B of quad 2.

Thus, according to the photogrammetric measurements (Table 1), the strike-shift across the entire ridge is 2.62 to 2.64 m, and most of this is accommodated on the main shear zone on the northeast side of the ridge. This leaves about 0.4 m of right shift that we measured with our resurvey of bench marks unaccounted for, but presumably it is distributed northeast or southwest the ladder of quadrilaterals.

The photogrammetric measurements also provide rather detailed information about the horizontal dilation of rock within the ridge. According to the photogrammetric measurements, there was net dilation of between 0.18 and 0.21 m between the most distant points outside the ridge, as measured from corner D of Q2 to corner A of Q3 and from corner C of Q2 to B of Q3, respectively. The dilation is somewhat larger for the most distant points within the ridge, between 0.21 and 0.30 m, as measured from corner A of Q2 to corner D of Q3 and from corner B of Q2 to corner C of Q3. The dilation within the ridge is expressed in part by a reverse fault dipping about 45° toward the northeast on the southwest side of the ridge and a very high angle reverse fault dipping about 86° toward the southwest on the northeast side of the ridge. These faults, though, do not account for the net dilation of 0.18 to 0.21 m for points outside the ridge.

Vertical Displacements

In late spring 1995, surveyors Kelley and Quinn from SoCalEd also releveled all the points that could be relocated. This included the network of control points for the northern half of Section 12 near Bessemer Mine Road, through Sections 1, 36, 25, over Tortoise Ridge, to the middle of Section 24 northeast of the ridge as well as all the wing points (wooden stakes) that we could find on either side of the line of sections (fig. 13 and Plate 1). They releveled along the same paths followed by the survey crew at the time of the first leveling in 1973 and 1976. The data are discussed in Appendix II.

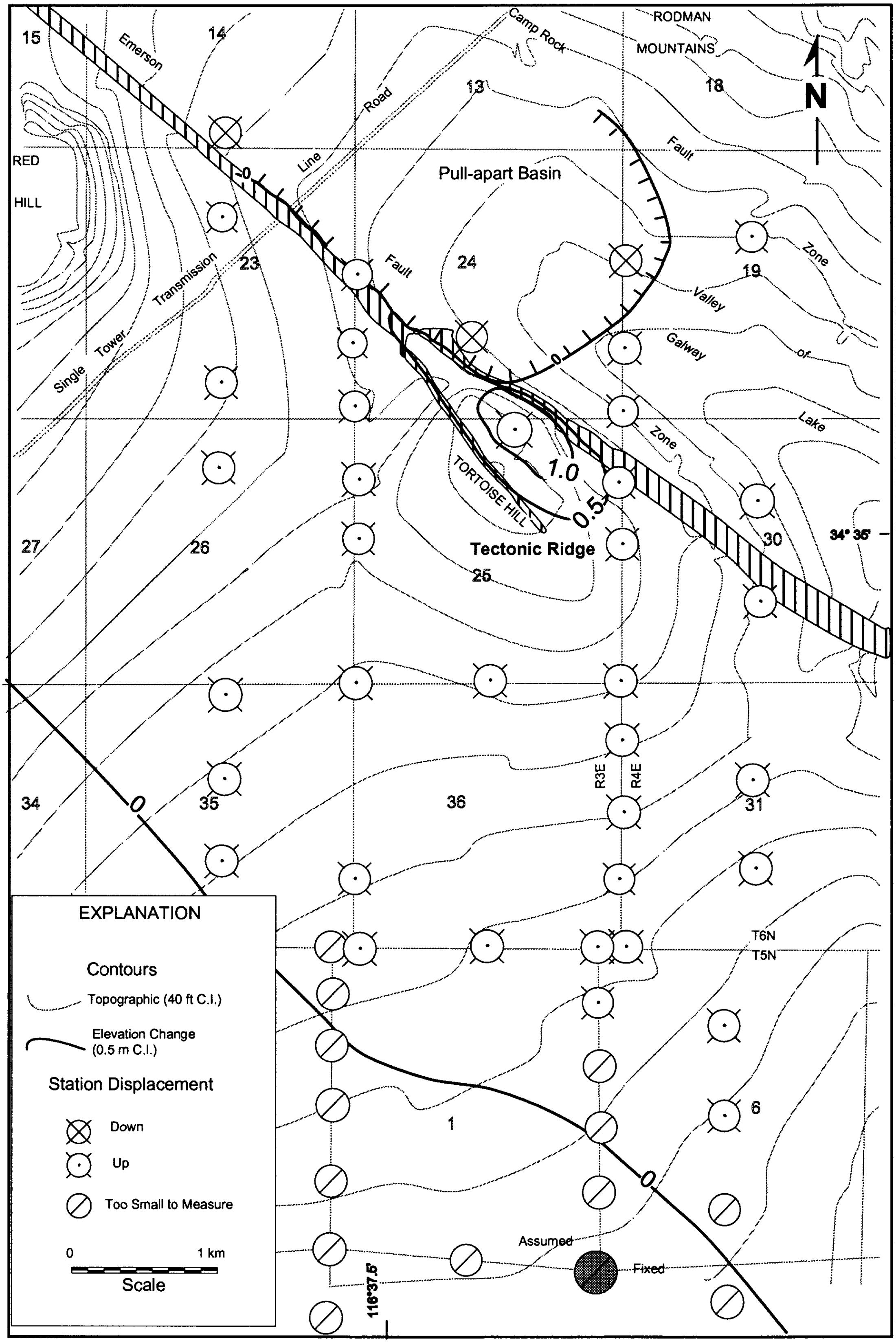

Figure 13. Contours of vertical displacement, relative to a point (large shaded circle) near Bessemer Mine Road, showing concentrated uplift at Tortoise Hill ridge, within Emerson fault zone. Land survey control points, surveyed in 1973 and 1994, shown with circles. Circles with cross (arrow moving away from observer) indicate downward movement. Circles with dot (and tips of feathers) indicate upward movement (arrow moving toward observer).

We have contoured the changes in altitude of control points and wing points, assuming that the point at the southeast corner of Section 1, T5N R3E did not change altitude. The changes in altitude are marked beside the diamond-shaped symbols representing the control or wing points in Plate 1. We have put three contours on the map with heavy lines, for 0 m, 0.5 m and 1.0 m of vertical uplift. The 0 m contour in the south was placed by interpolating the data and drawing a contour at 0.01 m and then offsetting the 0 m contour slightly to the southwest of it. Then we removed the 0.01 m contour. According to our results, the entire area south of the 0 m contour changed altitude insignificantly; the measurements indicate that we are ignoring changes in altitude smaller than 2 cm. Note in Table II-1 that this limit is about half the largest closure error for an entire level line.

The map with three solid contours of vertical uplift (fig. 13) is the main result of the regional leveling. In this contour map we see a highly localized uplift of Tortoise Hill ridge. The ridge was pushed upward about 1 m as about 3 m of right-lateral shift was accommodated across the Emerson fault zone during the Landers earthquake.

We can see more details of the uplift if we interpolate some intermediate contours, especially if we add some data from the photogrammetric analysis of quadrilaterals shown in Plate 4. The changes in altitude are indicated at corners of quadrilaterals in Plate 4. There we fixed the change in altitude of the western corner of Quad Q2 with the regional data presented in Plate 1. The more detailed map shows uplift of about 0.25 m at the southwest edge of the ridge, then further uplift to 0.7 to 0.8 m inside the belt of shear zones on the southwest side of the ridge, to about 0.8 to 0.9 m at mid-width of the ridge, and then back down to zero on the northeast side of the ridge. The ground northeast of the ridge appears to have been downdropped at least as much as 0.3 m. All these data are consistent with an uplift of 1.0 m at the control point in the middle of the ridge, shown at the right-hand edge of Plate 4. Thus we see in more detail how the 1 m of uplift was distributed across the width of the ridge.

Using both sets of data, the regional survey, and the photogrammetric survey of part of the ridge, we have constructed the map of contours of uplift shown in figure 13 and Plate 1. The regional pattern is an abrupt uplift of the ridge within the bounds of the surrounding belts of shear zones. Where the belt of shear zones on the southwest side of the ridge ends, the uplift of the ridge is less spectacular, but not absent. Thus, the greatest growth of the ridge is an elliptically-shaped domical area centered on the high ground of Tortoise Hill ridge. There the differential growth relative to the tilted surface to the southwest is about three-quarters of the total, or 0.7 to 0.8 m.

There is significant uplift (0.33 to 0.35 m) at wing points east and southeast of the ridge, suggesting that an area of unknown shape extends from Tortoise Hill in that direction. There is another topographic ridge about 3 km southeast of Tortoise Hill Ridge, bounded on the east by the Emerson fault zone, but we do not know whether it grew during the 1994 earthquake.

Another striking feature of the map of contours of altitude change in Plate 1 is a broad trough underlying the valley northeast of Tortoise Hill, between Tortoise Hill and Rodman Mountains to the northeast. The trough probably is a reflection of a pull-apart basin forming where the shift across the Emerson fault zone is decreasing and the shift across the Camp Rock fault zone is increasing. We described some of the tension cracks associated with about a 1 m transfer zone near the single-tower powerline near the northwest edge of the map in Plate 2.

There are other, more subtle, features in the contour map of uplift. One is a bench or very shallow trough in Sections 23, 25 and 26 (T6N R3E), just southwest Tortoise Hill ridge. Another is a decrease in the decrease of changes of altitude to the southwest. The slope of the uplift is very steep at the southwest edge of Tortoise Hill ridge. Near its edge, there is a belt where there is a change in altitude of 10 cm over a horizontal distance of about 50 m. In a much broader belt passing through Sections 23, 25 and 31, there is a 10 cm change in altitude over a horizontal distance of about 1 km. In an even broader belt to the south, between the 0.1 m and 0 m contours, the change is 4 to 5 cm in altitude over a horizontal distance of 1 km. The uplift, then, is not linear, it is essentially an exponential function of distance measured from the southwest toward the belt of shear zones on the southwest side of the ridge.

Summary and Discussion

Magnitudes of Displacements

The repeated land survey determined that 3.0 to 3.1 m of right-lateral, horizontal differential displacement was accommodated across Tortoise Hill relative to a fixed point southwest the ridge. It showed that the center of the ridge moved upward 1.0 m relative to the same reference. The same point moved about 0.57 m in a right-lateral sense. A point within the narrower belt of shear zones northwest of Tortoise Hill moved about 0.6 m in a right-lateral sense and was uplifted about 0.3 m.

The photogrammetric survey with a ladder of braced quadrilaterals shows how the vertical and horizontal displacements are distributed across Tortoise Hill, and show that the ground in the valley to the northeast moved downward, as much as 0.3 m, presumably reflecting the growth of a pullapart basin in that area (Plate 1).

Magnitudes of Strains

With the different methods of determining normalized length changes, we see a range of three orders of magnitude, from about 10^{-2} within the belt of shear zones of the Emerson fault zone on the northeast side of Tortoise Hill ridge, to about 10^{-3} within the belt of shear zones on the southwest side of Tortoise Hill ridge, to about 10^{-5} in ground to the north and south of the Emerson fault zone. The larger normalized length changes largely reflect right-lateral, permanent shearing within the Emerson fault zone whereas the smaller normalized length changes reflect left-lateral, elastic shearing of ground, apparently partly unloaded by a stress drop across the Emerson fault zone.

Our most detailed measurements are those made with quadrilaterals spanning Tortoise Hill. The measurements of normalized length changes develop a picture of belts of shear zones on either side of the ridge accommodating most of the right-lateral, permanent horizontal deformation that occurred here during the Landers earthquake. The measurements show that the ridge accommodated about 2.7 m of the total amount of 3.0 to 3.1 m of permanent right-lateral shearing across the belt of shear zones. Of the 2.7 m, a small part was distributed across the rupture zone bounding the southwest side of the ridge but most of it was distributed across the rupture zone bounding the northeast side of the ridge. The measurements normal to the belt of shear zones indicate that the ridge accommodated about 0.2 m of net dilation, between points outside the ridge on the southwest and points outside the ridge on the northeast. The dilation was slightly larger, about 0.25 m, for points most widely separated but within the ridge. The larger internal dilation is probably largely a result of thrusting along the southwest side of the ridge. However, the horizontal displacement of the control point for the land survey in the center of Tortoise Hill shows the same result, 0.8 m of movement of the ground of Tortoise Hill directly southward relative to a fixed point about 6 km south along Bessemer Mine Road (Plate 1).

The lack of measurable (larger than 3×10^{-4}) normalized horizontal length changes within the quadrilateral (Q0) near the center of Tortoise Hill shows that the deformations within the center of the Tortoise Hill were very small. Plate 4 shows a few of the elements of aplite dikes in the monzogranite of Tortoise Hill; these were mapped from the aerial photographs, and the numbers and extent of dikes are a minimum of what is there. The continuity of the dikes indicates that Tortoise Hill consists of relatively large, unfaulted blocks, not merely broken, sheared rock, again suggesting that the differential displacements are concentrated in the rupture zones on either side of the ridge.

The land survey mainly established that the measurable values of normalized length changes are smaller than about $3x10^{-4}$ southwest Tortoise Hill.

Subsurface Forms of Belts of Shear Zones

The subsurface form of the belt of shear zones and tectonic ridge at Tortoise Hill is, of course, unknown. We know of only two sets of observations that are relevant to subsurface conditions here. One is indirect evidence of zones 50 to 200 m wide at depths as great as 10 km that trapped seismic energy along the Homestead Valley and Johnson Valley belts of shear zones at Landers (Aki, 1994; Li and others, 1994a, 1994b). The other is the documentation of *flower structures* along some strike-slip faults. Flower structures have been described in seismic images of strike-slip fault zones (Harding and Lowell, 1979; Harding, 1983; Harding and others, 1983; D'Onfro and Glagola, 1983; Plawman, 1983) and in rifts (Genik, 1993; Roberts, 1983). They have a diagnostic branching appearance, from a supposed single branch at depth (generally many kilometers) to two branches above, and then four and so forth as the flower structure approaches the ground surface. The branching structures do not appear in vertical seismic sections of simple thrusting or extensional regimes (e.g., Bally, 1983). Flower structures appear to be complex in vertical sections because a vertical section of a strike-slip fault that is normal to the trace of the fault is a secondary view. A map view of a strike-slip fault is the principal view.

Observations Relevant to Mechanisms of Tectonic Ridge Formation

Several mechanisms have been suggested for the formation of tectonic ridges (and push ups) as well as analogous ridges known as *flank ridges* in large landslides. Tectonic ridges have been described many times (e.g., Sibson, 1980; Segall and Pollard, 1983; Aydin and Page, 1984; Sylvester, 1988; Bilham and King, 1989; Scholz, 1990). Flank ridges were described in several landslides in Utah by Fleming and Johnson (1989) and by Baum and others (1988a and 1988b) and the Slumgullion landslide in Colorado (Fleming and others, 1996).

Our observations at Tortoise Hill ridge at Landers provide some detailed information about the growth of a tectonic ridge:

1. Fractures define a broad belt of shear zones along the part of the Emerson fault zone that ruptured during the Landers earthquake, extending from somewhat north of the Single-Tower Transmission Line to at least the southern end of Tortoise Hill (Plates 1 and 2). The amount of right-lateral shift ranges from 2.9 m at the powerline to about 3.1 m at the southeast end of Tortoise Hill ridge.

2. Horizontal deformations in the vicinity of the Emerson fault zone show left-lateral shearing in rocks even a few hundred meters on either side of the belt of shear zones, representing stress drop and elastic rebound, and right-lateral shearing and probably dilation within Tortoise Hill ridge, reflecting permanent ground deformation within the belt of shear zones.

3. Differential vertical displacements show that Tortoise Hill ridge grew about 1 m in height much as an elongated dome centered on the highest point within the ridge as the Emerson fault zone accommodated about 3 m of right-lateral shift.

4. The elongate-dome-shaped region of growth is bounded on the northwest and southeast sides by belts of shear zones, accommodating both right-lateral and differential vertical shift.

5. Although the uplift of ground was largely concentrated in the ridge, the ground extending for at least 3 km southwest of the ridge was bent upwards. The ground is not merely tilted because the slope of the change in elevation increases as the southwest side of the ridge is approached from several kilometers away.

6. The present topography and geology of Tortoise Hill reiterates and echoes the growth that occurred during the 1992 earthquake (fig. 4). The northeast face of the ridge is steep and rugged where it rises abruptly above the valley of Galway Lake. The southwest face is much lower and extends only about 20 m above the pediment-like rock surface farther to the southwest the ridge. Most of the differential vertical displacement was on the steep, northeast side of the ridge. Sub-vertical scarps there are up to a meter high. The scarps of the low-angle reverse faults on the southwest side of the ridge are only a few tens of centimeters high.

7. Tortoise Hill contains spines of monzogranite near the northeast-bounding shear zone that appear to have been pushed upward differentially.

The measurements and observations at Tortoise Hill can be supplemented with data from landslides to identify potential mechanisms of ridge formation. Observations of map and cross-sectional views of flank ridges in landslides, documentation of differential displacements and strains within one ridge in the Aspen Grove landslide in Utah, and examination of maps of other ridges in that area suggest that there are several potential mechanisms of ridge formation (Fleming and Johnson, 1989).

Steps, Jogs or Bends

Tectonic ridges and push ups have been widely reported (e.g. Aydin and Page, 1984) to occur at opposite steps, jogs or bends along faults (i.e. restraining structures). An opposite bend or step would be a left step, jog, or a left bend in a right-lateral and would be a right step, jog, or a right bend in a left-lateral strike-slip fault. Our observations of structures that form at opposite steps at various places at Landers and in large landslides suggests that the main phenomena of restraining steps are near-surface phenomena such as folding or thrusting rather than the phenomena of ridge formation or another deeper, larger-scale process. For example, the small restraining bend between the second and third elements of the bounding rupture zone near the northwest end of Tortoise Hill produced compression structures. The two elements differ in strike by 10°, and, adjacent to the stepover zone between the elements there was a small dome and tension cracks on the southwest side and thrust faulting on the northeast side of the rupture belt (see left side of Plate 4).

The same was true in landslides. We generally saw low domes or thrust faults at opposite or restraining steps; we did not see ridges at such places (Fleming and Johnson, 1989). The structures that formed at restraining bends in flanks of landslides were restricted to the moving ground; non-moving ground outside the flanks did not contain the compressive structures. The ridges we saw in the landslides were fault-parallel and typically along straight stretches of rupture zones. In fault rupture, however, we note that the compressive structures are on both sides of the mis-aligned elements in the rupture zone.

Although there is no question that localized compression will be developed in ground in an area with an opposite step along a strike-slip fault, the importance of opposite steps in the formation of tectonic ridges remains to be demonstrated. Relations between the size, type, position, and orientation of the compressive features and the geometry of the constraining structure remain unresolved.

Dilatancy

The ridges, both in landslides and along faults, could result from dilatancy of rocks in shear zones (Johnson, 1995). We note that strike-slip faulting commonly occurs in belts of shear zones rather than across single fault surfaces, so ridges could be associated with the belts of shear zones rarther than individual fault strands.

The growth of several ridges along the flanks of landslides in Utah and Colorado might be analogous to ridge formation along strike-slip faults (Fleming and Johnson, 1989; Fleming and others, 1996). Specifically, our observations of ridges in landslides and along strike-slip faults lead us to suggest the following:

1. Ridges occur within belts of shear zones along faults with predominant strike-shift differential displacements. In the case of landslides, the belts of shearing are within the active landslide debris as are the ridges, but they are adjacent to the bounding or internal fault zones, not within non-deforming debris. In the case of tectonic ridges we have examined, the ridges are within a belt of shear zones.

2. The belts of shear zones occur at depth as well as at the ground surface.

3. Ridges are a result of localized increase in pressure and volume within the belts of shear zones beneath the ground surface. The increase in pressure and volume pushes the ground upward within the ridge.

4. The increase in pressure and volume can be a result of positive dilatancy of the fractured rock within the belt of shear zones beneath the ground surface (e.g., Johnson, 1995).

5. Some ridges form in certain materials that occur within belts of shear zones. The materials that produce ridges translate along the fault zone as the ridge grows, carrying the causative mechanism with them, and growing as a dome that presumably has roughly the area of the horizontal area of the mass of dilatant materials below. Where ridges are a result of dilatation, they have a finite period of growth because the material eventually dilates to a constant state volumetrically.

In contrast, if ridges were a result of a step or similar irregularity in the shape of a single fault, they would grow essentially at a point and then be translated away from the causative step and be dormant thereafter. The causative mechanism would be static. The active part of the ridge should be at one end of the ridge.

Wedging

Another mechanism for producing ridges is suggested by three observations: Tortoise Hill and some other tectonic ridges in the Landers area have an enveloping belt of shear zones. Flower structures at depth have been identified along some strike-slip faults with seismic exploration techniques. Finally, faults typically are straight in the direction of fault slip but are highly curved in the direction normal to the direction of slip. For example, normal and reverse faults are characterized by highly irregular and sinuous surface traces, but strike-slip faults are characterized by relatively straight surface traces. Thus we would expect the Emerson fault zone to have a highly sinuous trace if we would examine it in vertical section. A change in the sinuous trace with horizontal position near the ground surface could cause the ground to rise or fall near the trace of the fault.

The overall form of Tortoise Hill ridge is a wedge-shape, both in plan and, presumably, in cross section (fig. 14C). The dip of the bounding faults near the ground surface indicates that they would converge at depth. As shown in Plate 1, or especially Plate 2, the plan view of the northwest part of Tortoise Hill is a wedge, bounded on the northeast by the main rupture zone and on the southwest by the thrust/right-lateral rupture zone. The latter rupture zone is a splay that diverges from the main rupture zone. The trace of the trace of the splay is oriented with a clockwise trend with respect to the trend of the main, right-lateral, rupture zone on the northeast, in the sense that G K. Gilbert noted for faults along the surface rupture north of San Francisco following the 1906 earthquake and along normal faults in Utah (Gilbert, 1928, p. 13).

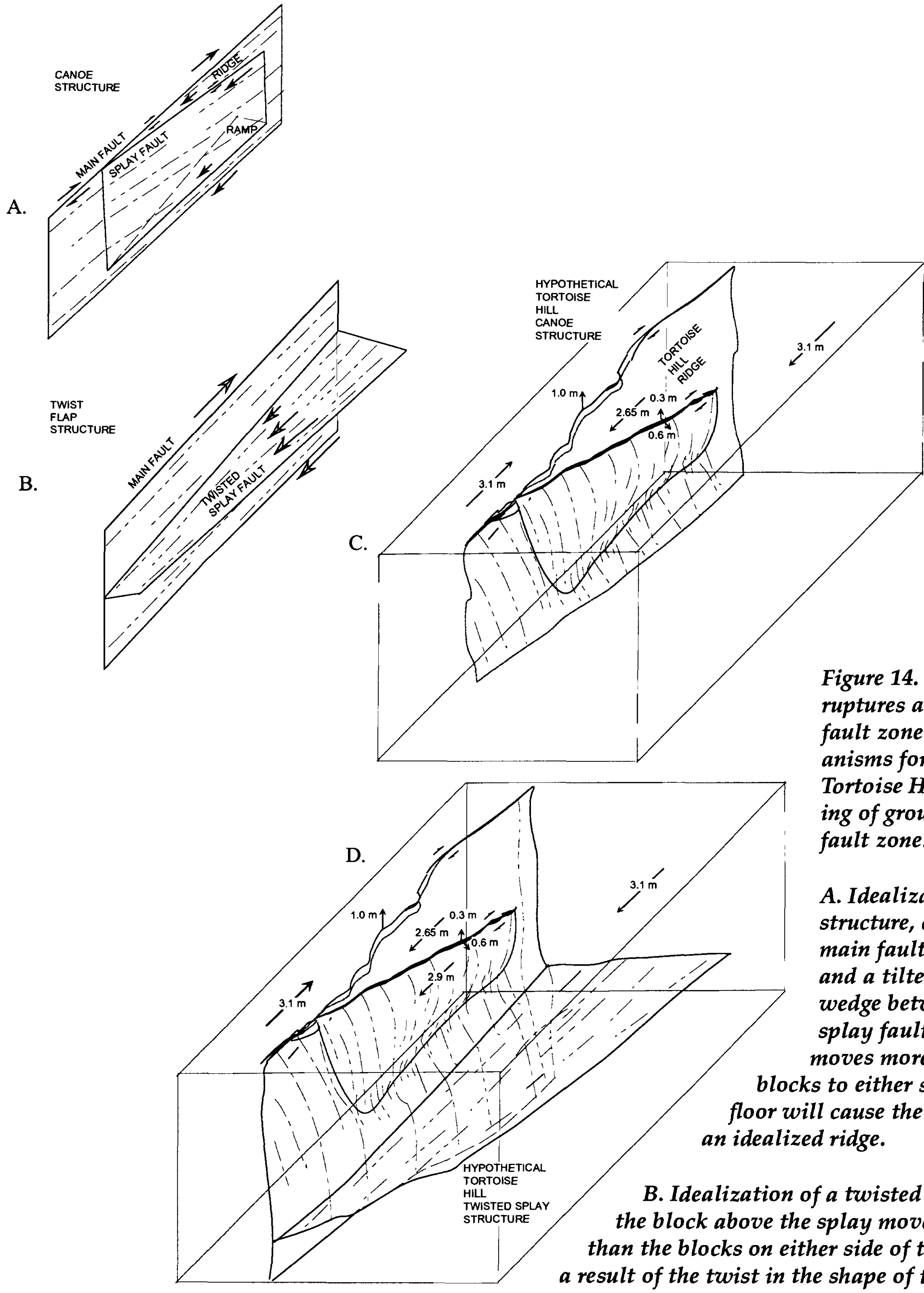

Figure 14. Idealizations of ruptures along Emerson fault zone suggesting mechanisms for growth of Tortoise Hill ridge and tilting of ground southwest of fault zone.

A. Idealization of canoe structure, consisting of a main fault, a splay fault, and a tilted floor of the wedge between the main and splay faults. If the wedge moves more slowly than the blocks to either side, the sloping floor will cause the wedge to rise, as an idealized ridge.

B. Idealization of a twisted splay. The part of the block above the splay moves more slowly than the blocks on either side of the main fault. As a result of the twist in the shape of the splay, part of the block near the fault tilts.

C. Idealization of proposed canoe structure beneath Tortoise Hill ridge.

D. Idealization of proposed twisted splay at deeper level beneath Tortoise Hill ridge.

Figure 14C shows Tortoise Hill interpreted as a simple flower structure, a wedge, within a belt of shear zones. The idealized mechanism of growth is illustrated in figure 14A. The mechanism has two essential parts, one geometric and the other kinematic. The geometric part is a sloping base or bottom of the wedge. The kinematic part is that the wedge moves more slowly than the block of ground on the same side of the main rupture. Specifically applied to Tortoise Hill, the block of ground to the east (left in fig. 14A) has a relative displacement toward the south. The block of ground to the west, except for the wedge, has the same relative displacement, but toward the north. The wedge has a smaller relative displacement toward the north. Thus the wedge is lifted as the block to the west moves beneath it.

At Tortoise Hill, the wedge is imagined to be shaped like half of a sway-backed canoe, with the front of the canoe deeper than the midlength. Thus, since Tortoise Hill moves more slowly, relatively, northwesterly, than the ground to the southwest, the hill rises, forming a tectonic ridge.

An appealing feature of this explanation of the growth of Tortoise Hill ridge, besides that it is consistent with the field observations and measuements, is that the same basic mechanism can explain the tilting of the pediment to the southwest of the ridge. If there is a deeper splay within the flower structure, perhaps nearly horizontal, but twisted about an axis parallel to the main fault, the same differential displacements discussed above would produce a tilting of the ground. The basic mechanism is illustrated in figure 14B and its application to Tortoise Hill is suggested in figure 14D.

Other reasons we favor this mechanism for some ridges is that ridges within wedge-like intersections of a main fault and a splay fault along right-lateral, strike-slip faults have been mapped throughout the Landers area. There are several along the Emerson fault zone next to Emerson Lake, one along the Calico fault zone about 8 km northeast of Tortoise Hill, and two along the Johnson Valley fault zone near Melville Lake (Dibblee, 1964, 1967a, 1967b). Finally, the proposed splay faults are similar to simple flower structures observed in seismic profiles of strike-slip and rifting areas throughout the world (e.g., Harding, 1983; Harding and Lowell, 1979; Harding and others, 1983; D'Onfro and Glagola, 1983; Genick, 1993).

Final Comments

We have identified geometric and material property conditions that could produce tectonic ridges. An opposite step or bend in a fault produces compression that may produce a dome and thrust faults and perhaps even a ridge. A dilative material in a broad shear zone near the ground surface could develop sufficient pressure at depth to intrude more mobile material at depth and extrude some material onto the ground surface. This is an important mechanism of ridge-formation in landslides, and may well be important along some faults. Simple flower structures within strike-slip fault zones that change shape along strike could produce tectonic ridges and tilt the ground on either side of a fault zone.

Presumably ridges can form in all these ways and it would be foolish to think there are not other ways. There is no reason to believe that structures with the one name must be produced by only one mechanism. In landslides, for example, we have not noticed ridges that have formed at splays of the main bounding shear zone. At Landers, many of the tectonic ridges occur between a splay and a main rupture zone. Perhaps many of these formed by wedging. But not all tectonic ridges occur adjacent to a splay.

Only the splay mechanism specifically addresses the tilting of the ground to form a pediment-like slope southwest the fault zone (Plate 1).

We have stretched our observations and survey data to and perhaps beyond logical limits in the search for a process model for ridge formation. Indeed, many of the survey measurements are near or below the threshold of accuracy. The data presented here do constrain various mechanisms of formation but do exclusively identify one. The most important outcome of this investigation is in the GPS/trilateration, survey, and photogrammetric data that provide an internally consistent description of real-time tectonics. The fractures, the displacement, the normalized length changes, and the vertical changes are each part of the larger deformational picture of a small part of the rupture zone that has heretofore been lacking in neotectonics. The integration of these different kinds of data dramatically illustrates the interrelationships between fracture orientations and kinematics with the measurable deformations.

References Cited

Aki, K., 1994, Seismological expressions of the fine scale structure of fault zones [abs.]: Baltimore, Maryland, Program of AGU Spring Meeting, p. 106.

Aydin, A., and Page, B.M., 1984, Diverse Pliocene-Quaternary tectonics in a transform environment, San Francisco Bay region, California: Geological Society of America Bulletin, 95, p. 1303-1317.

Bally, A.W., 1983, Seismic expression of structural styles—A picture and work atlas: American Association of Petroleum Geologists, Studies in Geology, Series 15, four volumes.

Baum, R.L., and Fleming, R.W., 1991, Use of longitudinal strain in identifying driving and resisting elements in landslides: Geological Society of America Bulletin., 103, p. 1121-1132.

Baum, R.L., Fleming, R.W., and Ellen, S.E., 1989, Maps showing landslide features and related ground deformation in the Woodlawn area of the Manoa Valley, City and County of Honolulu, Hawaii: U.S. Geological Survey Open-File Report 89-290, 16 p.

Baum, R.L., Fleming, R.W., and Johnson, A.M., 1988a, Kinematics of the Aspen Grove landslide, Ephraim Canyon, Central Utah: U.S. Geological Survey Bulletin 1842F, 34 p.

Baum, R.L., Johnson, A.M., and Fleming, R.W., 1988b, Measurement of slope deformation using quadrilaterals: U.S. Geological Survey Bulletin 1842B, 23 p.

Bilham, R., and King, G., 1989, The morphology of strike-slip faults; examples from the San Andreas fault, California: Journal of Geophysical Research, 94, p. 10204-10216.

Cruikshank, K.M., Zhao, G.Z., and Johnson, A.M., 1991, Duplex structures connecting fault elements in Entrada Sandstone: Journal of Structural Geology, 13, p. 1185–1196.

D'Onfro, P., and Glagola, P., 1983, Wrench fault, southeast Asia, *in* Bally, A.W., ed., Seismic expression of structural styles: Bulletin of the American Association of Petroleum Geologists, 4.2, p. 9-12.

Dibblee, T.W., Jr., 1964, Geologic map of the Rodman Mountains Quadrangle, San Bernardino County, California: Miscellaneous Investigation Map I-430.

Dibblee, T.W., Jr., 1967a, Geologic map of the Emerson Lake Quadrangle, San Bernardino County, California: Miscellaneous Investigation Map I-490.

Dibblee, T.W., Jr., 1967b, Geologic map of the Old Woman Springs Quadrangle, San Bernardino County, California: Miscellaneous Investigation Map I-518.

Fleming, R.W., and Johnson, A.M., 1989, Structures associated with strike–slip faults that bound landslide elements: Engineering Geology, 27, p. 39–114.

Fleming, R.W., Baum, R.L., and Savage, W.Z., 1996, The Slumgullion landslide, Hinsdale County, Colorado: Geological Society of America, Guidebook for Field Trips, 21 p.

Frazer, C.S., and Gruendig, L., 1985, The analysis of photogrammetric deformation measurements on Turtle Mountain: Photogrammetric Engineering and Remote Sensing, 51, p. 207-216.

Genik, G.J., 1993, Petroleum geology of Cretaceous-Tertiary rift basins in Niger, Chad, and Central African Republic: Bulletin of the American Association of Petroleum Geologists, 77, p. 1405-1434.

Harding, T.P., 1983, Divergent wrench fault and negative flower structure, Andaman Sea, *in* Bally, A.W., ed., Seismic expression of structural styles: Bulletin of the American Association of Petroleum Geologists, 4.2, p. 1-8.

Harding, T.P., and Lowell, J.D., 1979, Structural styles, their plate-tectonic habitats, and hydrocarbon traps in petroleum provinces: Bulletin of the American Association of Petroleum Geologists, 63, p. 1016-1058.

Harding, T.P., Gregory, R.F., and Stephens, L.H., 1983, Convergent wrench fault and positive flower structure, Ardmore Basin, Oklahoma, *in* Bally, A.W., ed., Seismic expression of structural styles: Bulletin of the American Association of Petroleum Geologists, 4.2, p. 13-17.

Hudnut, K.W., and many others, 1994, Co-seismic displacements of the 1992 Landers earthquake sequence: Bulletin of the Seismological Society of America, 84, p. 625-645.

Jennings, C.W., 1973, State of California, Preliminary fault and geologic map, south half, scale 1:750000: California Division of Mines and Geology, Preliminary Report 13.

Jennings, C.W., 1994, Fault Activity Map of California and Adjacent Areas: California Division of Mines and Geology, Geologic Data Map no. 6, scale 1:750,000.

Johnson, A.M., 1995, Orientations of faults determined by premonitory shear zones: Tectonophysics, v. 247, p. 161–238.

Johnson, A.M., and Fleming, R.W., 1993, Formation of left-lateral fractures within the Summit Ridge shear zone, 1989 Loma Prieta, California, earthquake: Journal of Geophysical Research, 98, p. 21,823-21,837.

Johnson, A.M., Fleming, R.W. , and Cruikshank, K.C., 1993, Broad Belts of Shear Zones as the Common Form of Surface Rupture Produced by the 28 June 1992 Landers, California, earthquake: U.S. Geological Survey Open-File Report 93-348, 61 p.

Johnson, A.M., Fleming, R.W., Cruikshank, K.M., Martosudarmo, S.Y., Johnson, N.A., Johnson, K.M., and Wei, W., 1997, Analecta of structures formed during the 28 June 1992 Landers-Big Bear, California, earthquake sequence: U.S. Geological Survey Open-File Report 97-94, 67 p., 7 plates.

King, N.E., and Savage, J.C., 1983, Strain-rate profile across the Elsinore, San Jacinto and San Andreas faults near Palm Springs, California, 1973-81: Geophysical Research Letters, 10, p. 55-57.

Li, Y.G., Vidale, J.E., Aki, K., Marone, C.J., and Lee, W.H.K., 1994a, Fine structure of the Landers fault zone: Elementation and the rupture process, Science, 265, p. 367-370.

Li., Y.G., Aki, K., Adams, D., and Hasemi, A., 1994b, Seismic guided waves trapped in the fault zone of the Landers, California, earthquake of 1992: Journal of Geophysical Research, 99, p. 11705-11722.

Martosudarmo, S.Y., Johnson, A.M., and Fleming, R.W. , 1997, Ground fracturing at southern end of Summit Ridge caused by October 17, 1989 Loma Prieta, California, earthquake sequence: U.S. Geological Survey Open-File Report 97-127, 42 p., 5 plates.

Plawman, T.L., 1983, Fault with reversal of displacement, central Montana, *in* Bally, A.W., ed., Seismic expression of structural styles: Bulletin of the American Association of Petroleum Geologists, 3.3, p. 1-12.

Prescott, W.H., and Lisowski, M., 1983, Strain accumulation along the San Andreas fault sytem east of San Francisco Bay, California: Tectonophysics, 94, p. 41-56.

Roberts, M.T., 1983, Seismic example of complex faulting from northwest shelf of Palawan, Philippines, *in* Bally, A.W., ed., Seismic expression of structural styles: American Association of Petroleum Geologists, 4.2, p. 18-24.

Savage, J.C., and Gu, G., 1985, The 1979 Palmdale, California, strain event in retrospect: Journal of Geophysical Research, 90, p. 10,301-10,309.

Scholz, C.H., 1990, The mechanics of earthquakes and faulting: Cambridge University Press, 439 p.

Segall, P., and Pollard, D.D., 1983b, Nucleation and growth of strike–slip faults in granite: Journal of Geophysical Research 88, p. 555–568.

Sibson, R.H., 1980, Transient discontinuities in ductile shear zones: Journal of Structural Geology, v. 2, p. 165–171.

Stein, R.S., and Thatcher, W., 1981, Seismic and aseismic deformation associated with the 1952 Kern County, California, earthquake and relationship to the Quaternary history of the White Wolf fault: Journal Geophysical Research, 86, p. 4913-4828.

Sylvester, A.G., 1988, Strike–slip faults: Geological Society of America Bulletin, v. 100, p. 166–1703.

Thatcher, W., 1975, Strain accumulation in northern California since 1906: Journal of Geophysical Research, 80, p. 4873-4880.

Thatcher, W., 1979, Horizontal crustal deformation from historic geodesic measurements in southern California: Journal of Geophysical Research, 84, p. 2351-2370.

Thatcher, W., 1983, Nonlinear strain buildup and the earthquake cycle on the San Andreas fault: Journal of Geophysical Research, 88, p. 5893-5902.

Thatcher, W., and Fujita, N., 1984, Deformation of the Mitaka rhombus; strain buildup following the 1923 Kanto earthquake, central Honshu, Japan: Journal of Geophysical Research, 89, p. 3102-3106.

Zachariasen, J., and Sieh, K., 1955, The transfer of slip between two *en-echelon* strike-slip faults—A case study from the 1992 Landers earthquake, southern California: Journal of Geophysical Research, 100, p. 15,281-15,301.

Appendix I. Determination of Displacements at Single-Tower Power Line

Surveyors use a method of measuring lengths of braced quadrilaterals in order to determine the position of points. We used the method to compute displacement across the narrow shear zone that passed between the legs of a damaged tower. The following sketch is a map of the legs:

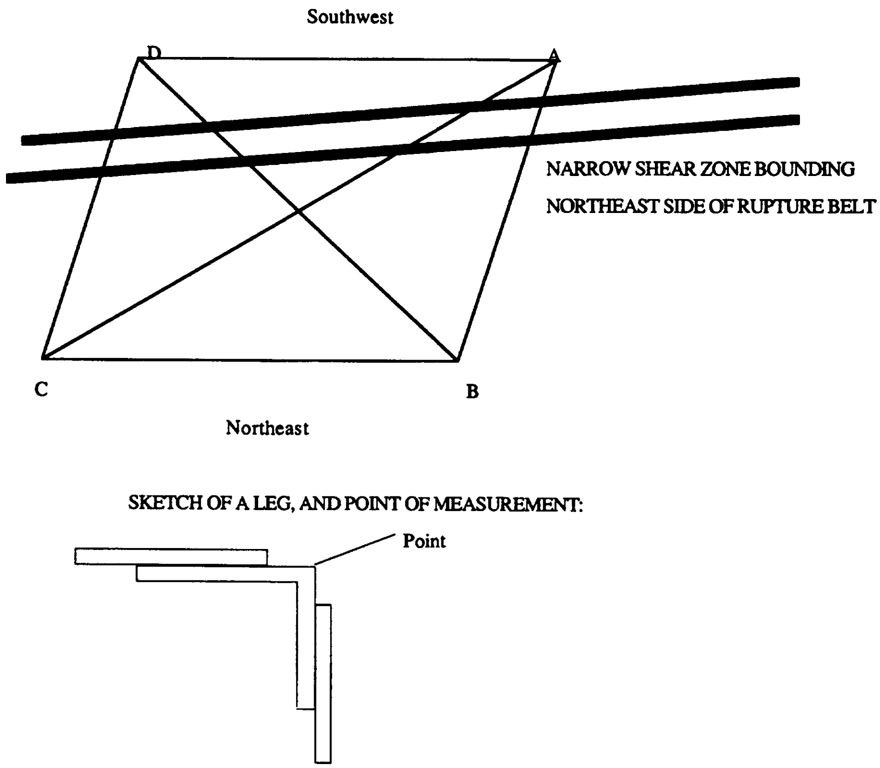

Figure I-1 Sketch of transmission tower, narrow shear zone and a tower leg.

Assuming that the points are essentially in the same plane, we use the measurements to compute all the interior angles of the quadrilateral and then compared the sum of the angles of the four corners, A...D, to 360°. The lengths of all sides except BD were then adjusted until the error was zero. These are the corrected lengths. The measurement error is about 2 mm.

Then we moved to the next tower (SoCalEd no. 150/2) to the northeast of the damaged tower and made the same set of measurements. The labels for the legs are the same. Note that we are assuming that there is no shearing in the legs of the towers outside the identifiable shear zone. Table I.2 shows the table of measurements.

Measurements were not as precise here because the tower was standing, and the points could not be directly measured by tape on the diagonals. The measurement error for this tower was about 2 cm, so changes of 2 cm or less are insignificant. We note primarily that the tower is a nearly perfect rectangle, about 7.9 m one way and 7.3 m the other.

Table I.1 Measurements and Corrected Lengths for Damaged Tower

From	To	Measurement (m)	Corrected
A	B	8.671	8.669
A	C	12.986	12.984
A	D	7.297	7.295
B	C	7.467	7.465
B	D	9.576	9.576 (assumed same)
C	D	8.733	8.731

In calculating the stretches in different directions as well as the differential displacement across the rupture zone that passed through the downed tower, we assume that side BC remained fixed in orientation but slightly lengthened whereas other sides changed orientation and changed length. We

Table I.2. Measurements and Corrected Lengths for Undisturbed Tower to northeast

From	To	Measurement (m)	Corrected
A	B	7.872	7.849
A	C	10.764	10.741
A	D	7.328	7.305
B	C	7.342	7.319
B	D	10.754	10.754 (assumed)
C	D	7.928	7.905

assume that the original lengths are those given in Table I.2.

Using the distances between the legs of the deformed tower, and the corresponding distances between the legs of a neighboring, undeformed tower, we calculated that the narrow shear zone that passed between pairs of legs of the tower accommodated 2.7 m of right–lateral differential displacement along, and 2 to 7 cm of dilation normal to the trace of the shear zone within the base of the tower. We noted an error of about 2 cm in our measurements of the reference tower, so we suspect that 2 to 7 cm of dilation is well within the limits of the combination of that known error and the inherent error caused by assuming that the deformed and undeformed towers originally had the same shape at their bases. We would have to suspect that the dilation was not detectable for the shear zone at the tower.

Our assumption that the deformed and intact towers had the same dimensions at ground level may be incorrect. We note that the legs of the tower are trapezoidal and, if they are buried to different depths or in markedly sloping ground, distances between legs will not be the same. If we assume only that the perimeter of the deformed tower was a rectangle before fault movement, we can calculate right-lateral displacement from the measurements of the sides and diagonals of the braced quadrilateral. This more accurate method results in a value of about 2.6 m of shear across the northeast side of the shear zone; and thus, qualitatively supports the more precise measurement method.

We determined differential shift across the entire belt of shear zones at the single-tower powerline as follows: We sight along corresponding legs of several towers in each direction and determine the net offset. The following sketch will help with the explanation. At the right is the typical quadrilateral, with corners A,B,C and D.

At the left is a series of three towers, two to southwest the rupture belt and the one within the rupture belt. The line xz is established by sighting along the leg D of the farthest tower and leg D of the next tower. Then the offset of leg D of the tower within the rupture zone defines part (0.21 m) of the offset across the rupture zone. One then turns around and sights northeast along legs D of two towers to the northwest,

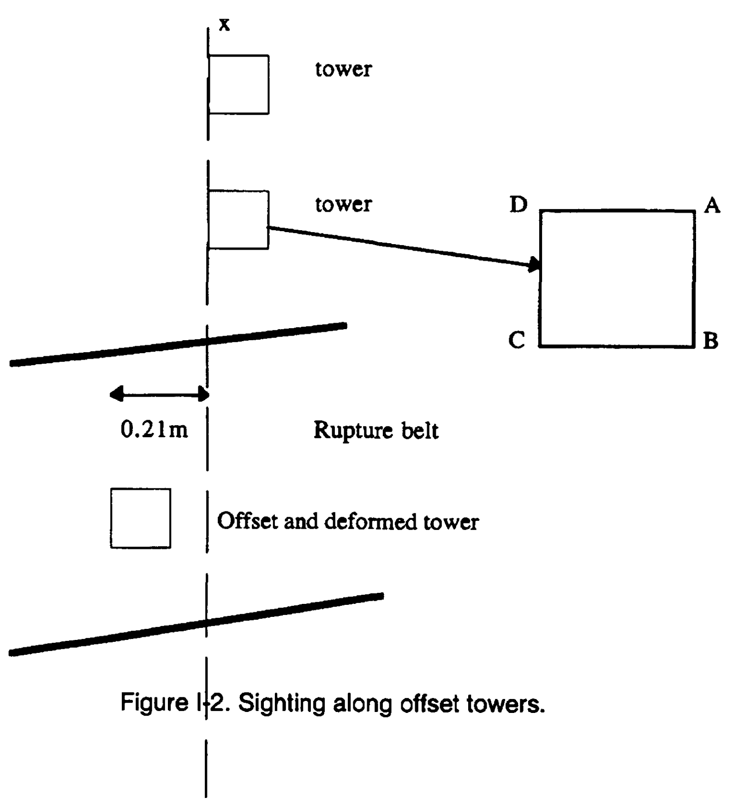

Figure I-2. Sighting along offset towers.

Table I.3 Estimates of Shift Across Emerson Fault Zone

Leg	Direction	Shift (m)	Total	Apparent Right-Lateral Shift NE of Shear Zone (m)
A	NE	3.27		0.6
	SW	0.21	3.48	
B	NE	1.04		1.0
	SW	2.77	3.81	
C	NE	0.72		0.7
	SW	2.8	3.52	
D	NE	3.39		0.7
	SW	0.21	3.6	

much as shown above, and establishes that the leg D of the tower within the rupture zone is offset 3.39 m (right-lateral) relative to those other towers. The total right-lateral offset, then is 3.6 m.

We made this same set of measurements for each of the legs of the tower within the rupture zone in order to determine the total shift as well as an estimate of the error of the method. The following table summarizes the results. The measurements of shift across the rupture belt in the direction of the power line indicate that the total shift is between 3.5 and 3.8 m and average about 3.6 m.

This estimate does not separate the right-lateral shift in the shear zone of the Emerson fault from right-lateral shift outside the shear zone. We have shown that the right-lateral shift across the northeast side of the rupture zone is about 2.7 m. Likewise, the right-lateral shift within the rest of the zone to the southwest contains an additional 0.2 m. The total right-lateral shift within the entire shear zone then is about 2.9 m. Note, however, that the legs B and C, which are outside the shear zone to the northeast also have an apparent right-lateral shift of 1.04 and 0.72 m with respect to the towers farther to the northeast. Apparently, the shift outside the belt of surface rupture is a result of opening of the swarm of tension cracks (Plate 3) that trend approximately N10°E toward the Camp Rock fault zone. The function of the tension cracks would be to transfer right-lateral displacement across a releasing stepover between the fault zones.

The line of towers is oblique to the direction of opening of the tension cracks by about 35°, and adjustment of the displacement to account for this produces an apparent displacement normal to the tension cracks of about 1.1 m.

Our best estimate of right-lateral shift within the shear zone at the deformed tower is 2.9 m. The balance of deformation obtained by sighting along the line of towers is the result of opening of tension fractures that apparently step between the Camp Rock fault and the Emerson fault. The amount of shift produced by this opening is about 1 m. If the fractures indicate displacement transfer between faults, then we expect displacement on the Emerson fault to the northwest to be markedly diminished. This is at least qualitatively true as rupture on the Emerson fault ends a short distance to the northwest.

Appendix II. Survey and Resurvey of Control Points

Permanent monuments were placed by Southern California Edison during the 1970's. The monuments consist of a pipe extending a few inches out of the ground and buried in a concrete-filed hole. The pipe was also filled with cement, and a mark about 1 mm in diameter was sunk in the center to mark the survey point. The monuments were set on each quarter-section along north-south sections lines and each half section on east-west section lines for sections 24, 25 and 36 as shown in the official record of the survey, Book 31, page 90, San Bernardino County.

We arranged to have the monuments resurveyed by contacting Richard Moses[4], SoCalEd, who participated in the survey work in the 1970's. The agreement was that the earlier survey would be retraced, so that we could compare lengths and angles between monuments. The purpose of the re-survey was to calculate strains, which involves comparison of the positions of the same material points, so we wanted the measurements to be directly comparable.

Horizontal Control Data

The horizontal control was established in 1994 by using a total station surveying instrument. According to Mr. Moses, angles should be accurate to within 5 seconds and distances should be accurate to within 10^{-5} for the distances to be shot. The measurements of distances and angle are shown inthe tables of data.

Vertical Control Data

All the monuments plus as many wing points as could be located were leveled, using a new bar-coded instrument. The wing points were marked only with wooden stakes, so it is remarkable that we found as many of them as we did. We found most of the wing points on the east side and at least half of those on the west side of the area. The wing points and monuments that were leveled are indicated by gray diamonds in Plate 1. The two or three-digit number written by each diamond is the change in elevation, relative to a point near the south end of the array marked with a black diamond in Plate 1.

The leveling was done over closed loops. For example, the line of wing points on the east side was started with point CP1, just north of Bessemer Mine Road and along the boundary between sections 12 and 7, which was part of an independent loop. The line extended from there eastward to the end wing point, and then straight northward along the line of wing points, across the ridge and to the wing point in section 19. From there the line extended to CP-19, which was part of another loop. The elevation of CP-19 was different by 4.1 cm. This error was redistributed back through the entire line, so one would expect errors for points along this line to be much smaller than 4.1 cm. The actual error for each point is probably less than 0.4 mm.

The closure errors for the 1995 survey are indicated in Table II.1.

Table II.1. Closure Errors of Level Lines

Location	Closure Error (mm)
Section 12	3
Section 1	0.4
Section 36	26
Sections 25 and 24	2.2
point in ridge	0.1
wing points on east side	41
wing points on west side	42

[4]Land Engineering Supervisor, Southern California Edison Company, 221 S. Brookhurst Rd., Fullerton, California 92633.[714-870-3127]

Comparison of the lengths, angles and elevations for the two surveys indicates that there must be errors in one data set or the other. For example, the elevation of CP30 on the southeastern boundary of Section 36 apparently moved downward 0.89 foot. We know from several lines of evidence that the point did not decrease in elevation. If the recorded elevation of the 1973-76 survey was in error by one foot, the elevation of point CP30 would have moved upward 0.11 foot. This is a reasonable value. If a 0.1-foot contour is drawn through the data, the resulting contour would trend N50°W, and the line would be defined by five other points that apparently are correct. Similarly, the elevation of CP35 apparently is incorrect. Other than these two readings, the elevations appear to be credible.

The differences in horizontal distances and angles also contain errors. They are more difficult to evaluate. Some of the computed changes in distances and angles are simply too large to be credible. As a result of the errors, the computed displacements are highly dependent on the path. Thus, when we compute displacements, we follow paths through the points defined by lengths and angles that appear to be correct. For the displacement data reported in our maps, we chose a path near the southwest side of the tectonic ridge. The path generally follows the east side of the survey data.

Appendix III. Photogrammetric Measurements

Method

There are two ways that the method of sequential aerial photogrammetry can supplement deformation measurements with other techniques. First, aerial photographs, in combination with adequate survey control of points that can be identified on the photographs, are an archival record of the three-dimensional configuration of the ground surface, containing an almost unlimited number of potential measurement points and lines. Other methods are limited to the points actually surveyed. Second, annual surveys of points in southern California, which are being taken by the Southern California Earthquake Center to provide essential data on the gross tectonic deformation of a region, are necessarily relatively sparse, whether the data are collected by surveying distances and angles, or by GPS measurements. In contrast, each aerial photograph potentially contains many measurement points, but necessarily covering a relatively small area, so aerial photographs are primarily useful for investigating deformations within and adjacent to fault zones.

At Landers, we had a set of photographs taken in 1976 by Southern California Edison, who established a network of monuments to control photogrammetric work with the photographs. The post-earthquake photographs contain no targets with known ground control, so we spent about two weeks surveying monuments that can be identified precisely on the 1992 photographs to serve as ground control of photogrammetric models.

The photogrammetric methods are being developed primarily in collaboration with Jim Messerich of the Geologic Division Plotter Laboratory at the U.S. Geological Survey in Denver, Colorado. Coordinates in deformed and non-deformed ground are measured using a Kern DSR-11 analytical stereoplotter. The stereoplotter has the capability of reproducing positions on an aerial photograph to plus or minus 5 microns. This limits the measurements of position on the 1:6000 aerial photographs to plus or minus 3 cm on the ground.

Measurements

After testing the photographic method for consistency and reproducibility, we set up a ladder of four quadrilaterals that span Tortoise Hill ridge just northwest of the culmination of the ridge (Plate 4). Quadrilateral 2 crosses the thrust/right lateral fault on the southwest side of the ridge, Quadrilateral 0 is next to 2 and includes no known faults. Quadrilateral 1 is next to 0 and crosses a minor fault. Quadrilateral 3 crosses the main rupture zone on the northeast side of the ridge.

We will describe the procedure used to process the data by using data from Quadrilateral 1. Table III.1 shows the data and computed results. For each quadrilateral, three complete series of measurements were made. The lengths, AB, BC, CD, DA, AC and BD were measured in each series. On the third and fourth page of Table III.1 are the three series of measurements for the 1976 photos and for the 1992 photos. The actual measurements are entered as bold-faced quantities. To the right of 1st data series for 1976 are the x-, y- and z- components of the sides or braces, such as AB. The same results are presented for each series.

The first check of the measurements is made by copying the data, pair by pair, onto page two of the Table III.1. The ones shown there are the last processed, data series three for 1976 and 1992. After the data are copied there, error analysis begins. The measurements are converted to those of a plane, horizontal quadrilateral. Then all the angles are calculated, as indicated. The angles are summed and then 360° are subtracted. The residual is identified as error in bold face. At this point we learn something about the size of the error in terms of lengths of sides and braces of the quadrilaterals. incl is the correction factor for the 1976 data and inc2 is the correction factor for the 1992 data (in this case, the corrections are in meters.) Thus, we note that to make the errors in angles essentially zero, we add about 1.5 cm to the lengths of the sides of the quadrilateral for the 1976 data and subtract about 2.4 cm from the lengths of the sides of the quadrilateral for the 1992 data. This gives us a good idea of the accuracy of the data. Finally, we compare the errors to the lengths of the sides of the quadrilateral to obtain estimates of the error due to measurement. In this case, the error for the 1976 data ranges from 1.3 to $2x10^{-4}$ and for the 1992 data the error ranges from 2 to $3x10^{-4}$. The idea is that strain measurements smaller than $3x10^{-4}$ would be negligible for this quadrilateral.

The errors (in percent) are given beneath each data set on pages 3 to 5 of Table III.1

At this point we typically make an adjustment of the data. If the errors are simply too large, or if we see obvious errors in the data, we adjust them as follows. Adjacent to the 1st data series on the third page is also a summary of the resultant lengths, $dr^2 = dx^2 + dy^2+dz^2$ for all three series, for comparison. Note that several of the numbers in the last four columns are in bold face. The *dr* value calculated for each of these was so different from those in the other series that is was rejected in favor of the average of the others. For example, the dr length for AB in the first series was computed from dx = 51.57, dy = –53.564 and dz = –0.747, so that dr = 74.358. This was judged to be too far from the value of 74.341 for the other two series, so it was replaced by 74.341. All these adjustments are shown in bold face numbers. In this example, four lengths were adjusted. Note that, after the adjustments, the errors are recalculated.

Tables III.2, 0, 1, and 3 present the data for all four quadrilaterals. Table III.4 presents data used to compute displacements of corners of quadrilaterals.

Table III.0

Program to check length measurements in a quadrilateral and to compute magnitudes of errors In boulder field within shear zone (near base camp). Known hereafter as Quad 0.
"Note that horizontal and vertical, not slope distances are to be measured."

Summary of Data (% strain)

Side:	AB	CD	AC	BD	BC	AD
	-0.1345	-0.0653	-0.0386	-0.0511	0.0345	0.0226
	-0.14376	-0.04206	-0.01219	-0.03035	0.01700	0.08156
	-0.12523	-0.04945	-0.02340	-0.00375	0.02576	0.05228
	-0.14710	-0.04516	-0.02425	-0.04699	0.05007	0.02211
	-0.15637	-0.02190	0.00214	-0.02624	0.03254	0.08103
	-0.13784	-0.02930	-0.00907	0.00036	0.04130	0.05176
	-0.16263	-0.03427	-0.05291	-0.05575	0.08445	-0.00533
	-0.17189	-0.01102	-0.02652	-0.03499	0.06692	0.05358
	-0.15337	-0.01841	-0.03773	-0.00840	0.07569	0.02432
Average:	-0.1481	-0.0352	-0.0247	-0.0286	0.0476	0.0427 in percent strain
	-1.48E-03	-3.52E-04	-2.47E-04	-2.86E-04	4.76E-04	4.27E-04 in strain
	2.05E-05	0.0001006	2.134E-05	5.635E-05	1.8964E-05	4.45906E-05
	2.075E-06	5.214E-06	1.745E-05	3.468E-07	0.00010393	0.000168096
	5.801E-05	2.254E-05	1.949E-07	6.849E-05	5.2924E-05	1.02936E-05
	1.05E-07	1.1E-05	2.474E-08	3.768E-05	6.8477E-07	4.69391E-05
	7.635E-06	1.966E-05	8.02E-05	6.084E-07	2.5132E-05	0.000163622
	1.164E-05	3.879E-06	2.724E-05	9.303E-05	4.3811E-06	9.20954E-06
	2.355E-05	9.774E-08	8.828E-05	8.201E-05	0.00015102	0.000255909
	6.304E-05	6.503E-05	3.6E-07	4.571E-06	4.1556E-05	1.32508E-05
	3.116E-06	3.135E-05	1.88E-05	4.525E-05	8.7749E-05	3.73801E-05

	AB	CD	AC	BD	BC	AD
Stndrd Dev.	0.0138	0.0161	0.0159	0.0197	0.0221	0.0274 in percent
	1.38E-04	1.61E-04	1.59E-04	1.97E-04	2.21E-04	2.74E-04 in strain
Coef. Var.:	9%	46%	64%	69%	46%	64%

Changes in Height (in meters)

Altitudes

"(e.g., AB is change in B relative to A)"

AB	CD	AC	BD	BC	AD	A	B	C	D
0.089	-0.066	0.005	-0.076	0.017	-0.024	#######	#######	#######	#######
0.006	-0.004	0.064	-0.083	0.06	-0.122	#######	#######	#######	#######
0.086	-0.11	0.011	-0.099	0.039	-0.095	#######			

	0.099	-0.086	0.008	-0.109	0.018	-0.014	#######
	0.016	-0.024	0.067	-0.116	0.061	-0.112	#######
	0.096	-0.13	0.014	-0.132	0.04	-0.085	#######
	0.134	-0.033	0.005	-0.092	0.043	0.003	#######
	0.051	0.029	0.064	-0.099	0.086	-0.095	#######
	0.131	-0.077	0.011	-0.115	0.065	-0.068	#######
average:	0.079	-0.056	0.028	-0.102	0.048	-0.068	#######
	0.00011	0.00011	0.00051	0.00069	0.00094	0.00194	0.00010
	0.00528	0.00267	0.00132	0.00037	0.00015	0.00292	0.00167
	0.00005	0.00295	0.00028	0.00001	0.00008	0.00073	0.00085
	0.00041	0.00092	0.00039	0.00004	0.00088	0.00292	0.00036
	0.00393	0.00100	0.00155	0.00019	0.00018	0.00194	0.00116
	0.00030	0.00553	0.00019	0.00088	0.00006	0.00029	0.00083
	0.00306	0.00051	0.00051	0.00011	0.00002	0.00504	0.00007
	0.00077	0.00717	0.00132	0.00001	0.00147	0.00073	0.00002
	0.00274	0.00046	0.00028	0.00016	0.00030	0.00000	0.00015
	AB	**CD**	**AC**	**BD**	**BC**	**AD**	
Stndrd Dev.	0.04	0.05	0.03	0.02	0.02	0.04	0.02
Coef. Var.:	55%	87%	96%	16%	45%	63%	0.00%

line lengths 1976					line lengths			
1st	2nd	3rd	average		1st	2nd	3rd	average
108.156	108.166	108.146	108.156	AB	108.011	107.997	107.980	107.996
113.114	113.088	113.096	113.100	CD	113.040	113.063	113.076	113.060
144.664	144.626	144.642	144.644	AC	**144.609**	144.629	144.588	144.609
132.364	132.336	132.301	132.333	BD	132.296	132.301	132.290	132.296
84.260	84.275	**84.267**	84.267	CB	84.289	84.302	84.331	84.307
82.980	82.931	82.955	82.955	AD	82.999	82.998	82.976	82.991

Values in bold have been modified.
Note: You are to enter values for bold-face quantities. The others are computed.
See data at bottom of spreadsheet

2nd Series 1976

						line lengths			
	Point	x	y	z		dx	dy	dz	dr
from	**A**	**736080.811**	**121960.444**	**1062.827**					
to	**B**	**736151.334**	**121878.551**	**1067.291**	AB	70.523	-81.893	4.464	108.166
from	**C**	**736094.321**	**121816.736**	**1072.967**					

to	**D**	**736021.227**	**121902.863**	**1067.646**	CD	-73.094	86.127	-5.321	113.088
from	**A**	**736080.810**	**121960.407**	**1062.880**					
to	**C**	**736094.304**	**121816.761**	**1072.904**	AC	13.494	-143.646	10.024	144.626
from	**B**	**736151.313**	**121878.589**	**1067.297**					
to	**D**	**736021.222**	**121902.859**	**1067.659**	BD	-130.091	24.270	0.362	132.336
from	**C**	**736094.344**	**121816.748**	**1072.929**					
to	**B**	**736151.312**	**121878.594**	**1067.279**	CB	56.968	61.846	-5.650	84.275
from	**A**	**736080.801**	**121960.402**	**1062.817**					
to	**D**	**736021.299**	**121902.838**	**1067.661**	AD	-59.502	-57.564	4.844	82.931

"note: AB, for example, is horizontal distance between A and B."

AB	BC	CD	AD	AC	BD			
108.074	84.085	112.963	82.790	144.278	132.336		Azimuth	
Differences in altitude:						N	139.3	E
A>B	B>C	C>D	A>D	A>C	B>D	N	42.7	E
4.464	5.650	-5.321	4.844	10.024	0.362			

1st Series 1992

line lengths

	Point	x	y	z		dx	dy	dz	dr
from	**a**	**736080.433**	**121960.946**	**1062.947**					
to	**b**	**736150.984**	**121879.283**	**1067.417**	AB	70.551	-81.663	4.470	108.011
from	**c**	**736094.014**	**121817.347**	**1073.015**					
to	**d**	**736020.862**	**121903.362**	**1067.690**	CD	-73.152	86.015	-5.325	113.040
from	**a**	**736080.443**	**121960.960**	**1062.923**					
to	**c**	**736094.042**	**121817.265**	**1073.011**	AC	13.599	-143.695	10.088	144.689
from	**b**	**736150.955**	**121879.272**	**1067.409**					
to	**d**	**736020.871**	**121903.361**	**1067.688**	BD	-130.084	24.089	0.279	132.296
from	**c**	**736094.035**	**121817.348**	**1073.010**					
to	**b**	**736150.941**	**121879.276**	**1067.420**	CB	56.906	61.928	-5.590	84.289
from	**a**	**736080.447**	**121960.959**	**1062.957**					
to	**d**	**736020.869**	**121903.366**	**1067.679**	AD	-59.578	-57.593	4.722	82.999

Ab	bc	cd	Ad	Ac	bc			
107.918	84.153	112.915	82.870	144.337	132.296		Azimuth	
A>b	b>c	c>d	A>d	A>c	b>d	N	139.2	E
-4.470	5.590	-5.325	4.722	10.088	0.279	N	42.6	E

The stakes of the quadrilaterals are arranged as follows:

Before:	A	B	After:	A	b
	D	C		d	c

Start of Error Computations:
The lengths of the sides of the plane quadrilaterals:

	AB	BC	CD	AD	AC	BD
before:	108.074	84.085	112.963	82.790	144.278	132.336
	Ab	bc	cd	Ad	Ac	bd
after:	107.918	84.153	112.915	82.870	144.337	132.296

Compute angles of plane quadrilaterals (in radians).

angle no:	1	2	3	4	5	6	7	8
angle:	CAB	ACB	CBD	CDB	ACD	DAC	ADB	ABD
before	0.617294811	0.83905444	1.010720798	0.682313522	0.609504007	0.896512995	0.953262245	0.674522723
angle:	cAb	Acb	cbd	cdb	Acd	dAc	Adb	Abd
after	0.617944276	0.83741827	1.010485353	0.683321998	0.610366909	0.896099922	0.951803699	0.675744626

"Now adjust lengths through increments, inc1 (before) and inc2 (after)"
Error Checking (angles in degrees).

angle no:	1	2	3	4	5	6	7	8
				Total Error (degrees)				
before	35.37	48.07	57.91	39.09	34.92	51.37	54.62	38.65
	ERROR	**1.3304E-05 degrees**						
after	35.41	47.98	57.90	39.15	34.97	51.34	54.53	38.72
	ERROR	**-1.46E-05 degrees**						

"Note: in following, AC and Ac are held fixed."
"correction for ""before"" data:" inc1= -0.02216 Adjust until error is (nearly) 0 degr.
"correction for ""after""data:" inc2= 0.03095 Adjust until error is (nearly) 0 degr.

AB	BC	CD	AD	AC	BD
108.052	84.063	112.941	82.767	144.278	132.313
Ab	bc	cd	Ad	Ac	bd
107.949	84.183	112.946	82.901	144.337	132.327

Errors in Triangles (angles in degrees)

triangle:	ACD	ACB	BDA	BDC
before	0.00	0.00	0.00	0.00
triangle:	Acd	Acb	bdA	bcd
after	0.00	0.00	0.00	0.00

Estimates of Errors in Lengths and Stretches:
"Apparent stretch and length change values, due solely to error, would be:"

side:	AB	BC	CD	AD	AC	BD	
Appar. S	1.00021	1.00026	1.00020	1.00027	1.00000	1.00017	App. Stretch
Appar. dL	0.02216	0.02216	0.02216	0.02216	0.00000	0.02216	"(e.g., metres)"
% error	0.02051	0.02636	0.01962	0.02677	0.00000	0.01675	percent

side:	Ab	bc	cd	Ad	Ac	bd	
Appar. S	0.99971	0.99963	0.99973	0.99963	1.00000	0.99977	App. Stretch
Appar. dL	-0.03095	-0.03095	-0.03095	-0.03095	0.00000	-0.03095	"(e.g., metres)"
% error	-0.02867	-0.03676	-0.02740	-0.03733	0.00000	-0.02339	percent

End of Error Analysis

Stretches of Line Segments in Quadrilateral
Stretch Values Computed from Slope-Distance Measurements of Qadrilateral

stakes:	AB	CD	AC	BD	BC	AD
stretch:	0.998562448	0.999579428	1.000435242	0.999696536	1.000169995	1.000815551
% strain	-0.143755	-0.042057	0.043524	-0.030346	0.016999	0.081555

These values need to be compared to two sets of error values given immediately above "in order to determine which stretch values, if any, are significantly greater than the errors."
"In this case, note that the stretch values are insignificant."
End of Spreadsheet

1976 Data

		1st Series 1976							line lengths			
	Point	x	y	z		dx	dy	dz	dr			
from	**A**	**736080.811**	**121960.415**	**1062.856**					1st	2nd	3rd	average
to	**B**	**736151.318**	**121878.616**	**1067.237**	AB	70.507	-81.799	4.381	108.156	108.166	108.146	108.156
from	**C**	**736094.298**	**121816.753**	**1072.896**								
to	**D**	**736021.160**	**121902.881**	**1067.637**	CD	-73.138	86.128	-5.259	113.114	113.088	113.096	113.100
from	**A**	**736080.817**	**121960.423**	**1062.805**								
to	**C**	**736094.325**	**121816.744**	**1072.888**	AC	13.508	-143.679	10.083	144.664	144.626	144.642	144.644
from	**B**	**736151.317**	**121878.563**	**1067.264**								
to	**D**	**736021.204**	**121902.865**	**1067.619**	BD	-130.113	24.302	0.355	132.364	132.336	132.301	132.333
from	**C**	**736094.363**	**121816.767**	**1072.931**								
to	**B**	**736151.372**	**121878.559**	**1067.324**	CB	57.009	61.792	-5.607	84.260	84.275	84.267	84.267
from	**A**	**736080.794**	**121960.425**	**1062.875**								
to	**D**	**736021.217**	**121902.860**	**1067.621**	AD	-59.577	-57.565	4.746	82.980	82.931	82.955	82.955

Estimates of Errors in Lengths and Stretches:
"Apparent stretch and length change values, due solely to error, would be:"

side:	AB	BC	CD	AD	AC	BD	
Appar. S	0.9998	0.9997	0.9998	0.9997	1.0000	0.9998	App. Stretch
Appar. dL	-0.0211	-0.0211	-0.0211	-0.0211	0.0000	-0.0211	"(e.g., metres)"
% error	-0.0195	-0.0251	-0.0187	-0.0255	0.0000	-0.0159	percent

2nd Series 1976

	Point	x	y	z		dx	dy	dz	dr
						line lengths			
from	**A**	**736080.811**	**121960.444**	**1062.827**					
to	**B**	**736151.334**	**121878.551**	**1067.291**	AB	70.523	-81.893	4.464	108.166
from	**C**	**736094.321**	**121816.736**	**1072.967**					
to	**D**	**736021.227**	**121902.863**	**1067.646**	CD	-73.094	86.127	-5.321	113.088
from	**A**	**736080.810**	**121960.407**	**1062.880**					
to	**C**	**736094.304**	**121816.761**	**1072.904**	AC	13.494	-143.646	10.024	144.626
from	**B**	**736151.313**	**121878.589**	**1067.297**					
to	**D**	**736021.222**	**121902.859**	**1067.659**	BD	-130.091	24.270	0.362	132.336
from	**C**	**736094.344**	**121816.748**	**1072.929**					
to	**B**	**736151.312**	**121878.594**	**1067.279**	CB	56.968	61.846	-5.650	84.275
from	**A**	**736080.801**	**121960.402**	**1062.817**					
to	**D**	**736021.299**	**121902.838**	**1067.661**	AD	-59.502	-57.564	4.844	82.931

Estimates of Errors in Lengths and Stretches:
"Apparent stretch and length change values, due solely to error, would be:"

side:	AB	BC	CD	AD	AC	BD	
Appar. S	1.00020	1.00026	1.00020	1.00027	1.00000	1.00017	App. Stretch
Appar. dL	0.02215	0.02215	0.02215	0.02215	0.00000	0.02215	"(e.g., metres)"
% error	0.02050	0.02635	0.01961	0.02676	0.00000	0.01674	percent

3rd series 1976

	Point	x	y	z		dx	dy	dz	dr
						line lengths			
from	**A**	**736080.778**	**121960.427**	**1062.854**					
to	**B**	**736151.324**	**121878.576**	**1067.238**	AB	70.546	-81.851	4.384	108.146
from	**C**	**736094.363**	**121816.733**	**1072.895**					
to	**D**	**736021.239**	**121902.852**	**1067.680**	CD	-73.124	86.119	-5.215	113.096
from	**A**	**736080.798**	**121960.416**	**1062.841**					
to	**C**	**736094.394**	**121816.767**	**1072.918**	AC	13.596	-143.649	10.077	144.642
from	**B**	**736151.332**	**121878.617**	**1067.286**					
to	**D**	**736021.272**	**121902.861**	**1067.664**	BD	-130.060	24.244	0.378	132.301
from	**C**	**736094.390**	**121816.762**	**1072.905**					
to	**B**	**736151.321**	**121878.529**	**1067.276**	CB	56.931	61.767	-5.629	84.267
from	**A**	**736080.794**	**121960.432**	**1062.858**					
to	**D**	**736021.259**	**121902.865**	**1067.675**	AD	-59.535	-57.567	4.817	82.955

Estimates of Errors in Lengths and Stretches:
"Apparent stretch and length change values, due solely to error, would be:"

side:	AB	BC	CD	AD	AC	BD	
Appar. S	1.00012	1.00015	1.00011	1.00016	1.00000	1.00010	App. Stretch
Appar. dL	0.01290	0.01290	0.01290	0.01290	0.00000	0.01290	"(e.g., metres)"
% error	0.01194	0.01536	0.01142	0.01558	0.00000	0.00975	percent

1992 Data

1st series

										line lengths					δ height	
	Point	x	y	z		dx	dy	dz	dr							
									2nd		3rd	average	1st	2nd	3rd	average
from	a	**736080.433**	**121960.946**	**1062.947**												
to	b	**736150.984**	**121879.283**	**1067.417**	AB	70.551	-81.663	4.470	108.011	107.997	107.980	107.99582	0.089	0.006	0.086	0.0603333
from	c	**736094.014**	**121817.347**	**1073.015**												
to	d	**736020.862**	**121903.362**	**1067.690**	CD	-73.152	86.015	-5.325	113.040	113.06327	113.076	113.05978	-0.066	-0.004	-0.11	-0.06
from	a	**736080.443**	**121960.960**	**1062.923**												
to	c	**736094.042**	**121817.265**	**1073.011**	AC	13.599	-143.695	10.088	144.609	144.62931	144.588	144.60858	0.005	0.064	0.011	0.0266667
from	b	**736150.955**	**121879.272**	**1067.409**												
to	d	**736020.871**	**121903.361**	**1067.688**	BD	-130.084	24.089	0.279	132.296	132.30133	132.290	132.29566	-0.076	-0.083	-0.099	-0.086
from	c	**736094.035**	**121817.348**	**1073.010**												
to	b	**736150.941**	**121879.276**	**1067.420**	CB	56.906	61.928	-5.590	84.289	84.301996	84.331	84.307287	0.017	0.06	0.039	0.0386667
from	a	**736080.447**	**121960.959**	**1062.957**												
to	d	**736020.869**	**121903.366**	**1067.679**	AD	-59.578	-57.593	4.722	82.999	82.998297	82.976	82.990852	-0.024	-0.122	-0.095	-0.080333

Estimates of Errors in Lengths and Stretches:
"Apparent stretch and length change values, due solely to error, would be:"

side:	Ab	bc	cd	Ad	Ac	bd	
Appar. S	0.9997	0.9996	0.9997	0.9996	1.0000	0.9998	App. Stretch
Appar. dL	-0.0310	-0.0310	-0.0310	-0.0310	0.0000	-0.0309	"(e.g., metres)"
% error	-0.0287	-0.0368	-0.0274	-0.0373	0.0000	-0.0234	percent

Stretches of Line Segments in Quadrilateral
1976 1st series
Stretch Values Computed from Slope-Distance Measurements of Qadrilateral

stakes:	AB	CD	AC	BD	BC	AD
Stretch:	0.9987	0.9993	0.9996	0.9995	1.0003	1.0002
% strain	-0.1345	-0.0653	-0.0386	-0.0511	0.0345	0.0226

1976 2nd series
Stretch Values Computed from Slope-Distance Measurements of Qadrilateral

stakes:	AB	CD	AC	BD	BC	AD
Stretch:	0.9986	0.9996	0.9999	0.9997	1.0002	1.0008
% strain	-0.1438	-0.0421	-0.0122	-0.0303	0.0170	0.0816

1976 3rd series

Stretch Values Computed from Slope-Distance Measurements of Qadrilateral

stakes:	AB	CD	AC	BD	BC	AD
Stretch:	0.9987	0.9995	0.9998	1.0000	1.0003	1.0005
% strain	-0.1252	-0.0494	-0.0234	-0.0038	0.0258	0.0523

2nd series **1992 data**

	Point	x	y	z		dx	dy	dz	0.04652 line lengths dr		δ height 1st	 2nd	 3rd	 average
from	**a**	**736080.450**	**121960.957**	**1062.944**										
to	**b**	**736150.954**	**121879.272**	**1067.424**	AB	70.504	-81.685	4.480	107.997	AB	0.099	0.016	0.096	0.070
from	**c**	**736094.050**	**121817.330**	**1073.019**										
to	**d**	**736020.876**	**121903.355**	**1067.674**	CD	-73.174	86.025	-5.345	113.063	CD	-0.086	-0.024	-0.130	-0.080
from	**a**	**736080.453**	**121960.959**	**1062.938**										
to	**c**	**736094.047**	**121817.324**	**1073.029**	AC	13.594	-143.635	10.091	144.629	AC	0.008	0.067	0.014	0.030
from	**b**	**736150.974**	**121879.291**	**1067.439**										
to	**d**	**736020.882**	**121903.367**	**1067.685**	BD	-130.092	24.076	0.246	132.301	BD	-0.109	-0.116	-0.132	-0.119
from	**c**	**736094.049**	**121817.333**	**1073.030**										
to	**b**	**736150.956**	**121879.278**	**1067.441**	CB	56.907	61.945	-5.589	84.302	CB	0.018	0.061	0.040	0.040
from	**a**	**736080.455**	**121960.962**	**1062.940**										
to	**d**	**736020.861**	**121903.387**	**1067.672**	AD	-59.594	-57.575	4.732	82.998	AD	-0.014	-0.112	-0.085	-0.070

Estimates of Errors in Lengths and Stretches:

"Apparent stretch and length change values, due solely to error, would be:"

side:	Ab	bc	cd	Ad	Ac	bd	
Appar. S	0.9999	0.9999	0.9999	0.9999	1.0000	0.9999	App. Stretch
Appar. dL	-0.0095	-0.0095	-0.0095	-0.0095	0.0000	-0.0095	"(e.g., metres)"
% error	-0.0088	-0.0113	-0.0084	-0.0115	0.0000	-0.0072	percent

Stretches of Line Segments in Quadrilateral

1976 1st series

Stretches of Line Segments in Quadrilateral

Stretch Values Computed from Slope-Distance Measurements of Qadrilateral

stakes:	AB	CD	AC	BD	BC	AD
Stretch:	0.9985	0.9995	0.9998	0.9995	1.0005	1.0002
% strain	-0.1471	-0.0452	-0.0243	-0.0470	0.0501	0.0221

1976 2nd series
Stretches of Line Segments in Quadrilateral
Stretch Values Computed from Slope-Distance Measurements of Qadrilateral

stakes:	AB	CD	AC	BD	BC	AD
Stretch:	0.9984	0.9998	1.0000	0.9997	1.0003	1.0008
% strain	-0.1564	-0.0219	0.0021	-0.0262	0.0325	0.0810

1976 3rd series
Stretches of Line Segments in Quadrilateral
Stretch Values Computed from Slope-Distance Measurements of Qadrilateral

stakes:	AB	CD	AC	BD	BC	AD
Stretch:	0.9986	0.9997	0.9999	1.0000	1.0004	1.0005
% strain	-0.1378	-0.0293	-0.0091	0.0004	0.0413	0.0518

1992 data

3rd series

	Point	x	y	z		dx	dy	dz	dr		δ height 1st	2nd	3rd	average
from	a	**736080.453**	**121960.937**	**1062.930**										
to	b	**736150.958**	**121879.277**	**1067.445**	AB	70.505	-81.660	4.515	107.980	AB	0.134	0.051	0.131	0.1053333
from	c	**736094.079**	**121817.336**	**1073.003**										
to	d	**736020.888**	**121903.366**	**1067.711**	CD	-73.191	86.030	-5.292	113.076	CD	-0.033	0.029	-0.077	-0.027
from	a	**736080.448**	**121960.936**	**1062.940**										
to	c	**736094.068**	**121817.345**	**1073.028**	AC	13.620	-143.591	10.088	144.588	AC	0.005	0.064	0.011	0.0266667
from	b	**736150.953**	**121879.279**	**1067.426**										
to	d	**736020.873**	**121903.356**	**1067.689**	BD	-130.080	24.077	0.263	132.290	BD	-0.092	-0.099	-0.115	-0.102
from	c	**736094.055**	**121817.322**	**1073.010**										
to	b	**736150.966**	**121879.305**	**1067.446**	CB	56.911	61.983	-5.564	84.331	CB	0.043	0.086	0.065	0.0646667
from	a	**736080.450**	**121960.952**	**1062.944**										
to	d	**736020.891**	**121903.375**	**1067.693**	AD	-59.559	-57.577	4.749	82.976	AD	0.003	-0.095	-0.068	-0.053333

Estimates of Errors in Lengths and Stretches:
"Apparent stretch and length change values, due solely to error, would be:"

side:	Ab	bc	cd	Ad	Ac	bd	
Appar. S	1.00001	1.00001	1.00001	1.00001	1.00000	1.00000	App. Stretch
Appar. dL	0.00057	0.00057	0.00057	0.00057	0.00000	0.00057	" (e.g., metres)"
% error	0.00053	0.00068	0.00050	0.00069	0.00000	0.00043	percent

Stretches of Line Segments in Quadrilateral

1976 1st series
Stretches of Line Segments in Quadrilateral
Stretch Values Computed from Slope-Distance Measurements of Qadrilateral

stakes:	AB	CD	AC	BD	BC	AD
Stretch:	0.9984	0.9997	0.9995	0.9994	1.0008	0.9999
% strain	-0.1626	-0.0343	-0.0529	-0.0557	0.0845	-0.0053

1976 2nd series
Stretches of Line Segments in Quadrilateral
Stretch Values Computed from Slope-Distance Measurements of Qadrilateral

stakes:	AB	CD	AC	BD	BC	AD
Stretch:	0.9983	0.9999	0.9997	0.9997	1.0007	1.0005
% strain	0.1719	-0.0110	-0.0265	-0.0350	0.0669	0.0536

1976 3rd series
Stretches of Line Segments in Quadrilateral
Stretch Values Computed from Slope-Distance Measurements of Qadrilateral

stakes:	AB	CD	AC	BD	BC	AD
Stretch:	0.9985	0.9998	0.9996	0.9999	1.0008	1.0002
% strain-0.1534-0.0184		-0.0377	-0.0084	0.0757	0.0243	

Table III.1

Program to check length measurements in a quadrilateral and to compute magnitudes of errors.
"Quad 1, just NE of quad 0 [In boulder field within shear zone (near base camp)]."
"Points A and B are new stations, points C and D correspond to points B and A, respectively, in Quad 0."
"Note that horizontal and vertical, not slope distances are to be measured."

Summary of Data (% strain)

Side:	AB	CD	AC	BD	BC	AD	
	-0.1700	-0.1037	-0.0540	0.2464	0.3327	0.2794	
	-0.17009	-0.09179	-0.05426	0.24065	0.32572	0.27127	
	-0.17016	-0.10002	-0.05412	0.23495	0.33826	0.27536	
	-0.16193	-0.08901	-0.05472	0.22761	0.32432	0.27135	
	-0.16201	-0.07711	-0.05499	0.22192	0.31734	0.26318	
	-0.16208	-0.08534	-0.05485	0.21622	0.32989	0.26727	
	-0.16597	-0.09411	-0.06227	0.23831	0.33986	0.27515	
	-0.16605	-0.08220	-0.06254	0.23261	0.33288	0.26697	
	-0.16612	-0.09043	-0.06241	0.22691	0.34543	0.27106	
Average:	-0.166	-0.090	-0.057	0.232	0.332	0.271	in percent
	-1.66E-03	-9.04E-04	-5.71E-04	2.32E-03	3.32E-03	2.71E-03	in strain
	1.746E-06	1.96E-05	1.09E-06	2.376E-05	8.4786E-08	7.50554E-06	
	1.815E-06	2.12E-07	9.16E-07	8.848E-06	4.1438E-06	2.08933E-10	
	1.884E-06	1.026E-05	1E-06	1.155E-06	4.6098E-06	1.89608E-06	
	1.884E-06	2.186E-07	6.44E-07	1.877E-06	6.2472E-06	1.76453E-09	
	1.815E-06	1.967E-05	5.09E-07	1.069E-05	2.3291E-05	7.19818E-06	
	1.746E-06	2.86E-06	5.75E-07	2.673E-05	4.1438E-07	1.74378E-06	
	6.543E-10	1.516E-06	2.94E-06	4.819E-06	7.1782E-06	1.70566E-06	
	1.718E-22	7.487E-06	3.25E-06	8.715E-08	1.2406E-07	2.01368E-06	
	6.543E-10	5.521E-11	3.1E-06	2.575E-06	2.0568E-05	3.20025E-09	
Stndrd Dev.	0.003	0.008	0.004	0.009	0.008	0.005	in percent
	3.30E-05	7.86E-05	3.75E-05	8.97E-05	8.16E-05	4.70E-05	in strain
coef. variation	1.99%	8.70%	6.56%	3.87%	2.46%	1.73%	

Changes in Height (in meters)

"(e.g., AB is change in B relative to A)"

AB	CD	AC	BD	BC	AD
0.00	-0.06	0.56	0.35	-0.45	0.41
0.04	-0.08	0.47	0.33	-0.49	0.43
0.01	-0.11	0.48	0.32	-0.47	0.37

	0.00	-0.11	0.57	0.33	-0.46	0.38
	0.05	-0.13	0.48	0.31	-0.51	0.39
	0.02	-0.15	0.49	0.31	-0.48	0.33
	0.02	-0.07	0.57	0.36	-0.45	0.41
	0.06	-0.09	0.47	0.34	-0.49	0.42
	0.03	-0.11	0.49	0.34	-0.47	0.36
average:	0.02	-0.10	0.51	0.33	-0.47	0.39
	8.301E-05	0.0001633	0.000297	3.6E-05	9.5605E-05	5.70864E-05
	3.468E-05	3.338E-05	0.000181	2.778E-06	2.7272E-05	0.000149383
	2.612E-05	1.494E-06	6.05E-05	5.444E-06	9.679E-06	6.04938E-05
	4.594E-05	1.264E-05	0.000382	1.111E-07	1.1864E-05	7.71605E-06
	6.76E-05	0.0001114	0.000123	5.378E-05	0.00013353	3.5679E-06
	7.716E-06	0.0003082	2.96E-05	6.4E-05	1.0383E-05	0.000328012
	9.679E-06	0.0001387	0.000357	9.344E-05	7.1309E-05	3.4679E-05
	0.0001413	2.283E-05	0.000139	4E-06	4.2975E-05	0.00011142
	7.901E-07	4.938E-06	3.73E-05	1.778E-06	3.1605E-06	8.91975E-05
Stndrd Dev.	0.02	0.03	0.04	0.02	0.02	0.03

line lengths (in meters) 1976					line lengths 1992			
1st	2nd	3rd	average		1st	2nd	3rd	average
74.341	74.341	**74.341**	74.341	AB	74.215	74.221	**74.218**	74.218
108.107	108.094	108.103	108.102	CD	107.995	108.011	108.006	108.004
138.093	138.093	**138.093**	138.093	AC	138.018	138.017	138.007	138.014
116.698	**116.705**	116.712	116.705	BD	116.986	116.964	116.976	116.975
96.376	96.383	96.370	96.376	CB	96.696	96.688	96.703	96.696
85.811	85.818	**85.814**	85.814	AD	86.051	86.044	86.047	86.047

Note: Values in bold have been adjusted.

Note: You are to enter values for bold-face quantities. The others are computed. See data at bottom of spreadsheet

3rd series 1976

	Point	x	y	z		dx	dy	dz (line lengths)	dr
from	A	**736145.773**	**122016.281**	**1057.484**					
to	B	**736197.337**	**121962.734**	**1056.770**	AB	51.564	-53.547	-0.714	74.341
from	C	**736151.333**	**121878.614**	**1067.219**					
to	D	**736080.814**	**121960.435**	**1062.891**	CD	-70.519	81.821	-4.328	108.103

from	A	**736145.789**	**122016.272**	**1057.485**					
to	C	**736151.340**	**121878.613**	**1067.244**	AC	5.551	-137.659	9.759	138.116
from	B	**736197.330**	**121962.781**	**1056.765**					
to	D	**736080.804**	**121960.400**	**1062.899**	BD	-116.526	-2.381	6.134	116.712
from	C	**736151.355**	**121878.607**	**1067.247**					
to	B	**736197.291**	**121962.678**	**1056.796**	CB	45.936	84.071	-10.451	96.370
from	A	**736145.773**	**122016.274**	**1057.483**					
to	D	**736080.781**	**121960.422**	**1062.903**	AD	-64.992	-55.852	5.420	85.865

AB	BC	CD	AD	AC	BD			
74.338	95.802	108.017	85.694	137.771	116.550		Azimuth	

Differences in altitude:

						N	136.1	E
A>B	B>C	C>D	A>D	A>C	B>D	N	28.7	E
-0.714	10.451	-4.328	5.420	9.759	6.134			

3rd series 1992

	Point	x	y	z		dx	dy (line lengths)	dz	dr
from	**a**	**736145.669**	**122016.809**	**1057.174**					
to	**b**	**736197.254**	**121963.497**	**1056.487**	AB	51.585	-53.312	-0.687	74.187
from	**c**	**736151.001**	**121879.266**	**1067.413**					
to	**d**	**736080.460**	**121960.933**	**1062.977**	CD	-70.541	81.667	-4.436	108.006
from	**a**	**736145.674**	**122016.804**	**1057.180**					
to	**c**	**736150.985**	**121879.281**	**1067.429**	AC	5.311	-137.523	10.249	138.007
from	**b**	**736197.249**	**121963.477**	**1056.494**					
to	**d**	**736080.479**	**121960.945**	**1062.963**	BD	-116.770	-2.532	6.469	116.976
from	**c**	**736150.987**	**121879.280**	**1067.423**					
to	**b**	**736197.234**	**121963.503**	**1056.503**	CB	46.247	84.223	-10.920	96.703
from	**a**	**736145.666**	**122016.811**	**1057.177**					
to	**d**	**736080.486**	**121960.934**	**1062.957**	AD	-65.180	-55.877	5.780	86.047

Ab	bc	cd	Ad	Ac	bc			
74.183	96.095	107.914	85.875	137.626	116.797		Azimuth	
A>b	b>c	c>d	A>d	A>c	b>d	N	135.9	E
0.687	10.920	-4.436	5.780	10.249	6.469	N	28.8	E

The stakes of the quadrilaterals are arranged as follows:

Before:	A	B	After:	A	b
	D	C		d	c

Start of Error Computations:
The lengths of the sides of the plane quadrilaterals:

	AB	BC	CD	AD	AC	BD
before:	74.338	95.802	108.017	85.694	137.771	116.550
	Ab	bc	cd	Ad	Ac	bd
After:	74.183	96.095	107.914	85.875	137.626	116.797

Compute angles of plane quadrilaterals (in radians).

angle no:	1	2	3	4	5	6	7	8
angle:	CAB	ACB	CBD	CDB	ACD	DAC	ADB	ABD
before	0.72547531	0.540845146	1.050884629	0.878431116	0.671431763	0.901304761	0.690425013	0.824387569
angle:	cAb	Acb	cbd	cdb	Acd	dAc	Adb	Abd
after	0.730009054	0.540750164	1.046849557	0.880402345	0.673590587	0.900986068	0.686613654	0.823983878

"Now adjust lengths through increments, inc1 (before) and inc2 (after)"

Error Checking (angles in degrees).

angle no:	1	2	3	4	5	6	7	8
			Total Error (degrees)					
before	41.57	30.99	60.21	50.33	38.47	51.64	39.56	47.23
	ERROR	**8.49229E-09**	**degrees**					
after	41.83	30.98	59.98	50.44	38.59	51.62	39.34	47.21
	ERROR	**-8.33893E-11**	**degrees**					

"Note: in following, AC and Ac are held fixed."
"correction for ""before"" data:" inc1=0.01479388 Adjust until error is (nearly) 0 degr.
"correction for ""after""data:" inc2=-0.02361917 Adjust until error is (nearly) 0 degr.

AB	BC	CD	AD	AC	BD
74.353	95.817	108.031	85.708	137.771	116.565
Ab	bc	cd	Ad	Ac	bd
74.160	96.071	107.891	85.851	137.626	116.774

Errors in Triangles (angles in degrees)

triangle:	ACD	ACB	BDA	BDC
before	0.00	0.00	0.00	0.00
triangle:	Acd	Acb	bdA	bcd
after	0.00	0.00	0.00	0.00

Estimates of Errors in Lengths and Stretches:
"Apparent stretch and length change values, due solely to error, would be:"

side: AB	BC	CD	AD	AC	BD		
Appar. S	0.99980	0.99985	0.99986	0.99983	1.00000	0.99987	App. Stretch
Appar. dL	-0.01479	-0.01479	-0.01479	-0.01479	0.00000	-0.01479	"(e.g., metres)"
% error	-0.01990	-0.01544	-0.01369	-0.01726	0.00000	-0.01269	percent

side:	Ab	bc	cd	Ad	Ac	bd	
Appar. S	1.00032	1.00025	1.00022	1.00028	1.00000	1.00020	App. Stretch
Appar. dL	0.02362	0.02362	0.02362	0.02362	0.00000	0.02362	"(e.g., metres)"
% error	0.03185	0.02459	0.02189	0.02751	0.00000	0.02023	percent

End of Error Analysis

Stretches of Line Segments in Quadrilateral
Stretch Values Computed from Slope-Distance Measurements of Qadrilateral

stakes:	AB	CD	AC	BD	BC	AD
Stretch:	0.997918489	0.999095659	0.999207391	1.002269114	1.003454286	1.002120259
% strain	-0.208151	-0.090434	-0.079261	0.226911	0.345429	0.212026

These values need to be compared to two sets of error values given immediately above "in order to determine which stretch values, if any, are significantly greater than the errors."
"In this case, note that the stretch values are insignificant."
End of Spreadsheet

1976 Data

28-Dec-94

1st Series 1976

	Point	x	y	z		dx	dy	dz	dr 1st	line lengths 2nd	3rd	average
from	**A**	**736145.776**	**122016.254**	**1057.473**								
to	**B**	**736197.340**	**121962.707**	**1056.771**	AB	51.564	-53.547	-0.702	74.341	**74.341**	74.341	74.341
from	**C**	**736151.327**	**121878.579**	**1067.243**								
to	**D**	**736080.837**	**121960.428**	**1062.873**	CD	-70.490	81.849	-4.370	108.107	108.094	108.103	108.102
from	**A**	**736145.721**	**122016.240**	**1057.516**								
to	**C**	**736151.315**	**121878.601**	**1067.200**	AC	5.594	-137.639	9.684	138.093	138.093	**138.093**	138.093
from	**B**	**736197.315**	**121962.673**	**1056.778**								
to	**D**	**736080.799**	**121960.391**	**1062.887**	BD	-116.516	-2.282	6.109	116.698	**116.705**	116.712	116.705
from	**C**	**736151.312**	**121878.631**	**1067.232**								
to	**B**	**736197.315**	**121962.669**	**1056.761**	CB	46.003	84.038	-10.471	96.376	96.383	96.370	96.376
from	**A**	**736145.748**	**122016.256**	**1057.484**								
to	**D**	**736080.815**	**121960.414**	**1062.858**	AD	-64.933	-55.842	5.374	85.811	85.818	**85.814**	85.814

Estimates of Errors in Lengths and Stretches:
"Apparent stretch and length change values, due solely to error, would be:"

side:	AB	BC	CD	AD	AC	BD
Appar. S	0.999785325	0.99983342	0.999852252	0.999813656	1	0.999863052 App. Stretch
Appar. dL	-0.015961904	-0.015961904	-0.015961904	-0.015961904	0	-0.015961904 "(e.g., metres)"
% error	-0.021	-0.017	-0.015	-0.019	0.000	-0.014 percent

2nd Series 1976

	Point	x	y	z		dx	line lengths dy	dz	dr
from	**A**	**736145.737**	**122016.263**	**1057.521**					
to	**B**	**736197.307**	**121962.699**	**1056.774**	AB	51.570	-53.564	-0.747	**74.341**
from	**C**	**736151.307**	**121878.620**	**1067.216**					
to	**D**	**736080.825**	**121960.460**	**1062.867**	CD	-70.482	81.840	-4.349	108.094
from	**A**	**736145.742**	**122016.241**	**1057.469**					
to	**C**	**736151.308**	**121878.607**	**1067.245**	AC	5.566	-137.634	9.776	138.093
from	**B**	**736197.306**	**121962.738**	**1056.746**					
to	**D**	**736080.830**	**121960.433**	**1062.878**	BD	-116.476	-2.305	6.132	**116.705**
from	**C**	**736151.320**	**121878.644**	**1067.237**					
to	**B**	**736197.329**	**121962.692**	**1056.811**	CB	46.009	84.048	-10.426	96.383
from	**A**	**736145.758**	**122016.234**	**1057.507**					
to	**D**	**736080.806**	**121960.402**	**1062.867**	AD	-64.952	-55.832	5.360	85.818

Estimates of Errors in Lengths and Stretches:
"Apparent stretch and length change values, due solely to error, would be:"

side:	AB	BC	CD	AD	AC	BD
Appar. S	1.000229834	1.000178343	1.000158211	1.000199516	1	1.000146677 App. Stretch
Appar. dL	0.017085236	0.017085236	0.017085236	0.017085236	0	0.017085236 "(e.g., metres)"
% error	0.023	0.018	0.016	0.020	0.000	0.015 percent

3rd series 1976

	Point	x	y	z		dx	line lengths dy	dz	dr
from	**A**	**736145.773**	**122016.281**	**1057.484**					
to	**B**	**736197.337**	**121962.734**	**1056.770**	AB	51.564	-53.547	-0.714	74.341
from	**C**	**736151.333**	**121878.614**	**1067.219**					
to	**D**	**736080.814**	**121960.435**	**1062.891**	CD	-70.519	81.821	-4.328	108.103
from	**A**	**736145.789**	**122016.272**	**1057.485**					
to	**C**	**736151.340**	**121878.613**	**1067.244**	AC	5.551	-137.659	9.759	**138.093**
from	**B**	**736197.330**	**121962.781**	**1056.765**					
to	**D**	**736080.804**	**121960.400**	**1062.899**	BD	-116.526	-2.381	6.134	116.712

from	**C**	**736151.355**	**121878.607**	**1067.247**					
to	**B**	**736197.291**	**121962.678**	**1056.796**	CB	45.936	84.071	-10.451	96.370
from	**A**	**736145.773**	**122016.274**	**1057.483**					
to	**D**	**736080.781**	**121960.422**	**1062.903**	AD	-64.992	-55.852	5.420	**85.814**

Estimates of Errors in Lengths and Stretches:
"Apparent stretch and length change values, due solely to error, would be:"

side:	AB	BC	CD	AD	AC	BD
Appar. S	0.999801031	0.999845603	0.99986306	0.999827393	1	0.999873085 App. Stretch
Appar. dL	-0.01479388	-0.01479388	-0.01479388	-0.01479388	0	-0.01479388 "(e.g., metres)"
% error	-0.020	-0.015	-0.014	-0.017	0.000	-0.013 percent

1992 Data

1st series 1992

	Point	x	y	z		dx	dy	dz	dr	line lengths 1992			δ height			
									1st	2nd	3rd	average	1st	2nd	3rd	average
from	**a**	**736145.646**	**122016.821**	**1057.182**												
to	**b**	**736197.260**	**121963.498**	**1056.477**	AB	51.614	-53.323	-0.705	74.215	74.221	74.218	74.218	-0.003	0.042	0.009	0.016
from	**c**	**736150.988**	**121879.276**	**1067.396**												
to	**d**	**736080.465**	**121960.945**	**1062.963**	CD	-70.523	81.669	-4.433	107.995	108.011	108.006	108.004	-0.063	-0.084	-0.105	-0.084
from	**a**	**736145.667**	**122016.826**	**1057.173**												
to	**c**	**736151.000**	**121879.292**	**1067.417**	AC	5.333	-137.534	10.244	138.018	138.017	138.007	138.014	0.560	0.468	0.485	0.504
from	**b**	**736197.239**	**121963.504**	**1056.507**												
to	**d**	**736080.460**	**121960.926**	**1062.965**	BD	-116.779	-2.578	6.458	116.986	116.964	116.976	116.975	0.349	0.326	0.324	0.333
from	**c**	**736151.001**	**121879.284**	**1067.428**												
to	**b**	**736197.260**	**121963.493**	**1056.512**	CB	46.259	84.209	-10.916	96.696	96.688	96.703	96.696	-0.445	-0.490	-0.465	-0.467
from	**a**	**736145.645**	**122016.815**	**1057.173**												
to	**d**	**736080.458**	**121960.941**	**1062.958**	AD	-65.187	-55.874	5.785	86.051	86.044	86.047	86.047	0.411	0.425	0.365	0.400

Estimates of Errors in Lengths and Stretches:
"Apparent stretch and length change values, due solely to error, would be:"

side:	Ab	bc	cd	Ad	Ac	bd
Appar. S	1.000280943	1.000216948	1.000193203	1.000242785	1	1.000178474 App. Stretch
Appar. dL	0.020843351	0.020843351	0.020843351	0.020843351	0	0.020843351 "(e.g., metres)"
% error	0.028	0.022	0.019	0.024	0.000	0.018 percent

Stretches of Line Segments in Quadrilateral
1976 1st series
Stretch Values Computed from Slope-Distance Measurements of Qadrilateral

stakes:	AB	CD	AC	BD	BC	AD
Stretch:	0.9983	0.9990	0.9995	1.0025	1.0033	1.0028
% strain	-0.1700	-0.1037	-0.0540	0.2464	0.3327	0.2794
δ height	-0.7050					

1976 2nd series

Stretch Values Computed from Slope-Distance Measurements of Qadrilateral

stakes:	AB	CD	AC	BD	BC	AD
Stretch:	0.9983	0.9991	0.9995	1.0024	1.0033	1.0027
% strain	-0.1701	-0.0918	-0.0543	0.2406	0.3257	0.2713

1976 3rd series

Stretch Values Computed from Slope-Distance Measurements of Qadrilateral

stakes:	AB	CD	AC	BD	BC	AD
Stretch:	0.9983	0.9990	0.9995	1.0023	1.0034	1.0028
% strain	-0.1702	-0.1000	-0.0541	0.2349	0.3383	0.2754

2nd series 1992

	Point	x	y	z		line lengths dx	dy	dz	dr		δ height 1st	2nd	3rd	average
from	**a**	**736145.653**	**122016.832**	**1057.175**										
to	**b**	**736197.253**	**121963.487**	**1056.477**	AB	51.600	-53.345	-0.698	74.221	AB	0.004	0.049	0.016	0.023
from	**c**	**736151.037**	**121879.278**	**1067.426**										
to	**d**	**736080.487**	**121960.942**	**1062.944**	CD	-70.550	81.664	-4.482	108.011	CD	-0.112	-0.133	-0.154	-0.133
from	**a**	**736145.660**	**122016.811**	**1057.153**										
to	**c**	**736151.005**	**121879.279**	**1067.404**	AC	5.345	-137.532	10.251	138.017	AC	0.567	0.475	0.492	0.511
from	**b**	**736197.249**	**121963.496**	**1056.489**										
to	**d**	**736080.490**	**121960.962**	**1062.930**	BD	-116.759	-2.534	6.441	116.964	BD	0.332	0.309	0.307	0.316
from	**c**	**736151.012**	**121879.290**	**1067.427**										
to	**b**	**736197.246**	**121963.501**	**1056.492**	CB	46.234	84.211	-10.935	96.688	CB	-0.464	-0.509	-0.484	-0.486
from	**a**	**736145.659**	**122016.833**	**1057.173**										
to	**d**	**736080.493**	**121960.942**	**1062.927**	AD	-65.166	-55.891	5.754	86.044	AD	0.380	0.394	0.334	0.369

Estimates of Errors in Lengths and Stretches:
"Apparent stretch and length change values, due solely to error, would be:"

side:	Ab	bc	cd	Ad	Ac	bd
Appar. S	1.000180956	1.000139807	1.00012444	1.000156447	1	1.000114989 App. Stretch
Appar. dL	0.013427676	0.013427676	0.013427676	0.013427676	0	0.013427676 "(e.g., metres)"
% error	0.018	0.014	0.012	0.016	0.000	0.011 percent

Stretches of Line Segments in Quadrilateral

1976 1st series
Stretches of Line Segments in Quadrilateral
Stretch Values Computed from Slope-Distance Measurements of Qadrilateral

stakes:	AB	CD	AC	BD	BC	AD
Stretch:	0.9984	0.9991	0.9995	1.0023	1.0032	1.0027
% strain	-0.1619	-0.0890	-0.0547	0.2276	0.3243	0.2714

1976 2nd series
Stretches of Line Segments in Quadrilateral
Stretch Values Computed from Slope-Distance Measurements of Qadrilateral

stakes:	AB	CD	AC	BD	BC	AD
Stretch:	0.9984	0.9992	0.9995	1.0022	1.0032	1.0026
% strain	-0.1620	-0.0771	-0.0550	0.2219	0.3173	0.2632

1976 3rd series
Stretches of Line Segments in Quadrilateral
Stretch Values Computed from Slope-Distance Measurements of Qadrilateral

stakes:	AB	CD	AC	BD	BC	AD
Stretch:	0.9984	0.9991	0.9995	1.0022	1.0033	1.0027
% strain	-0.1621	-0.0853	-0.0549	0.2162	0.3299	0.2673

3rd series 1992

						line lengths						δ height			
	Point	x	y	z		dx	dy	dz	dr		1st	2nd	3rd	average
from	**a**	**736145.669**	**122016.809**	**1057.174**										
to	**b**	**736197.254**	**121963.497**	**1056.487**	AB	51.585	-53.312	-0.687	74.218	AB	0.015	0.060	0.027	0.034
from	**c**	**736151.001**	**121879.266**	**1067.413**										
to	**d**	**736080.460**	**121960.933**	**1062.977**	CD	-70.541	81.667	-4.436	108.006	CD	-0.066	-0.087	-0.108	-0.087
from	**a**	**736145.674**	**122016.804**	**1057.180**										
to	**c**	**736150.985**	**121879.281**	**1067.429**	AC	5.311	-137.523	10.249	138.007	AC	0.565	0.473	0.490	0.509
from	**b**	**736197.249**	**121963.477**	**1056.494**										
to	**d**	**736080.479**	**121960.945**	**1062.963**	BD	-116.770	-2.532	6.469	116.976	BD	0.360	0.337	0.335	0.344
from	**c**	**736150.987**	**121879.280**	**1067.423**										
to	**b**	**736197.234**	**121963.503**	**1056.503**	CB	46.247	84.223	-10.920	96.703	CB	-0.449	-0.494	-0.469	-0.471
from	**a**	**736145.666**	**122016.811**	**1057.177**										
to	**d**	**736080.486**	**121960.934**	**1062.957**	AD	-65.180	-55.877	5.780	86.047	AD	0.406	0.420	0.360	0.395

Estimates of Errors in Lengths and Stretches:

"Apparent stretch and length change values, due solely to error, would be:"

side:	Ab	bc	cd	Ad	Ac	bd	
Appar. S	1.00031849	1.000245851	1.000218917	1.000275118	1	1.000202264	App. Stretch
Appar. dL	0.023619166	0.023619166	0.023619166	0.023619166	0	0.023619166	"(e.g., metres)"
% error	0.032	0.025	0.022	0.028	0.000	0.020	percent

Stretches of Line Segments in Quadrilateral

1st series

A B

Stretches of Line Segments in Quadrilateral
Stretch Values Computed from Slope-Distance Measurements of Qadrilateral

stakes:	AB	CD	AC	BD	BC	AD
Stretch:	0.9983	0.9991	0.9994	1.0024	1.0034	1.0028
% strain	-0.1660	-0.0941	-0.0623	0.2383	0.3399	0.2751

D C

1976 2nd series
Stretches of Line Segments in Quadrilateral
Stretch Values Computed from Slope-Distance Measurements of Qadrilateral

stakes:	AB	CD	AC	BD	BC	AD
Stretch:	0.9983	0.9992	0.9994	1.0023	1.0033	1.0027
% strain	-0.1660	-0.0822	-0.0625	0.2326	0.3329	0.2670

1976 3rd series
Stretches of Line Segments in Quadrilateral
Stretch Values Computed from Slope-Distance Measurements of Qadrilateral

stakes:	AB	CD	AC	BD	BC	AD
Stretch:	0.9983	0.9991	0.9994	1.0023	1.0035	1.0027
% strain	-0.1661	-0.0904	-0.0624	0.2269	0.3454	0.2711

Table III.2

Program to check length measurements in a quadrilateral and to compute magnitudes of errors.
"Quad 2, just SW of quad 0 [In boulder field within shear zone (near base camp)]."
"Points C and D are new stations, points A and B correspond to points D and C, respectively, in Quad 0."
Quad crosses thrust fault on west side of 2-T Ridge.
"Note that horizontal and vertical, not slope distances are to be measured."

Summary of Data (% strain)

Side:	AB	CD	AC	BD	BC	AD
	-0.0114	0.0478	-0.1764	0.0451	-0.2601	-0.1615
	-0.00442	0.05842	-0.16572	0.04886	-0.25578	-0.15952
	-0.00792	0.05310	-0.15505	0.05257	-0.25146	-0.15751
	-0.01191	0.04322	-0.17088	0.04938	-0.26930	-0.16527
	-0.00491	0.05386	-0.16021	0.05309	-0.26498	-0.16326
	-0.00841	0.04854	-0.14953	0.05680	-0.26065	-0.16126
	-0.01166	0.04873	-0.18190	0.04092	-0.25092	-0.15777
	-0.00467	0.05937	-0.17123	0.04463	-0.24659	-0.15577
	-0.00817	0.05405	-0.16056	0.04834	-0.24227	-0.15376
Average:	-0.008	0.052	-0.166	0.049	-0.256	-0.160
	1.177E-06	1.883E-06	1.27E-05	1.531E-06	2.0777E-06	4.46737E-07
	1.557E-06	4.731E-06	6.42E-14	9.369E-16	1.7358E-15	8.0087E-17
	6.611E-09	1.61E-07	1.27E-05	1.531E-06	2.0779E-06	4.46749E-07
	1.557E-06	8.363E-06	2.96E-06	2.998E-08	2.0298E-05	3.67684E-06
	1.177E-06	4.297E-07	3.38E-06	1.99E-06	9.3886E-06	1.5604E-06
	6.62E-09	1.25E-06	2.91E-05	7.012E-06	2.6331E-06	3.37307E-07
	1.36E-06	1.117E-06	2.91E-05	7.012E-06	2.6324E-06	3.37259E-07
	1.36E-06	6.203E-06	3.38E-06	1.99E-06	9.388E-06	1.56035E-06
	7.402E-16	5.137E-07	2.96E-06	3E-08	2.0301E-05	3.67706E-06
Stndrd Dev.	0.003	0.005	0.010	0.005	0.008	0.003

Q1

Q0

A B

Q2

D C

Changes in Height (in meters)

"(e.g., AB is change in B relative to A)"

AB	CD	AC	BD	BC	AD
0.03	-0.04	-0.43	-0.51	0.47	-0.56
0.02	0.01	-0.48	-0.44	0.46	-0.48
0.01	-0.11	-0.43	-0.52	0.47	-0.48
0.05	-0.08	-0.44	-0.52	0.48	-0.54
0.04	-0.03	-0.49	-0.45	0.46	-0.47

	0.03	-0.15	-0.44	-0.53	0.47	-0.47	
	0.04	-0.05	-0.44	-0.52	0.48	-0.56	
	0.03	0.00	-0.49	-0.45	0.47	-0.48	
	0.02	-0.12	-0.44	-0.54	0.47	-0.48	
average:	0.03	-0.06	-0.45	-0.50	0.47	-0.50	in percent
	2.97E-04	-6.33E-04	-4.53E-03	-4.98E-03	4.70E-03	-5.03E-03	in strain
	2.42E-06	5.057E-05	8.5E-05	1.186E-05	3.0864E-07	0.000304309	
	1.264E-05	0.0005975	5.54E-05	0.0003443	1.4272E-05	4.29753E-05	
	4.298E-05	0.0002217	7.32E-05	7.705E-05	6.0494E-07	6.22346E-05	
	3.735E-05	3.468E-05	1.26E-05	3.338E-05	4.9383E-06	0.000189827	
	1.69E-05	0.000131	0.000172	0.0002632	4.4568E-06	0.000104494	
	1.235E-06	0.0007778	8.35E-06	0.0001235	7.9012E-07	0.000133531	
	5.975E-06	1.186E-05	2.08E-05	5.542E-05	8.3457E-06	0.000328012	
	1.975E-07	0.0004317	0.000147	0.0002119	2.0864E-06	3.4679E-05	
	6.531E-06	0.0003443	1.51E-05	0.0001633	2.4198E-06	5.21605E-05	
Stndrd Dev.	0.01	0.05	0.02	0.04	0.01	0.04	in percent
	1.12E-04	5.10E-04	2.43E-04	3.58E-04	6.18E-05	3.54E-04	in strain
Coef. Var.	37.87%	80.53%	5.36%	7.20%	1.31%	7.04%	
	AB	CD	AC	BD	BC	AD	

line lengths (in meters) 1976 **line lengths 1992**

1st	2nd	3rd	average		1st	2nd	3rd	average
113.120	113.112	113.116	113.116	AB	113.107	113.106	113.106	113.106
107.359	107.348	107.353	107.353	CD	107.410	107.406	107.411	107.409
163.434	163.417	163.399	163.417	AC	163.146	163.155	163.137	163.146
140.707	140.702	140.696	140.702	BD	140.770	140.776	140.764	140.770
98.677	98.673	98.668	98.673	CB	98.420	98.411	98.429	98.420
112.554	112.551	112.549	112.551	AD	112.372	112.368	112.376	112.372

Note: Values in bold have been adjusted.
Note: You are to enter values for bold-face quantities. The others are computed.

See data at bottom of spreadsheet

3rd series 1976

	Point	x	y	z		line lengths dx	dy	dz	dr
from	**A**	**736021.168**	**121902.871**	**1067.657**					
to	**B**	**736094.331**	**121816.796**	**1072.915**	AB	73.163	-86.075	5.258	113.090
from	**C**	**736032.357**	**121740.066**	**1076.582**					
to	**D**	**735953.680**	**121812.864**	**1071.720**	CD	-78.677	72.798	-4.862	107.300

from	**A**	**736021.168**	**121902.858**	**1067.670**					
to	**C**	**736032.337**	**121740.086**	**1076.608**	AC	11.169	-162.772	8.938	163.399
from	**B**	**736094.320**	**121816.775**	**1072.902**					
to	**D**	**735953.683**	**121812.873**	**1071.678**	BD	-140.637	-3.902	-1.224	140.696
from	**C**	**736032.364**	**121740.060**	**1076.608**					
to	**B**	**736094.320**	**121816.763**	**1072.930**	CB	61.956	76.703	-3.678	98.668
from	**A**	**736021.196**	**121902.872**	**1067.690**					
to	**D**	**735953.720**	**121812.881**	**1071.677**	AD	-67.476	-89.991	3.987	112.549

AB	BC	CD	AD	AC	BD			
112.968	98.600	107.190	112.478	163.155	140.691		Azimuth	

Differences in altitude:

						N	139.6	E
A>B	B>C	C>D	A>D	A>C	B>D	N	38.9	E
5.258	3.678	-4.862	3.987	8.938	-1.224			

3rd series 1992

	Point	x	y	z		line lengths dx	dy	dz	dr
from	**a**	**736020.882**	**121903.378**	**1067.704**					
to	**b**	**736094.109**	**121817.337**	**1072.984**	AB	73.227	-86.041	5.280	113.107
from	**c**	**736032.258**	**121740.835**	**1076.206**					
to	**d**	**735953.392**	**121813.585**	**1071.225**	CD	-78.866	72.750	-4.981	107.411
from	**a**	**736020.884**	**121903.366**	**1067.692**					
to	**c**	**736032.259**	**121740.848**	**1076.189**	AC	11.375	-162.518	8.497	163.137
from	**b**	**736094.103**	**121817.308**	**1072.972**					
to	**d**	**735953.398**	**121813.615**	**1071.212**	BD	-140.705	-3.693	-1.760	140.764
from	**c**	**736032.237**	**121740.830**	**1076.191**					
to	**b**	**736094.095**	**121817.326**	**1072.988**	CB	61.858	76.496	-3.203	98.429
from	**a**	**736020.902**	**121903.387**	**1067.732**					
to	**d**	**735953.404**	**121813.609**	**1071.238**	AD	-67.498	-89.778	3.506	112.376

Ab	bc	cd	Ad	Ac	bc			
112.983	98.377	107.296	112.320	162.916	140.753		Azimuth	
A>b	b>c	c>d	A>d	A>c	b>d	N	139.6	E
-5.280	3.203	-4.981	3.506	8.497	-1.760	N	39.0	E

The stakes of the quadrilaterals are arranged as follows:

Before:	A	B	After:	A	b
	D	C		d	c

Start of Error Computations:
The lengths of the sides of the plane quadrilaterals:

	AB	BC	CD	AD	AC	BD
before:	112.968	98.600	107.190	112.478	163.155	140.691
	Ab	bc	cd	Ad	Ac	bd
After:	112.983	98.377	107.296	112.320	162.916	140.753

Compute angles of plane quadrilaterals (in radians).

angle no:	1	2	3	4	5	6	7	8
angle:	CAB	ACB	CBD	CDB	ACD	DAC	ADB	ABD
before	0.635729395	0.748165694	0.863549811	0.7743233890.755553760.7121310730.8995844320.894147754				
angle:	cAb	Acb	cbd	cdb	Acd	dAc	Adb	Abd
after	0.635217062	0.749759747	0.864303122	0.77177320.7557565840.7143896220.8996732470.892312722				

"Now adjust lengths through increments, inc1 (before) and inc2 (after)"

Error Checking (angles in degrees).

angle no:	1	2	3	4	5	6	7	8
Total Error (degrees)								
before	36.42	42.87	49.48	44.37	43.29	40.80	51.54	51.23
ERROR	0	degrees						
after	36.40	42.96	49.52	44.22	43.30	40.93	51.55	51.13
ERROR	-0	degrees						

"Note: in following, AC and Ac are held fixed."
"correction for ""before"" data:" inc1= -0.0071558Adjust until error is (nearly) 0 degr.
"correction for ""after""data:" inc2= -0.01776815Adjust until error is (nearly) 0 degr.

AB	BC	CD	AD	AC	BD
112.961	98.593	107.182	112.471	163.155	140.684
Ab	bc	cd	Ad	Ac	bd
112.966	98.360	107.278	112.302	162.916	140.736

Errors in Triangles (angles in degrees)

triangle:		ACD	ACB	BDA	BDC
before	0.00	0.00	0.00	0.00	
triangle:		Acd	Acb	bdA	bcd
after	0.00	0.00	0.00	0.00	

Estimates of Errors in Lengths and Stretches:
"Apparent stretch and length change values, due solely to error, would be:"

side: AB	BC	CD	AD	AC	BD		
Appar. S	1.00006	1.00007	1.00007	1.00006	1.00000	1.00005	App. Stretch
Appar. dL	0.00716	0.00716	0.00716	0.00716	0.00000	0.00716	"(e.g., metres)"
% error	0.00633	0.00726	0.00668	0.00636	0.00000	0.00509	percent

side: Ab	bc	cd	Ad	Ac	bd		
Appar. S	1.00016	1.00018	1.00017	1.00016	1.00000	1.00013	App. Stretch
Appar. dL	0.01777	0.01777	0.01777	0.01777	0.00000	0.01777	"(e.g., metres)"
% error	0.01573	0.01806	0.01656	0.01582	0.00000	0.01263	percent

End of Error Analysis

Stretches of Line Segments in Quadrilateral
Stretch Values Computed from Slope-Distance Measurements of Qadrilateral

stakes:	AB	CD	AC	BD	BC	AD
Stretch:	1.00014655	1.001040026	0.998394395	1.000483411	0.997577323	0.99846236
% strain	0.014655	0.104003	-0.160561	0.048341	-0.242268	-0.153764

These values need to be compared to two sets of error values given immediately above
"in order to determine which stretch values, if any, are significantly greater than the errors."
"In this case, note that the stretch values are insignificant."
End of Spreadsheet

1976 Data

28-Dec-94

1st Series 1976

									line lengths		1976	
	Point	x	y	z		dx	dy	dz	dr			
									1st	2nd	3rd	average
from	**A**	**736021.177**	**121902.888**	**1067.660**								
to	**B**	**736094.342**	**121816.775**	**1072.903**	AB	73.165	-86.113	5.243	113.120	113.112	113.116	113.116
from	**C**	**736032.399**	**121740.051**	**1076.616**								
to	**D**	**735953.698**	**121812.906**	**1071.688**	CD	-78.701	72.855	-4.928	107.359	107.348	107.353	107.353
from	**A**	**736021.187**	**121902.880**	**1067.675**								
to	**C**	**736032.344**	**121740.072**	**1076.611**	AC	11.157	-162.808	8.936	163.434	163.417	163.399	163.417
from	**B**	**736094.365**	**121816.780**	**1072.915**								
to	**D**	**735953.718**	**121812.867**	**1071.675**	BD	-140.647	-3.913	-1.240	140.707	140.702	140.696	140.702
from	**C**	**736032.341**	**121740.069**	**1076.599**								
to	**B**	**736094.324**	**121816.761**	**1072.917**	CB	61.983	76.692	-3.682	98.677	98.673	98.668	98.673
from	**A**	**736021.203**	**121902.866**	**1067.620**								
to	**D**	**735953.688**	**121812.902**	**1071.688**	AD	-67.515	-89.964	4.063	112.554	112.551	112.549	112.551

Estimates of Errors in Lengths and Stretches:

"Apparent stretch and length change values, due solely to error, would be:"

side:	AB	BC	CD	AD	AC	BD	
Appar. S	1.000170342	1.000195205	1.00017948	1.0001711271		1.000136798	App. Stretch
Appar. dL	0.019245077	0.019245077	0.019245077	0.0192450770		0.019245077	"(e.g., metres)"
% error	0.017034232	0.019520542	0.017948022	0.0171126730		0.013679826	percent

2nd Series 1976

	Point	x	y	z		dx	dy	dz	dr
						line lengths			
from	**A**	**736021.206**	**121902.848**	**1067.668**					
to	**B**	**736094.323**	**121816.705**	**1072.917**	AB	73.117	-86.143	5.249	113.112
from	**C**	**736032.371**	**121740.019**	**1076.648**					
to	**D**	**735953.687**	**121812.872**	**1071.668**	CD	-78.684	72.853	-4.980	107.348
from	**A**	**736021.189**	**121902.850**	**1067.666**					
to	**C**	**736032.399**	**121740.114**	**1076.652**	AC	11.210	-162.736	8.986	163.417
from	**B**	**736094.334**	**121816.772**	**1072.945**					
to	**D**	**735953.683**	**121812.851**	**1071.639**	BD	-140.651	-3.921	-1.306	140.702
from	**C**	**736032.368**	**121740.089**	**1076.598**					
to	**B**	**736094.362**	**121816.797**	**1072.929**	CB	61.994	76.708	-3.669	98.673
from	**A**	**736021.206**	**121902.851**	**1067.677**					
to	**D**	**735953.691**	**121812.901**	**1071.668**	AD	-67.515	-89.950	3.991	112.551

Estimates of Errors in Lengths and Stretches:
"Apparent stretch and length change values, due solely to error, would be:"

side:	AB	BC	CD	AD	AC	BD	
Appar. S	1.000449169	1.000514612	1.000473298	1.00045125	1	1.000360661	App. Stretch
Appar. dL	0.050728783	0.050728783	0.050728783	0.050728783	0	0.050728783	"(e.g., metres)"
% error	0.044916917	0.051461221	0.047329834	0.045125031	0	0.036066129	percent

3rd series 1976

	Point	x	y	z		dx	dy	dz	dr
						line lengths			
from	**A**	**736021.168**	**121902.871**	**1067.657**					
to	**B**	**736094.331**	**121816.796**	**1072.915**	AB	73.163	-86.075	5.258	113.116
from	**C**	**736032.357**	**121740.066**	**1076.582**					
to	**D**	**735953.680**	**121812.864**	**1071.720**	CD	-78.677	72.798	-4.862	107.353
from	**A**	**736021.168**	**121902.858**	**1067.670**					
to	**C**	**736032.337**	**121740.086**	**1076.608**	AC	11.169	-162.772	8.938	163.399
from	**B**	**736094.320**	**121816.775**	**1072.902**					
to	**D**	**735953.683**	**121812.873**	**1071.678**	BD	-140.637	-3.902	-1.224	140.696
from	**C**	**736032.364**	**121740.060**	**1076.608**					

to	B	736094.320	121816.763	1072.930	CB	61.956	76.703	-3.678	98.668
from	A	736021.196	121902.872	1067.690					
to	D	735953.720	121812.881	1071.677	AD	-67.476	-89.991	3.987	112.549

Estimates of Errors in Lengths and Stretches:
"Apparent stretch and length change values, due solely to error, would be:"

side:	AB	BC	CD	AD	AC	BD	
Appar. S	1.000063348	1.00007258	1.000066763	1.000063623	1	1.000050864	App. Stretch
Appar. dL	0.007155796	0.007155796	0.007155796	0.007155796	0	0.007155796	"(e.g., metres)"
% error	0.006334768	0.00725795	0.006676274	0.006362334	0	0.005086433	percent

1992 Data

1st series 1992

								line lengths 1992					δ height			
Point		x	y	z		dx	dy	dz	dr							
									1st	2nd	3rd	average	1st	2nd	3rd	average
from	**a**	**736020.890**	**121903.379**	**1067.728**												
to	**b**	**736094.085**	**121817.310**	**1072.996**	AB	73.195	-86.069	5.268	113.107	113.106	113.106	113.106	0.025	0.019	0.010	0.018
from	**c**	**736032.250**	**121740.832**	**1076.200**												
to	**d**	**735953.381**	**121813.578**	**1071.230**	CD	-78.869	72.746	-4.970	107.410	107.406	107.411	107.409	-0.042	0.010	-0.108	-0.047
from	**a**	**736020.888**	**121903.369**	**1067.711**												
to	**c**	**736032.240**	**121740.877**	**1076.222**	AC	11.352	-162.492	8.511	163.146	163.155	163.137	163.146	-0.425	-0.475	-0.427	-0.442
from	**b**	**736094.070**	**121817.322**	**1073.002**												
to	**d**	**735953.402**	**121813.592**	**1071.254**	BD	-140.668	-3.730	-1.748	140.770	140.776	140.764	140.770	-0.508	-0.442	-0.524	-0.491
from	**c**	**736032.243**	**121740.836**	**1076.202**												
to	**b**	**736094.052**	**121817.312**	**1072.992**	CB	61.809	76.476	-3.210	98.420	98.411	98.429	98.420	0.472	0.459	0.468	0.466
from	**a**	**736020.883**	**121903.379**	**1067.725**												
to	**d**	**735953.374**	**121813.585**	**1071.233**	AD	-67.509	-89.794	3.508	112.372	112.368	112.376	112.372	-0.555	-0.483	-0.479	-0.506

Estimates of Errors in Lengths and Stretches:
"Apparent stretch and length change values, due solely to error, would be:"

side:	Ab	bc	cd	Ad	Ac	bd	
Appar. S	1.000402904	1.000462889	1.000424274	1.000405225	1	1.000323472	App. Stretch
Appar. dL	0.045503387	0.045503387	0.045503387	0.045503387	0	0.045503387	"(e.g., metres)"
% error	0.040290418	0.046288853	0.042427447	0.04052253	0	0.032347166	percent

Stretches of Line Segments in Quadrilateral

1976 1st series

Stretch Values Computed from Slope-Distance Measurements of Qadrilateral

stakes:	AB	CD	AC	BD	BC	AD
Stretch:	0.9999	1.0005	0.9982	1.0005	0.9974	0.9984
% strain	-0.0114	0.0478	-0.1764	0.0451	-0.2601	-0.1615
δ height	5.2680					

1976 2nd series

Stretch Values Computed from Slope-Distance Measurements of Qadrilateral

stakes:	AB	CD	AC	BD	BC	AD
Stretch:	1.0000	1.0006	0.9983	1.0005	0.9974	0.9984
% strain	-0.0044	0.0584	-0.1657	0.0489	-0.2558	-0.1595

1976 3rd series

Stretch Values Computed from Slope-Distance Measurements of Qadrilateral

stakes:	AB	CD	AC	BD	BC	AD
Stretch:	0.9999	1.0005	0.9984	1.0005	0.9975	0.9984
% strain	-0.0079	0.0531	-0.1550	0.0526	-0.2515	-0.1575

2nd series 1992

Point		x	y	z		line lengths dx	dy	dz	dr		δ height 1st	2nd	3rd	average
from	a	**736020.885**	**121903.383**	**1067.705**										
to	b	**736094.101**	**121817.334**	**1072.996**	AB	73.216	-86.049	5.291	113.106	AB	0.048	0.042	0.033	0.041
from	c	**736032.273**	**121740.856**	**1076.208**										
to	d	**735953.391**	**121813.578**	**1071.199**	CD	-78.882	72.722	-5.009	107.406	CD	-0.081	-0.029	-0.147	-0.086
from	a	**736020.869**	**121903.388**	**1067.713**										
to	c	**736032.276**	**121740.854**	**1076.207**	AC	11.407	-162.534	8.494	163.155	AC	-0.442	-0.492	-0.444	-0.459
from	b	**736094.096**	**121817.325**	**1072.977**										
to	d	**735953.380**	**121813.595**	**1071.222**	BD	-140.716	-3.730	-1.755	140.776	BD	-0.515	-0.449	-0.531	-0.498
from	c	**736032.257**	**121740.850**	**1076.192**										
to	b	**736094.112**	**121817.325**	**1072.987**	CB	61.855	76.475	-3.205	98.411	CB	0.477	0.464	0.473	0.471
from	a	**736020.874**	**121903.386**	**1067.703**										
to	d	**735953.420**	**121813.586**	**1071.222**	AD	-67.454	-89.800	3.519	112.368	AD	-0.544	-0.472	-0.468	-0.495

Estimates of Errors in Lengths and Stretches:

"Apparent stretch and length change values, due solely to error, would be:"

side:	Ab	bc	cd	Ad	Ac	bd	
Appar. S	0.999918909	0.99990684	0.999914606	0.999918442	1	0.999934913	App. Stretch
Appar. dL	-0.009162578	-0.009162578	-0.009162578	-0.009162578	0	-0.009162578	"(e.g., metres)"
% error	-0.008109085	-0.009315976	-0.008539387	-0.008155823	0	-0.006508687	percent

Stretches of Line Segments in Quadrilateral

1976 1st series
Stretches of Line Segments in Quadrilateral
Stretch Values Computed from Slope-Distance Measurements of Qadrilateral

stakes:	AB	CD	AC	BD	BC	AD
Stretch:	0.9999	1.0004	0.9983	1.0005	0.9973	0.9983
% strain	-0.0119	0.0432	-0.1709	0.0494	-0.2693	-0.1653

1976 2nd series
Stretches of Line Segments in Quadrilateral
Stretch Values Computed from Slope-Distance Measurements of Qadrilateral

stakes:	AB	CD	AC	BD	BC	AD
Stretch:	1.0000	1.0005	0.9984	1.0005	0.9974	0.9984
% strain	-0.0049	0.0539	-0.1602	0.0531	-0.2650	-0.1633

976 3rd series
Stretches of Line Segments in Quadrilateral
Stretch Values Computed from Slope-Distance Measurements of Qadrilateral

stakes:	AB	CD	AC	BD	BC	AD
Stretch:	0.9999	1.0005	0.9985	1.0006	0.9974	0.9984
% strain	-0.0084	0.0485	-0.1495	0.0568	-0.2607	-0.1613

3rd series 1992

Point		x	y	z		line lengths dx	dy	dz	dr		δ height 1st	2nd	3rd	average
from	a	**736020.882**	**121903.378**	**1067.704**										
to	b	**736094.109**	**121817.337**	**1072.984**	AB	73.227	-86.041	5.280	113.106	AB	0.037	0.031	0.022	0.030
from	c	**736032.258**	**121740.835**	**1076.206**										
to	d	**735953.392**	**121813.585**	**1071.225**	CD	-78.866	72.750	-4.981	107.411	CD	-0.053	-0.001	-0.119	-0.058
from	a	**736020.884**	**121903.366**	**1067.692**										
to	c	**736032.259**	**121740.848**	**1076.189**	AC	11.375	-162.518	8.497	163.137	AC	-0.439	-0.489	-0.441	-0.456
from	b	**736094.103**	**121817.308**	**1072.972**										
to	d	**735953.398**	**121813.615**	**1071.212**	BD	-140.705	-3.693	-1.760	140.764	BD	-0.520	-0.454	-0.536	-0.503
from	c	**736032.237**	**121740.830**	**1076.191**										
to	b	**736094.095**	**121817.326**	**1072.988**	CB	61.858	76.496	-3.203	98.429	CB	0.479	0.466	0.475	0.473
from	a	**736020.902**	**121903.387**	**1067.732**										
to	d	**735953.404**	**121813.609**	**1071.238**	AD	-67.498	-89.778	3.506	112.376	AD	-0.557	-0.485	-0.481	-0.508

Estimates of Errors in Lengths and Stretches:
"Apparent stretch and length change values, due solely to error, would be:"

side:	Ab	bc	cd	Ad	Ac	bd	
Appar. S	1.000157288	1.000180645	1.000165627	1.000158217	1	1.000126252	App. Stretch
Appar. dL	0.017768151	0.017768151	0.017768151	0.017768151	0	0.017768151	"(e.g., metres)"
% error	0.015728812	0.018064484	0.016562697	0.015821715	0	0.012625192	percent

Stretches of Line Segments in Quadrilateral

1976 1st series
Stretches of Line Segments in Quadrilateral
Stretch Values Computed from Slope-Distance Measurements of Qadrilateral

stakes:	AB	CD	AC	BD	BC	AD		
							A	B
Stretch:	0.9999	1.0005	0.9982	1.0004	0.9975	0.9984		
% strain	-0.0117	0.0487	-0.1819	0.0409	-0.2509	-0.1578	D	C

1976 2nd series
Stretches of Line Segments in Quadrilateral
Stretch Values Computed from Slope-Distance Measurements of Qadrilateral

stakes:	AB	CD	AC	BD	BC	AD
Stretch:	1.0000	1.0006	0.9983	1.0004	0.9975	0.9984
% strain	-0.0047	0.0594	-0.1712	0.0446	-0.2466	-0.1558

1976 3rd series
Stretches of Line Segments in Quadrilateral
Stretch Values Computed from Slope-Distance Measurements of Qadrilateral

stakes:	AB	CD	AC	BD	BC	AD
Stretch:	0.9999	1.0005	0.9984	1.0005	0.9976	0.9985
% strain	-0.0082	0.0540	-0.1606	0.0483	-0.2423	-0.1538

Table III.3

Program to check length measurements in a quadrilateral and to compute magnitudes of errors.
"New Quad 3, just NE of quad 1 , extending across main fault."
"Points A and B are new stations, points C and D correspond to points B and A, respectively, in Quad 1."
Quad crosses main rupturet on east side of 2-T Ridge.
"Note that horizontal and vertical, not slope distances are to be measured."

Summary of Data (% strain)

Side:	AB	CD	AC	BD	BC	AD				
	0.104	-0.148	-2.331	1.868	1.778	1.023		A		B
	0.104	-0.148	-2.331	1.868	1.778	1.023				
	0.104	-0.148	-2.331	1.868	1.778	1.023			Q3	
	0.104	-0.148	-2.331	1.868	1.778	1.023				
	0.104	-0.148	-2.331	1.868	1.778	1.023		D		C
	0.104	-0.148	-2.331	1.868	1.778	1.023				
	0.104	-0.148	-2.331	1.868	1.778	1.023			Q1	
	0.104	-0.148	-2.331	1.868	1.778	1.023				
	0.104	-0.148	-2.331	1.868	1.778	1.023			Q0	
Average:	0.104	-0.148	-2.331	1.868	1.778	1.023			Q2	
	0	0	0	2.191E-32		2.1913E-32		0		
	0	0	0	2.191E-32		2.1913E-32		0		
	0	0	0	2.191E-32		2.1913E-32		0		
	0	0	0	2.191E-32		2.1913E-32		0		
	0	0	0	2.191E-32		2.1913E-32		0		
	0	0	0	2.191E-32		2.1913E-32		0		
	0	0	0	2.191E-32		2.1913E-32		0		
	0	0	0	2.191E-32		2.1913E-32		0		
	0	0	0	2.191E-32		2.1913E-32		0		
Stndrd Dev.		0.000	0.000	0.000	0.000	0.000	0.000			

Changes in Height (in meters)

"(e.g., AB is change in B relative to A)"

AB	CD	AC	BD	BC	AD
-0.02	-0.02	0.86	0.73	-0.82	0.70
-0.02	-0.02	0.86	0.73	-0.82	0.70
-0.02	-0.02	0.86	0.73	-0.82	0.70
-0.02	-0.02	0.86	0.73	-0.82	0.70
-0.02	-0.02	0.86	0.73	-0.82	0.70
-0.02	-0.02	0.86	0.73	-0.82	0.70
-0.02	-0.02	0.86	0.73	-0.82	0.70

	-0.02	-0.02	0.86	0.73	-0.82	0.70	
	-0.02	-0.02	0.86	0.73	-0.82	0.70	
average:	-0.02	-0.02	0.86	0.73	-0.82	0.70	
	0	0	0	0	0	0	
	0	0	0	0	0	0	
	0	0	0	0	0	0	
	0	0	0	0	0	0	
	0	0	0	0	0	0	
	0	0	0	0	0	0	
	0	0	0	0	0	0	
	0	0	0	0	0	0	
	0	0	0	0	0	0	
Stndrd Dev.		0.00	0.00	0.00	0.00	0.00	0.00

line lengths (in meters) 1976 | **line lengths 1992**

1st	2nd	3rd	average		1st	2nd	3rd	average
92.271	92.271	92.271	92.271	AB	92.368	92.368	92.368	92.368
74.293	74.293	74.293	74.293	CD	74.183	74.183	74.183	74.183
85.056	85.056	85.056	85.056	AC	83.073	83.073	83.073	83.073
119.995	119.995	119.995	119.995	BD	122.237	122.237	122.237	122.237
68.570	68.570	68.570	68.570	CB	69.789	69.789	69.789	69.789
56.997	56.997	56.997	56.997	AD	57.580	57.580	57.580	57.580

Note: Values in bold have been adjusted.

Note: You are to enter values for bold-face quantities. The others are computed.
See data at bottom of spreadsheet

1st series 1976

	Point	x	y	z	line lengths	dx	dy	dz	dr
from	**A**	**736193.104**	**122047.498**	**1052.228**					
to	**B**	**736261.684**	**121985.767**	**1051.956**	AB	68.580	-61.731	-0.272	92.271
from	**C**	**736197.296**	**121962.742**	**1056.779**					
to	**D**	**736145.769**	**122016.257**	**1057.484**	CD	-51.527	53.515	0.705	74.293
from	**A**	**736193.117**	**122047.494**	**1052.237**					
to	**C**	**736197.340**	**121962.662**	**1056.737**	AC	4.223	-84.832	4.500	85.056
from	**B**	**736261.692**	**121985.746**	**1051.942**					
to	**D**	**736145.776**	**122016.261**	**1057.521**	BD	-115.916	30.515	5.579	119.995

from	**C**	**736197.321**	**121962.695**	**1056.790**					
to	**B**	**736261.675**	**121985.869**	**1051.957**	CB	64.354	23.174	-4.833	68.570
from	**A**	**736193.108**	**122047.551**	**1052.177**					
to	**D**	**736145.775**	**122016.248**	**1057.503**	AD	-47.333	-31.303	5.326	56.997

AB	BC	CD	AD	AC	BD			
92.271	68.399	74.289	56.748	84.937	119.865		Azimuth	
					N	132.0	E	

Differences in altitude:

A>B	B>C	C>D	A>D	A>C	B>D	N	70.3	E
-0.272	4.833	0.705	5.326	4.500	5.579			

1st series 1992

	Point	x	y	z		dx	dy (line lengths)	dz	dr
from	**a**	**736194.710**	**122046.390**	**1051.159**					
to	**b**	**736263.500**	**121984.749**	**1050.868**	AB	68.790	-61.641	-0.291	92.368
from	**c**	**736197.250**	**121963.515**	**1056.475**					
to	**d**	**736145.662**	**122016.819**	**1057.162**	CD	-51.588	53.304	0.687	74.183
from	**a**	**736194.705**	**122046.373**	**1051.133**					
to	**c**	**736197.245**	**121963.512**	**1056.495**	AC	2.540	-82.861	5.362	83.073
from	**b**	**736263.466**	**121984.768**	**1050.852**					
to	**d**	**736145.675**	**122016.820**	**1057.158**	BD	-117.791	32.052	6.306	122.237
from	**c**	**736197.243**	**121963.513**	**1056.499**					
to	**b**	**736263.472**	**121984.779**	**1050.844**	CB	66.229	21.266	-5.655	69.789
from	**a**	**736194.712**	**122046.387**	**1051.144**					
to	**d**	**736145.663**	**122016.834**	**1057.166**	AD	-49.049	-29.553	6.022	57.580

Ab	bc	cd	Ad	Ac	bc			
92.367	69.570	74.180	57.260	82.900	122.074		Azimuth	
A>b	b>c	c>d	A>d	A>c	b>d	N	131.9	E
0.291	5.655	0.687	6.022	5.362	6.306	N	72.2	E

The stakes of the quadrilaterals are arranged as follows:

Before:	A	B	After:	A	b
	D	C		d	c

Start of Error Computations:
The lengths of the sides of the plane quadrilaterals:

	AB	BC	CD	AD	AC	BD
before:	92.271	68.399	74.289	56.748	84.937	119.865
	Ab	bc	cd	Ad	Ac	bd
After:	92.367	69.570	74.180	57.260	82.900	122.074

Compute angles of plane quadrilaterals (in radians).

angle no:	1	2	3	4	5	6	7	8
angle:	CAB	ACB	CBD	CDB	ACD	DAC	ADB	ABD
before	0.788601317	1.275957564	0.600883275	0.547509293	0.717242522	1.036061582	0.840779257	0.476150498
angle:	cAb	Acb	cbd	cdb	Acd	dAc	Adb	Abd
after	0.80933167	1.291120001	0.576227352	0.536330989	0.737914311	1.058605503	0.80874185	0.46491363

"Now adjust lengths through increments, inc1 (before) and inc2 (after)"
Error Checking (angles in degrees).

angle no:	1	2	3	4	5	6	7	8
				Total Error (degrees)				
before	45.18	73.11	34.43	31.37	41.09	59.36	48.17	27.28
	ERROR	0	degrees					
after	46.37	73.98	33.02	30.73	42.28	60.65	46.34	26.64
	ERROR	-0	degrees					

"Note: in following, AC and Ac are held fixed."
"correction for ""before"" data:" inc1= 0.025190418 Adjust until error is (nearly) 0 degr.
"correction for ""after""data:" inc2= -0.03734157 Adjust until error is (nearly) 0 degr.

AB	BC	CD	AD	AC	BD
92.296	68.425	74.314	56.773	84.937	119.890
Ab	bc	cd	Ad	Ac	bd
92.330	69.532	74.142	57.222	82.900	122.037

Errors in Triangles (angles in degrees)

triangle:	ACD	ACB	BDA	BDC
before	0.00	0.00	0.00	0.00
triangle:	Acd	Acb	bdA	bcd
after	0.00	0.00	0.00	0.00

Estimates of Errors in Lengths and Stretches:
"Apparent stretch and length change values, due solely to error, would be:"

side:	AB	BC	CD	AD	AC	BD	
Appar. S	0.99973	0.99963	0.99966	0.99956	1.00000	0.99979	App. Stretch
Appar. dL	-0.02519	-0.02519	-0.02519	-0.02519	0.00000	-0.02519	"(e.g., metres)"
% error	-0.02729	-0.03681	-0.03390	-0.04437	0.00000	-0.02101	percent

side:	Ab	bc	cd	Ad	Ac	bd	
Appar. S	1.00040	1.00054	1.00050	1.00065	1.00000	1.00031	App. Stretch
Appar. dL	0.03734	0.03734	0.03734	0.03734	0.00000	0.03734	"(e.g., metres)"
% error	0.04044	0.05370	0.05036	0.06526	0.00000	0.03060	percent

End of Error Analysis
Stretches of Line Segments in Quadrilateral
Stretch Values Computed from Slope-Distance Measurements of Qadrilatera

side:	AB	BC	CD	AD	AC	BD
Stretch:	1.001042146	0.998524667	0.976685746	1.018681453	1.017778882	1.010227595
% strain	0.104215	-0.147533	-2.331425	1.868145	1.777888	1.022760

These values need to be compared to two sets of error values given immediately above
"in order to determine which stretch values, if any, are significantly greater than the errors."
"In this case, note that the stretch values are insignificant."

End of Spreadsheet

1976 Data

28-Dec-94

1st Series 1976

	Point	x	y	z		dx	dy	dz	dr 1st	2nd	3rd	average
from	A	**736193.104**	**122047.498**	**1052.228**								
to	B	**736261.684**	**121985.767**	**1051.956**	AB	68.580	-61.731	-0.272	92.271	92.271	92.271	92.271
from	C	**736197.296**	**121962.742**	**1056.779**								
to	D	**736145.769**	**122016.257**	**1057.484**	CD	-51.527	53.515	0.705	74.293	74.293	74.293	74.293
from	A	**736193.117**	**122047.494**	**1052.237**								
to	C	**736197.340**	**121962.662**	**1056.737**	AC	4.223	-84.832	4.500	85.056	85.056	85.056	85.056
from	B	**736261.692**	**121985.746**	**1051.942**								
to	D	**736145.776**	**122016.261**	**1057.521**	BD	-115.916	30.515	5.579	119.995	119.995	119.995	119.995
from	C	**736197.321**	**121962.695**	**1056.790**								
to	B	**736261.675**	**121985.869**	**1051.957**	CB	64.354	23.174	-4.833	68.570	68.570	68.570	68.570
from	A	**736193.108**	**122047.551**	**1052.177**								
to	D	**736145.775**	**122016.248**	**1057.503**	AD	-47.333	-31.303	5.326	56.997	56.997	56.997	56.997

Estimates of Errors in Lengths and Stretches:
"Apparent stretch and length change values, due solely to error, would be:"

side:	AB	BC	CD	AD	AC	BD		
Appar. S		0.99972707	0.999631851	0.999661029	0.999556294	1	0.999789888	App. Stretch
Appar. dL		-0.025190418	-0.025190418	-0.025190418	-0.025190418	0	-0.025190418	"(e.g., metres)"
% error		-0.027293028	-0.036814887	-0.033897088	-0.04437058	0	-0.021011194	percent

2nd Series 1976

						line lengths			
	Point	x	y	z		dx	dy	dz	dr
from	**A**	**736193.104**	**122047.498**	**1052.228**					
to	**B**	**736261.684**	**121985.767**	**1051.956**	AB	68.580	-61.731	-0.272	92.271
from	**C**	**736197.296**	**121962.742**	**1056.779**					
to	**D**	**736145.769**	**122016.257**	**1057.484**	CD	-51.527	53.515	0.705	74.293
from	**A**	**736193.117**	**122047.494**	**1052.237**					
to	**C**	**736197.340**	**121962.662**	**1056.737**	AC	4.223	-84.832	4.500	85.056
from	**B**	**736261.692**	**121985.746**	**1051.942**					
to	**D**	**736145.776**	**122016.261**	**1057.521**	BD	-115.916	30.515	5.579	119.995
from	**C**	**736197.321**	**121962.695**	**1056.790**					
to	**B**	**736261.675**	**121985.869**	**1051.957**	CB	64.354	23.174	-4.833	68.570
from	**A**	**736193.108**	**122047.551**	**1052.177**					
to	**D**	**736145.775**	**122016.248**	**1057.503**	AD	-47.333	-31.303	5.326	56.997

Estimates of Errors in Lengths and Stretches:
"Apparent stretch and length change values, due solely to error, would be:"

side:	AB	BC	CD	AD	AC	BD	
Appar. S							App. Stretch
Appar. dL							"(e.g., metres)"
% error							percent

3rd series 1976

						line lengths			
	Point	x	y	z		dx	dy	dz	dr
from	**A**	**736193.104**	**122047.498**	**1052.228**					
to	**B**	**736261.684**	**121985.767**	**1051.956**	AB	68.580	-61.731	-0.272	92.271
from	**C**	**736197.296**	**121962.742**	**1056.779**					
to	**D**	**736145.769**	**122016.257**	**1057.484**	CD	-51.527	53.515	0.705	74.293
from	**A**	**736193.117**	**122047.494**	**1052.237**					
to	**C**	**736197.340**	**121962.662**	**1056.737**	AC	4.223	-84.832	4.500	85.056
from	**B**	**736261.692**	**121985.746**	**1051.942**					
to	**D**	**736145.776**	**122016.261**	**1057.521**	BD	-115.916	30.515	5.579	119.995
from	**C**	**736197.321**	**121962.695**	**1056.790**					
to	**B**	**736261.675**	**121985.869**	**1051.957**	CB	64.354	23.174	-4.833	68.570
from	**A**	**736193.108**	**122047.551**	**1052.177**					
to	**D**	**736145.775**	**122016.248**	**1057.503**	AD	-47.333	-31.303	5.326	56.997

Estimates of Errors in Lengths and Stretches:
"Apparent stretch and length change values, due solely to error, would be:"

side:	AB	BC	CD	AD	AC	BD	
Appar. S							App. Stretch
Appar. dL							"(e.g., metres)"
% error							percent

1992 Data

1st series 1992

	Point	x	y	z		dx	dy	dz	dr	line lengths 1992			δ height			
from	a	**736194.710**	**122046.390**	**1051.159**					1st	2nd	3rd	average	1st	2nd	3rd	average
to	b	**736263.500**	**121984.749**	**1050.868**	AB	68.790	-61.641	-0.291	92.368	92.368	92.368	92.368	-0.019	-0.019	-0.019	-0.019
from	c	**736197.250**	**121963.515**	**1056.475**												
to	d	**736145.662**	**122016.819**	**1057.162**	CD	-51.588	53.304	0.687	74.183	74.183	74.183	74.183	-0.018	-0.018	-0.018	-0.018
from	a	**736194.705**	**122046.373**	**1051.133**												
to	c	**736197.245**	**121963.512**	**1056.495**	AC	2.540	-82.861	5.362	83.073	83.073	83.073	83.073	0.862	0.862	0.862	0.862
from	b	**736263.466**	**121984.768**	**1050.852**												
to	d	**736145.675**	**122016.820**	**1057.158**	BD	-117.791	32.052	6.306	122.237	122.237	122.237	122.237	0.727	0.727	0.727	0.727
from	c	**736197.243**	**121963.513**	**1056.499**												
to	b	**736263.472**	**121984.779**	**1050.844**	CB	66.229	21.266	-5.655	69.789	69.789	69.789	69.789	-0.822	-0.822	-0.822	-0.822
from	a	**736194.712**	**122046.387**	**1051.144**												
to	d	**736145.663**	**122016.834**	**1057.166**	AD	-49.049	-29.553	6.022	57.580	57.580	57.580	57.580	0.696	0.696	0.696	0.696

Estimates of Errors in Lengths and Stretches:
"Apparent stretch and length change values, due solely to error, would be:"

side:	Ab	bc	cd	Ad	Ac	bd	
Appar. S	1.000404437	1.000537039	1.000503647	1.000652571	1	1.000305987	App. Stretch
Appar. dL	0.037341574	0.037341574	0.037341574	0.037341574	0	0.037341574	"(e.g., metres)"
% error	0.040443714	0.053703868	0.05036465	0.065257149	0	0.030598665	percent

Stretches of Line Segments in Quadrilateral

1976 1st series
Stretch Values Computed from Slope-Distance Measurements of Qadrilateral

stakes:	AB	CD	AC	BD	BC	AD
Stretch:	1.0010	0.9985	0.9767	1.0187	1.0178	1.0102
% strain	0.1042	-0.1475	-2.3314	1.8681	1.7779	1.0228
δ height	-0.2910					

1976 2nd series

Stretch Values Computed from Slope-Distance Measurements of Qadrilateral

stakes:	AB	CD	AC	BD	BC	AD
Stretch:	1.0010	0.9985	0.9767	1.0187	1.0178	1.0102
% strain	0.1042	-0.1475	-2.3314	1.8681	1.7779	1.0228

1976 3rd series

Stretch Values Computed from Slope-Distance Measurements of Qadrilateral

stakes:	AB	CD	AC	BD	BC	AD
Stretch:	1.0010	0.9985	0.9767	1.0187	1.0178	1.0102
% strain	0.1042	-0.1475	-2.3314	1.8681	1.7779	1.0228

2nd series 1992

						line lengths					δ height			
	Point	x	y	z		dx	dy	dz	dr		1st	2nd	3rd	average
from	**a**	**736194.710**	**122046.390**	**1051.159**										
to	**b**	**736263.500**	**121984.749**	**1050.868**	AB	68.790	-61.641	-0.291	92.368	AB	-0.019	-0.019	-0.019	-0.019
from	**c**	**736197.250**	**121963.515**	**1056.475**										
to	**d**	**736145.662**	**122016.819**	**1057.162**	CD	-51.588	53.304	0.687	74.183	CD	-0.018	-0.018	-0.018	-0.018
from	**a**	**736194.705**	**122046.373**	**1051.133**										
to	**c**	**736197.245**	**121963.512**	**1056.495**	AC	2.540	-82.861	5.362	83.073	AC	0.862	0.862	0.862	0.862
from	**b**	**736263.466**	**121984.768**	**1050.852**										
to	**d**	**736145.675**	**122016.820**	**1057.158**	BD	-117.791	32.052	6.306	122.237	BD	0.727	0.727	0.727	0.727
from	**c**	**736197.243**	**121963.513**	**1056.499**										
to	**b**	**736263.472**	**121984.779**	**1050.844**	CB	66.229	21.266	-5.655	69.789	CB	-0.822	-0.822	-0.822	-0.822
from	**a**	**736194.712**	**122046.387**	**1051.144**										
to	**d**	**736145.663**	**122016.834**	**1057.166**	AD	-49.049	-29.553	6.022	57.580	AD	0.696	0.696	0.696	0.696

Estimates of Errors in Lengths and Stretches:

"Apparent stretch and length change values, due solely to error, would be:"

side:	Ab	bc	cd	Ad	Ac	bd	
Appar. S							App. Stretch
Appar. dL							"(e.g., metres)"
% error							percent

Stretches of Line Segments in Quadrilateral

1976 1st series

Stretches of Line Segments in Quadrilateral

Stretch Values Computed from Slope-Distance Measurements of Qadrilateral

stakes:	AB	CD	AC	BD	BC	AD
Stretch:	1.0010	0.9985	0.9767	1.0187	1.0178	1.0102
% strain	0.1042	-0.1475	-2.3314	1.8681	1.7779	1.0228

1976 2nd series

Stretches of Line Segments in Quadrilateral

Stretch Values Computed from Slope-Distance Measurements of Qadrilateral

stakes:	AB	CD	AC	BD	BC	AD
Stretch:	1.0010	0.9985	0.9767	1.0187	1.0178	1.0102
% strain	0.1042	-0.1475	-2.3314	1.8681	1.7779	1.0228

1976 3rd series

Stretches of Line Segments in Quadrilateral

Stretch Values Computed from Slope-Distance Measurements of Qadrilateral

stakes:	AB	CD	AC	BD	BC	AD
Stretch:	1.0010	0.9985	0.9767	1.0187	1.0178	1.0102
% strain	0.1042	-0.1475	-2.3314	1.8681	1.7779	1.0228

3rd series 1992

						line lengths					δ height			
	Point	x	y	z		dx	dy	dz	dr		1st	2nd	3rdaverage	
from	**a**	**736194.710**	**122046.390**	**1051.159**										
to	**b**	**736263.500**	**121984.749**	**1050.868**	AB	68.790	-61.641	-0.291	92.368	AB	-0.019	-0.019	-0.019	-0.019
from	**c**	**736197.250**	**121963.515**	**1056.475**										
to	**d**	**736145.662**	**122016.819**	**1057.162**	CD	-51.588	53.304	0.687	74.183	CD	-0.018	-0.018	-0.018	-0.018
from	**a**	**736194.705**	**122046.373**	**1051.133**										
to	**c**	**736197.245**	**121963.512**	**1056.495**	AC	2.540	-82.861	5.362	83.073	AC	0.862	0.862	0.862	0.862
from	**b**	**736263.466**	**121984.768**	**1050.852**										
to	**d**	**736145.675**	**122016.820**	**1057.158**	BD	-117.791	32.052	6.306	122.237	BD	0.727	0.727	0.727	0.727
from	**c**	**736197.243**	**121963.513**	**1056.499**										
to	**b**	**736263.472**	**121984.779**	**1050.844**	CB	66.229	21.266	-5.655	69.789	CB	-0.822	-0.822	-0.822	-0.822
from	**a**	**736194.712**	**122046.387**	**1051.144**										
to	**d**	**736145.663**	**122016.834**	**1057.166**	AD	-49.049	-29.553	6.022	57.580	AD	0.696	0.696	0.696	0.696

Estimates of Errors in Lengths and Stretches:

"Apparent stretch and length change values, due solely to error, would be:"

side:	Ab	bc	cd	Ad	Ac	bd	
Appar. S							App. Stretch
Appar. dL							"(e.g., metres)"
% error							percent

Stretches of Line Segments in Quadrilateral

1976 1st series A B

Stretches of Line Segments in Quadrilateral

Stretch Values Computed from Slope-Distance Measurements of Qadrilateral

stakes:	AB	CD	AC	BD	BC	AD		
Stretch:	1.0010	0.9985	0.9767	1.0187	1.0178	1.0102		
% strain	0.1042	-0.1475	-2.3314	1.8681	1.7779	1.0228	D	C

1976 2nd series
Stretches of Line Segments in Quadrilateral
Stretch Values Computed from Slope-Distance Measurements of Qadrilateral

stakes:	AB	CD	AC	BD	BC	AD
Stretch:	1.0010	0.9985	0.9767	1.0187	1.0178	1.0102
% strain	0.1042	-0.1475	-2.3314	1.8681	1.7779	1.0228

1976 3rd series
Stretches of Line Segments in Quadrilateral
Stretch Values Computed from Slope-Distance Measurements of Qadrilateral

stakes:	AB	CD	AC	BD	BC	AD
Stretch:	1.0010	0.9985	0.9767	1.0187	1.0178	1.0102
% strain	0.1042	-0.1475	-2.3314	1.8681	1.7779	1.0228

Table III.4

DATA USED TO DETERMINE DISPLACEMENTS OF CORNERS OF LADDER OF BRACED QUADRILATERALS
ALL MEASUREMENTS MADE PHOTOGRAMMETRICALLY BY JAMES MESSERICH

1976 Data **co=** **57.29578**

Quad 2. Crosses thrust fault on west side of 2-T Ridge.

		x	y	z		B			C			D	
1st series 1976													
from	A	736021.177	121902.888	1067.660									
to	B				736094.342	121816.775	1072.903						
from	C							736032.399	121740.051	1076.616			
to	D										735953.698	121812.906	1071.688
from	A	736021.187	121902.880	1067.675									
to	C							736032.344	121740.072	1076.611			
from	B				736094.365	121816.780	1072.915						
to	D										735953.718	121812.867	1071.675
from	C							736032.341	121740.069	1076.599			
to	B				736094.324	121816.761	1072.917						
from	A	736021.203	121902.866	1067.620									
to	D										735953.688	121812.902	1071.683
2nd series													
	A	736021.206	121902.848	1067.668									
	B				736094.323	121816.705	1072.917						
	C							736032.371	121740.019	1076.648			
	D										735953.687	121812.872	1071.668
	A	736021.189	121902.850	1067.666									
	C							736032.399	121740.114	1076.652			
	B				736094.334	121816.772	1072.945						
	D										735953.683	121812.851	1071.639
	C							736032.368	121740.089	1076.598			
	B				736094.362	121816.797	1072.929						
	A	736021.206	121902.851	1067.677									
	D										735953.691	121812.901	1071.668
3rd series													
	A	736021.168	121902.871	1067.657									
	B				736094.331	121816.796	1072.915						
	C							736032.357	121740.066	1076.582			
	D										735953.680	121812.864	1071.720
	A	736021.168	121902.858	1067.670									
	C							736032.337	121740.086	1076.608			

	B				736094.320	121816.775	1072.902						
	D										735953.683	121812.873	1071.678
	C							736032.364	121740.060	1076.608			
	B				736094.320	121816.763	1072.930						
	A	736021.196	121902.872	1067.690									
	D										735953.720	121812.881	1071.677

Quad 0. Near midwidth of 2-T Ridge.

from	A	736080.811	121960.415	1062.856									
to	B				736151.318	121878.616	1067.237						
from	C							736094.298	121816.753	1072.896			
to	D										736021.160	121902.881	1067.637
from	A	736080.817	121960.423	1062.805									
to	C							736094.325	121816.744	1072.888			
from	B				736151.317	121878.563	1067.264						
to	D										736021.204	121902.865	1067.619
from	C							736094.363	121816.767	1072.931			
to	B				736151.372	121878.559	1067.324						
from	A	736080.794	121960.425	1062.875									
to	D										736021.217	121902.860	1067.621
2nd series													
	A	736080.811	121960.444	1062.827									
	B				736151.334	121878.551	1067.291						
	C							736094.321	121816.736	1072.967			
	D										736021.227	121902.863	1067.646
	A	736080.81	121960.407	1062.88									
	C							736094.304	121816.761	1072.904			
	B				736151.313	121878.589	1067.297						
	D										736021.222	121902.859	1067.659
	C							736094.344	121816.748	1072.929			
	B				736151.312	121878.594	1067.279						
	A	736080.801	121960.402	1062.817									
	D										736021.299	121902.838	1067.661
3rd series													
	A	736080.778	121960.427	1062.854									
	B				736151.324	121878.576	1067.238						
	C							736094.363	121816.733	1072.895			
	D										736021.239	121902.852	1067.680
	A	736080.798	121960.416	1062.841									
	C							736094.394	121816.767	1072.918			

	B				736151.332	121878.617	1067.286						
	D										736021.272	121902.861	1067.664
	C							736094.390	121816.762	1072.905			
	B				736151.321	121878.529	1067.276						
	A	736080.794	121960.432	1062.858									
	D										736021.259	121902.865	1067.675

Quad 1. Between midwidth and E side of 2-T Ridge.

from	A	736145.776	122016.254	1057.473									
to	B				736197.340	121962.707	1056.771						
from	C							736151.327	121878.579	1067.243			
to	D										736080.837	121960.428	1062.873
from	A	736145.721	122016.240	1057.516									
to	C							736151.315	121878.601	1067.200			
from	B				736197.315	121962.673	1056.778						
to	D										736080.799	121960.391	1062.887
from	C							736151.312	121878.631	1067.232			
to	B				736197.315	121962.669	1056.761						
from	A	736145.748	122016.256	1057.484									
to	D										736080.815	121960.414	1062.858
2nd series													
	A	736145.737	122016.263	1057.521									
	B				736197.307	121962.699	1056.774						
	C							736151.307	121878.620	1067.216			
	D										736080.825	121960.460	1062.867
	A	736145.742	122016.241	1057.469									
	C							736151.308	121878.607	1067.245			
	B				736197.306	121962.738	1056.746						
	D										736080.830	121960.433	1062.878
	C							736151.320	121878.644	1067.237			
	B				736197.329	121962.692	1056.811						
	A	736145.758	122016.234	1057.507									
	D										736080.806	121960.402	1062.867
3rd series													
	A	736145.773	122016.281	1057.484									
	B				736197.337	121962.734	1056.770						
	C							736151.333	121878.614	1067.219			
	D										736080.814	121960.435	1062.891
	B				736197.330	121962.781	1056.765						
	D										736080.804	121960.400	1062.899

	C							736151.355	121878.607	1067.247			
	B				736197.291	121962.678	1056.796						
	A	736145.773	122016.274	1057.483									
	D										736080.781	121960.422	1062.903
		"Quad 3.On E side of 2_T Ridge, across bounding fault.."											
from	A	736193.104	122047.498	1052.228									
to	B				736261.684	121985.767	1051.956						
from	C							736197.296	121962.742	1056.779			
to	D										736145.769	122016.257	1057.484
from	A	736193.117	122047.494	1052.237									
to	C							736197.340	121962.662	1056.737			
from	B				736261.692	121985.746	1051.942						
to	D										736145.776	122016.261	1057.521
from	C							736197.321	121962.695	1056.790			
to	B				736261.675	121985.869	1051.957						
from	A	736193.108	122047.551	1052.177									
to	D										736145.775	122016.248	1057.503
2nd series													
	A	736193.104	122047.498	1052.228									
	B				736261.684	121985.767	1051.956						
	C							736197.296	121962.742	1056.779			
	D										736145.769	122016.257	1057.484
	A	736193.117	122047.494	1052.237									
	C							736197.340	121962.662	1056.737			
	B				736261.692	121985.746	1051.942						
	D										736145.776	122016.261	1057.521
	C							736197.321	121962.695	1056.790			
	B				736261.675	121985.869	1051.957						
	A	736193.108	122047.551	1052.177									
	D										736145.775	122016.248	1057.503
3rd series													
	A	736193.104	122047.498	1052.228									
	B				736261.684	121985.767	1051.956						
	C							736197.296	121962.742	1056.779			
	D										736145.769	122016.257	1057.484
	A	736193.117	122047.494	1052.237									
	C							736197.340	121962.662	1056.737			
	B				736261.692	121985.746	1051.942						
	D										736145.776	122016.261	1057.521

C							736197.321	121962.695	1056.790			
B				736261.675	121985.869	1051.957						
A	736193.108	122047.551	1052.177									
D										736145.775	122016.248	1057.503

1976 Data

	x	y	z		x	y	z
A	736193.110	122047.514	1052.214	B	736261.684	121985.794	1051.952
				(3)			
D	736145.773	122016.255	1057.503	C	736197.319	121962.700	1056.769
A	736145.757	122016.257	1057.491	B	736197.319	121962.708	1056.775
				(1)			
D	736080.812	121960.421	1062.880	C	736151.324	121878.613	1067.231
A	736080.802	121960.421	1062.846	B	736151.327	121878.577	1067.277
				(0)			
D	736021.233	121902.860	1067.651	C	736094.345	121816.752	1072.915
A	736021.189	121902.865	1067.665	B	736094.336	121816.769	1072.919
				(2)			
D	735953.694	121812.880	1071.677	C	736032.364	121740.070	1076.614
	x	y	z		x	y	z

1992 Data

Quad 2. Crosses thrust fault on west side of 2-T Ridge.

		x	y	z		B			C				
1st series 1992													
from	A	736020.890	121903.379	1067.728									
to	B				736094.085	121817.310	1072.996						
from	C							736032.250	121740.832	1076.200			
to	D										735953.381	121813.578	1071.230
from	A	736020.888	121903.369	1067.711									
to	C							736032.240	121740.877	1076.222			
from	B				736094.070	121817.322	1073.002						
to	D										735953.402	121813.592	1071.254
from	C							736032.243	121740.836	1076.202			
to	B				736094.052	121817.312	1072.992						
from	A	736020.883	121903.379	1067.725									
to	D										735953.374	121813.585	1071.233
2nd series													
	A	736020.885	121903.383	1067.705									
	B				736094.101	121817.334	1072.996						
	C							736032.273	121740.856	1076.208			
	D										735953.391	121813.578	1071.199
	A	736020.869	121903.388	1067.713									
	C							736032.276	121740.854	1076.207			
	B				736094.096	121817.325	1072.977						
	D										735953.380	121813.595	1071.222
	C							736032.257	121740.850	1076.192			
	B				736094.112	121817.325	1072.987						
	A	736020.874	121903.386	1067.703									
	D										735953.420	121813.586	1071.222
3rd series													
	A	736020.882	121903.378	1067.704									
	B				736094.109	121817.337	1072.984						
	C							736032.258	121740.835	1076.206			
	D										735953.392	121813.585	1071.225
	A	736020.884	121903.366	1067.692									
	C							736032.259	121740.848	1076.189			
	B				736094.103	121817.308	1072.972						
	D										735953.398	121813.615	1071.212

	C							736032.237	121740.830	1076.191			
	B				736094.095	121817.326	1072.988						
	A	736020.902	121903.387	1067.732									
	D										735953.404	121813.609	1071.238
		Quad 0. Near midwidth of 2-T Ridge.											
from	A	736080.433	121960.946	1062.947									
to	B				736150.984	121879.283	1067.417						
from	C							736094.014	121817.347	1073.015			
to	D										736020.862	121903.362	1067.690
from	A	736080.443	121960.960	1062.923									
to	C							736094.042	121817.265	1073.011			
from	B				736150.955	121879.272	1067.409						
to	D										736020.871	121903.361	1067.688
from	C							736094.035	121817.348	1073.010			
to	B				736150.941	121879.276	1067.420						
from	A	736080.447	121960.959	1062.957									
to	D										736020.869	121903.366	1067.679
2nd series													
	A	736080.450	121960.957	1062.944									
	B				736150.954	121879.272	1067.424						
	C							736094.050	121817.330	1073.019			
	D										736020.876	121903.355	1067.674
	A	736080.453	121960.959	1062.938									
	C							736094.047	121817.324	1073.029			
	B				736150.974	121879.291	1067.439						
	D										736020.882	121903.367	1067.685
	C							736094.049	121817.333	1073.030			
	B				736150.956	121879.278	1067.441						
	A	736080.455	121960.962	1062.940									
	D										736020.861	121903.387	1067.672
3rd series													
	A	736080.453	121960.937	1062.930									
	B				736150.958	121879.277	1067.445						
	C							736094.079	121817.336	1073.003			
	D										736020.888	121903.366	1067.711
	A	736080.448	121960.936	1062.940									
	C							736094.068	121817.345	1073.028			
	C							736094.055	121817.322	1073.010			
	B				736150.966	121879.305	1067.446						

	A	736080.450	121960.952	1062.944									
	D										736020.891	121903.375	1067.693

Quad 1. Between midwidth and E side of 2-T Ridge.

from	A	736145.646	122016.821	1057.182									
to	B				736197.260	121963.498	1056.477						
from	C							736150.988	121879.276	1067.396			
to	D										736080.465	121960.945	1062.963
from	A	736145.667	122016.826	1057.173									
to	C							736151.000	121879.292	1067.417			
from	B				736197.239	121963.504	1056.507						
to	D										736080.460	121960.926	1062.965
from	C							736151.001	121879.284	1067.428			
to	B				736197.260	121963.493	1056.512						
from	A	736145.645	122016.815	1057.173									
to	D										736080.458	121960.941	1062.958
2nd series													
	A	736145.653	122016.832	1057.175									
	B				736197.253	121963.487	1056.477						
	C							736151.037	121879.278	1067.426			
	D										736080.487	121960.942	1062.944
	A	736145.660	122016.811	1057.153									
	C							736151.005	121879.279	1067.404			
	B				736197.249	121963.496	1056.489						
	D										736080.490	121960.962	1062.930
	C							736151.012	121879.290	1067.427			
	B				736197.246	121963.501	1056.492						
	A	736145.659	122016.833	1057.173									
	D										736080.493	121960.942	1062.927
3rd series													
	A	736145.669	122016.809	1057.174									
	B				736197.254	121963.497	1056.487						
	C							736151.001	121879.266	1067.413			
	D										736080.460	121960.933	1062.977
	A	736145.674	122016.804	1057.180									
	C							736150.985	121879.281	1067.429			
	B				736197.249	121963.477	1056.494						
	D										736080.479	121960.945	1062.963
	C							736150.987	121879.280	1067.423			
	B				736197.234	121963.503	1056.503						

	A	736145.666	122016.811	1057.177									
	D										736080.486	121960.934	1062.957

"Quad 3. On E side of 2_T Ridge, across bounding fault.."

from	A	736194.710	122046.390	1051.159									
to	B				736263.500	121984.749	1050.868						
from	C							736197.250	121963.515	1056.475			
to	D										736145.662	122016.819	1057.162
from	A	736194.705	122046.373	1051.133									
to	C							736197.245	121963.512	1056.495			
from	B				736263.466	121984.768	1050.852						
to	D										736145.675	122016.820	1057.158
from	C							736197.243	121963.513	1056.499			
to	B				736263.472	121984.779	1050.844						
from	A	736194.712	122046.387	1051.144									
to	D										736145.663	122016.834	1057.166
2nd series													
	A	736194.710	122046.390	1051.159									
	B				736263.500	121984.749	1050.868						
	C							736197.250	121963.515	1056.475			
	D										736145.662	122016.819	1057.162
	A	736194.705	122046.373	1051.133									
	C							736197.245	121963.512	1056.495			
	B				736263.466	121984.768	1050.852						
	D										736145.675	122016.820	1057.158
	C							736197.243	121963.513	1056.499			
	B				736263.472	121984.779	1050.844						
	A	736194.712	122046.387	1051.144									
	D										736145.663	122016.834	1057.166
3rd series													
	A	736194.710	122046.390	1051.159									
	B				736263.500	121984.749	1050.868						
	C							736197.250	121963.515	1056.475			
	D										736145.662	122016.819	1057.162
	A	736194.705	122046.373	1051.133									
	C							736197.245	121963.512	1056.495			
	B				736263.466	121984.768	1050.852						
	D										736145.675	122016.820	1057.158
	C							736197.243	121963.513	1056.499			
	B				736263.472	121984.779	1050.844						

A	736194.712	122046.387	1051.144				
D					736145.663	122016.834	1057.166

1992 Data

	x	y	z		x	y	z
A	736194.709	122046.383	1051.145	B	736263.479	121984.765	1050.855
				(3)			
D	736145.667	122016.824	1057.162	C	736197.246	121963.513	1056.490
A	736145.660	122016.818	1057.173	B	736197.249	121963.495	1056.493
				(1)			
D	736080.475	121960.941	1062.954	C	736151.002	121879.281	1067.418
A	736080.448	121960.952	1062.940	B	736150.960	121879.281	1067.430
				(0)			
D	736020.875	121903.366	1067.687	C	736094.049	121817.328	1073.017
A	736020.884	121903.379	1067.713	B	736094.091	121817.322	1072.988
				(2)			
D	735953.394	121813.591	1071.226	C	736032.255	121740.846	1076.202
	x	y	z		x	y	z

1992 Averaged Results

	x	y	z		x	y	z
A	736194.709	122046.383	1051.145	B	736263.479	121984.765	1050.855
				(3)			
D				C			
	736145.663	122016.821	1057.168		736197.248	121963.504	1056.491
A				B			
				(1)			
D				C			
	736080.482	121960.947	1062.947		736150.981	121879.281	1067.424
A				B			
				(0)			
D				C			
	736020.879	121903.373	1067.700		736094.070	121817.325	1073.003
A				B			
				(2)			
D	735953.394	121813.591	1071.226	C	736032.255	121740.846	1076.202
	x	y	z		x	y	z

1976 Averaged Results

	x	y	z		x	y	z
A	736193.110	122047.514	1052.214	B	736261.684	121985.794	1051.952
				(3)			
D				C			
	736145.765	122016.256	1057.497		736197.319	121962.704	1056.772
A				B			
				(1)			
D				C			
	736080.807	121960.421	1062.863		736151.326	121878.595	1067.254
A				B			
				(0)			
D				C			
	736021.211	121902.863	1067.658		736094.340	121816.761	1072.917
A				B			
				(2)			
D	735953.694	121812.880	1071.677	C	736032.364	121740.070	1076.614
	x	y	z		x	y	z

Determine Displacements

		u(x)	u(y)	u(z)		u(x)	u(y)	u(z)
	A	1.60	-1.13	-1.07	B	1.80	-1.03	-1.10
Quad 3					(3)			
	D				C			
		-0.10	0.56	-0.33		-0.07	0.80	-0.28
	A				B			
Quad 1					(1)			
	D				C			
		-0.35	0.53	0.08		-0.34	0.69	0.17
	A				B			
Quad 0					(0)			
	D				C			

		-0.33	0.51	0.04		-0.27	0.56	0.09
	A				B			
Quad 2					(2)			
	D	-0.30	0.71	-0.45	C	-0.11	0.78	-0.41

Transform Displacements to Parallel and Normal to Side AB of Quad 3.
"(new coordinates, x' and y')"
Theta (AB) = -0.837951147 Angle between x-axis and side AB

		u(x')	u(y')	u(z)		u(x')	u(y')	u(z)
	A	1.91	0.43	-1.07	B	1.97	0.65	-1.10
Quad 3					(3)			
	D				C			
		-0.49	0.30	-0.33		-0.64	0.48	-0.28
	A				B			
Quad 1					(1)			
	D				C			
		-0.62	0.10	0.08		-0.74	0.20	0.17
	A				B			
Quad 0					(0)			
	D				C			
		-0.60	0.09	0.04		-0.60	0.18	0.09
	A				B			
Quad 2					(2)			
	D	-0.73	0.25	-0.45	C	-0.65	0.44	-0.41

Relative Displacements (holding A and B of Quad 3 fixed)

		du(x')	du(y')	du(z)		du(x')	du(y')	du(z)
	A	0.00	0.00	0.00	B	0.00	0.00	0.00
Quad 3					(3)			
	D				C			
		-2.40	-0.13	0.74		-2.61	-0.16	0.82
	A				B			
Quad 1					(1)			
	D				C			
		-2.53	-0.34	1.15		-2.71	-0.44	1.27
	A				B			
Quad 0					(0)			
	D				C			
		-2.51	-0.34	1.11		-2.57	-0.47	1.18
	A				B			
Quad 2					(2)			
	D	-2.64	-0.18	0.62	C	-2.62	-0.21	0.69

Relative Displacements (holding C and D of Quad 2 fixed (only C for vertical))

for point C of quad. 2		fix du(z)=		0.210	0.661height correction			
		du(x')	du(y')	du(z)		du(x')	du(y')	du(z)
	A	2.64	0.18	-0.41	B	2.62	0.21	-0.44
Quad 3					(3)			
	D				C			
		0.24	0.05	0.33		0.01	0.04	0.38
	A				B			
Quad 1					(1)			
	D				C			
		0.11	-0.16	0.75		-0.09	-0.24	0.83
	A				B			
Quad 0					(0)			
	D				C			
		0.13	-0.16	0.70		0.05	-0.26	0.75
	A				B			
Quad 2					(2)			
	D	0.00	0.00	0.21	C	0.00	0.00	0.25